

7. SITE 436: JAPAN TRENCH OUTER RISE, LEG 56

Shipboard Scientific Party¹

HOLE 436

Date Occupied: 1 October 1977 (1500)

Date Departed: 6 October 1977 (1340)

Time on Hole: 4 days, 22.7 hours

Position: 39°55.96'N, 145°33.47'E

Water Depth (sea level): 5240 corrected meters, echo-sounding

Water Depth (rig floor): 5250 corrected meters, echo-sounding

Bottom Felt (meters, drill pipe): 5248

Penetration: 397.5 meters

Number of Cores: 42

Total Length of Cored Section: 397.5 meters

Total Core Recovery: 240.8 meters

Principal results:

The drill hole at Site 436 penetrated to a sub-bottom depth of 397.5 meters, and continuous coring was carried out. At Site 437, about 13 km west-southwest of 436, only a mudline core was attempted, and trace amounts of sea floor sediments were obtained. Hole 437 results will not be discussed further in this section.

The cores from Hole 436 represent the most complete record of the upper two-thirds of Neogene biostratigraphy of the northwestern Pacific sea floor yet collected. This stratigraphy contains the record of the depositional environment in this area of the Pacific during the past 15 m.y. The Pleistocene is represented by 80 to 90 meters of diatomaceous ooze. Diatom stratigraphy indicates a sedimentation rate of about 60 m/m.y. (Figure 1). We infer ice-rafting during the late Pleistocene from the occurrence in the upper 40 meters, of planktonic shelf-type benthic foraminifers and pebbles in the

deep-water sediments. Volcanic vitric ash is a major component of the sediment, and there are several discrete ash layers. In the Pliocene section we encountered an increased number of ash layers, reflecting increased ash falls due to the peak in volcanic activity on the Japanese Islands during this period. Overall, however, the lithology of the Pliocene sediments, consisting of diatom-rich hemipelagic deposits, is similar to those of the Pleistocene. The Pliocene-Miocene boundary occurs at 220 to 230 meters sub-bottom. In the interval from 235 to 312 meters, the sediments become distinctly more lithified but are compositionally similar to the overlying units. The microfossil assemblages are late Miocene and diatoms noticeably rarer. The sedimentation rate decreases steadily through this interval. Below 312 meters, there is a striking change in the coloration of the sediment. The grayish olive green of the younger units gives way to a pinkish-tan claystone. This unit belongs to the middle Miocene and is characterized as well by isolated occurrences of rhodochrosite and native copper. There is a rapid transition in Core 38 (359 meters sub-bottom) from tan claystone to chocolate-brown zeolitic clays. These clays are without microfossils but contain some fish teeth and many micronodules. We found nodules of chert and porcellanite in Cores 39 to 41. Some of these cherts contain radiolarian bits that are Late Cretaceous, Albian, or Cenomanian.

A noteworthy aspect of this sedimentary sequence is that the accumulation of biogenic sediments begins abruptly in the middle Miocene. Earlier Tertiary deposits are represented by very thin layers of zeolitic clays, if at all. Much of the Paleogene may be missing altogether. This is essentially the same stratigraphy as at Sites 303 and 304 on DSDP Leg 32. The sudden onset of biogenic sedimentation in the middle Miocene occurs at the same time at Sites 436 and 303, as nearly as can be deduced. If the increase in biogenous sediments is caused by the migration of sites into the high productivity zone, as they rode westward on the Pacific Plate, then the onset of increased sedimentation should have occurred nearly 14 m.y. earlier at Site 436 than at Sites 303 or 304. Since this is not borne out, the mid-Miocene bloom of microfossils must be the result of a ubiquitous major oceanographic change in surface waters in the northwestern Pacific and not of a transgression of sites into a pre-existing high productivity zone. This possibility has already been proposed by Lancelot and Larson (1975).

Correlating the stratigraphy at Sites 436 with the seismic reflection record of Figure 2, using the seismic velocity measurements made on the cores, indicates that the occurrence of the cherts corresponds to the top of the strongly reflecting layers at 0.5-second sub-bottom two-way travel time. This would indicate an interval velocity for the faintly stratified sediments of 1.52

¹ Marcus Langseth (Co-Chief Scientist), Lamont-Doherty Geological Observatory, Palisades, New York; Hakuyu Okada (Co-Chief Scientist), Shizuoka University, Shizuoka, Japan; Charles Adelseck, Deep Sea Drilling Project, Scripps Institution of Oceanography, La Jolla, California; Terry Bruns, United States Geological Survey, Menlo Park, California; Howard E. Harper, Jr., Atlantic Richfield Company, Dallas, Texas; Victor Kurnosov, U. S. S. R. Academy of Sciences, Vladivostok, U. S. S. R.; German Müller, Universität Heidelberg, Heidelberg, Federal Republic of Germany; Ivar Murdmaa, U. S. S. R. Academy of Sciences, Moscow, U. S. S. R.; Kenneth A. Pisciotto, University of California, Santa Cruz, California; Paul Robinson, University of California, Riverside, California; Toyosaburo Sakai, Tohoku University, Sendai, Japan; Peter R. Thompson, Lamont-Doherty Geological Observatory, Palisades, New York; Jean Whelan, Woods Hole Oceanographic Institution, Woods Hole, Massachusetts; Henk Worries, Union Oil Company of California, Los Angeles, California.

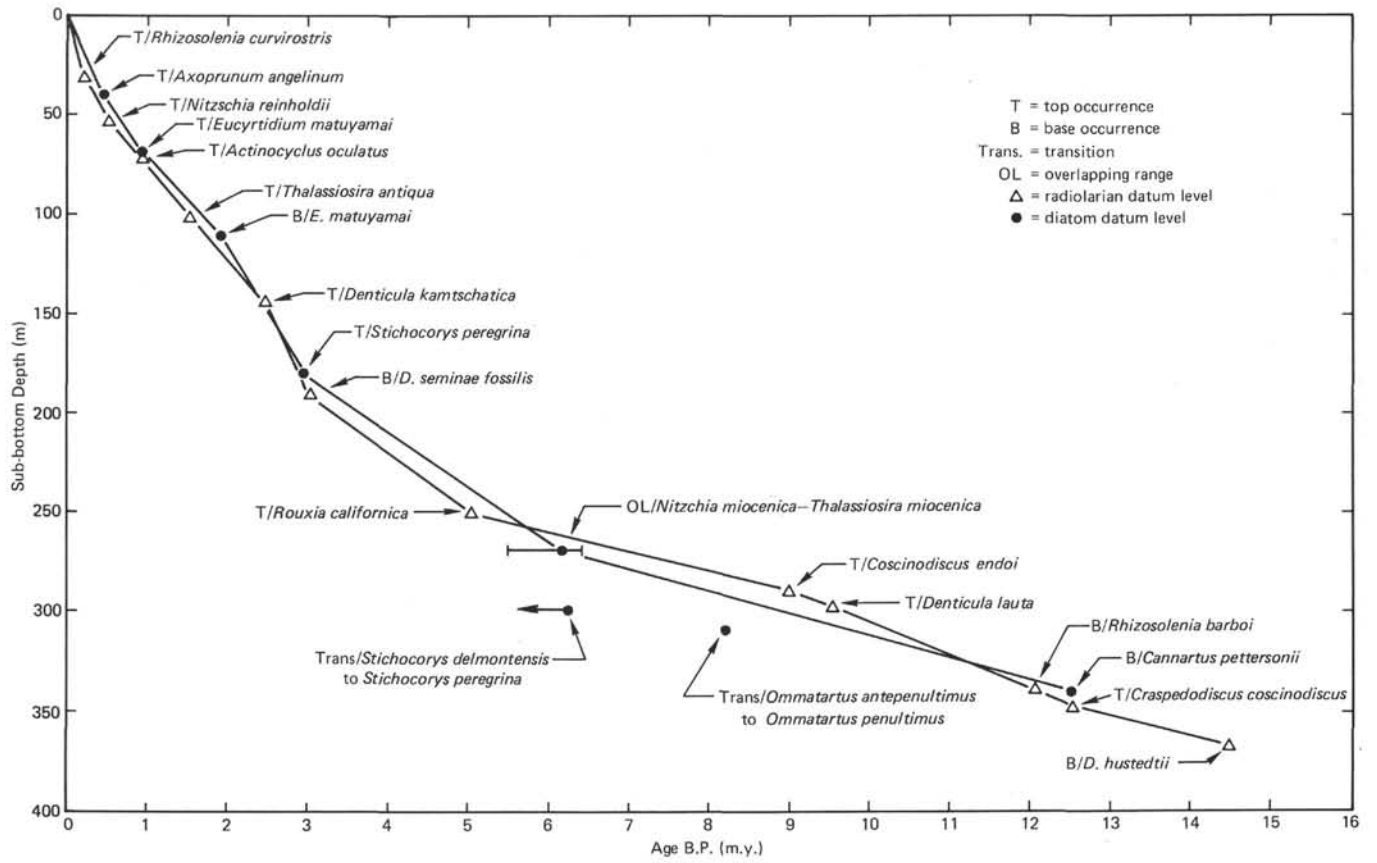


Figure 1. Sediment age versus depth curve for Site 436.

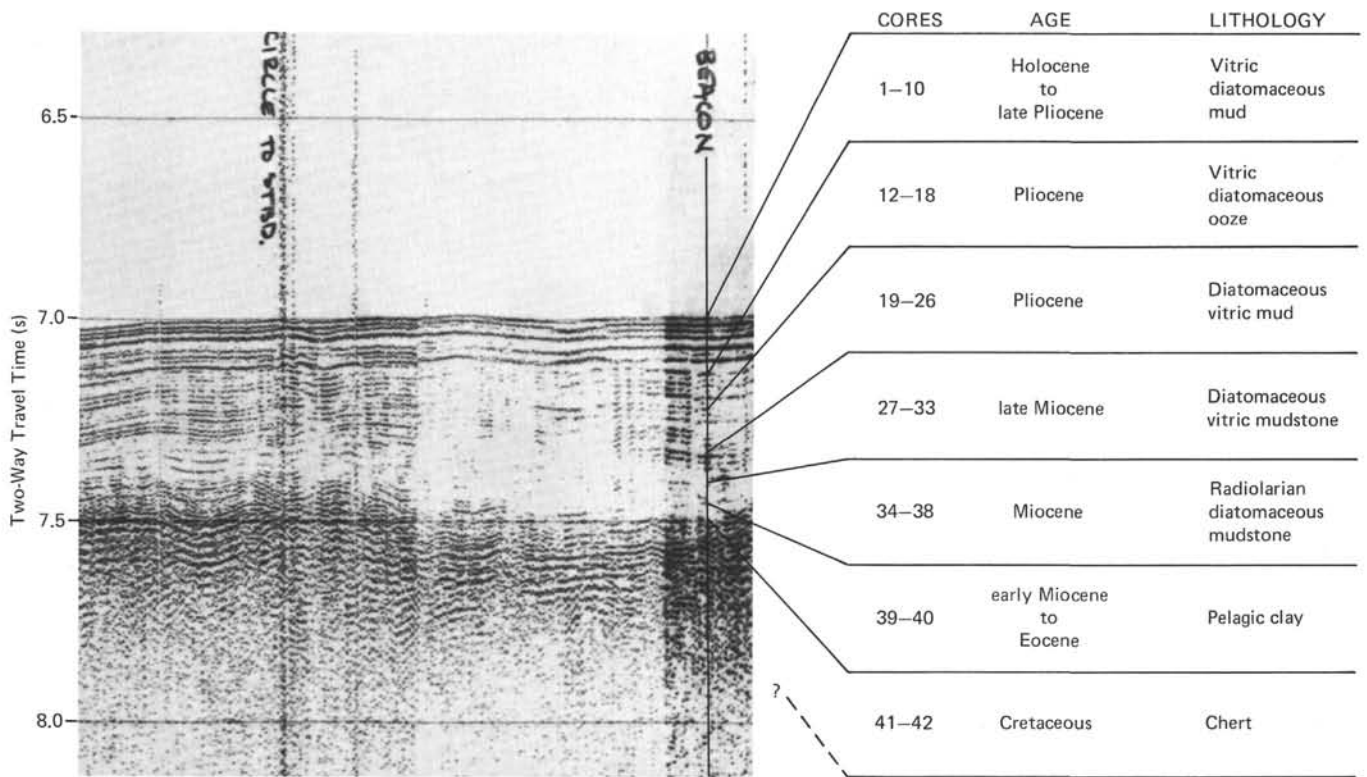


Figure 2. Correlation of seismic reflection data with lithology.

km/s. This compares with an average of 1.56 km/s for core samples (see Physical Properties) and 1.54 km/s from the sonobuoy wide-angle reflections. These velocities are not significantly different from sea water. The faint reflectors throughout this layer are probably thin ash deposits which onboard measurements show to have somewhat higher velocities.

Five *in situ* pore water samples were taken more or less uniformly spaced over the interval from 98 to 318 meters. The major chemical properties of these samples showed good, but not exact, agreement with pore water squeezed from the cores. The pore water alkalinity shows a rapid increase in the upper 35 to 80 meters to about nine times that of sea water but gradually decreases at greater depths sub-bottom. The abundance of calcium was observed to increase with depth, and magnesium shows a decrease. We detected no methane in the cored sediments at this site.

BACKGROUND

Site 436 is located near the crest of the outer swell seaward of the Japan Trench in a water depth of 5240 meters. The outer swell is a broad arching of the sea floor thought to be a dynamically supported feature that results from flexure of the entire oceanic lithosphere in response to overthrusting of the Japanese Island Arc at the trench (Watts and Talwani, 1974). Several detailed single-channel seismic (SCS) reflection lines have been made in the vicinity of the site. All of these tracks were made using a relatively low-energy air-gun sound source. The lines closest to the sites are those made by the Geological Survey of Japan (Honza, 1977; and Honza et al., this volume); three additional lines of seismic reflection data made by the University of Tokyo Ocean Research Institute (Nasu and Kobayashi, 1980); and a single line of SCS reflection data made by the Lamont-Doherty Geological Observatory of *Vema* Cruise 32. The *Glomar Challenger* made additional SCS profiles while surveying for an appropriate site.

The seismic reflection profiles show the sedimentary layer to be about 600 meters thick and generally conformably draped over the oceanic igneous basement. A portion of the record from a line across Site 436 is shown in Figure 2. Across the upper 0.5 second of two-way travel time, the record shows an acoustically stratified sequence. In the frequency range of the seismic reflection system used, the reflectivity of these layers is relatively low. The interval velocity over this section, based on V_p velocities on core samples, is 1.56 km/s, implying a depth of 390 meters for the bottom of the layer. Below 0.5 second two-way travel time (greater than 7.5 seconds in Figure 2), strata are more highly reflective over an interval 0.15 to 0.2 seconds thick. The bottom of this zone is not clearly defined, and its thickness is highly variable across the region. Figure 3, which shows a longer seismic reflection section across the outer swell, illustrates the strong acoustical stratification, general smoothness, and variability in thickness of the zone. This layer is thought to be not igneous basement, but rather a sequence of chert, porcellanite, and carbonate layers. If we assume that a velocity for this in-

terval is equal to those measured on some porcellanite samples (2.7 km/s), then the thickness of the layer ranges from 200 to 270 meters at the drill site. The igneous basement is not clearly seen by reflection profiles; rather, its presence is evident from the disruption of the well-stratified sequence (see Figure 3). The thickness of the highly reflective zone is difficult to determine; if the foregoing figures are correct, the depth to the basement sub-bottom is 590 to 660 meters. A sonobuoy refraction profile was made at the site by launching the buoy from the *Glomar Challenger* while on the drilling site. The northward-flowing surface current was fast enough to carry the buoy 10 km in four hours (Figure 4), far enough to obtain a single well-defined refractor. The velocity of the refractor was calculated to be 5.4 km/s (a typical Layer 2 value). For an interval velocity over the first 0.7 second of two-way travel time of 1.86 km/s, the depth to the basement reflector is 640 meters. This is in good agreement with the depth determined by reflection results. Another sonobuoy was run just 30 miles east of the drill site on a cruise by L-DGO's research vessel *Vema* (V32-13 SB#157) yielded two basement refractors, one with a velocity of 5.4 and a deeper layer of 6.05.

Sites 436 and 437 are located in the Japanese magnetic anomaly lineations (Uyeda et al., 1967; Larson and Chase, 1972). The sites are in an east-northeast-trending magnetic low, south of anomaly M10 in the Mesozoic sequence. This location should make the site somewhat older than anomaly M10 time. Based on the time scale of Hilde et al. (1976), the age of the basement at these sites is 120 to 125 m.y.—i.e., late Valanginian or early Hauterivian. Reconstruction of north Pacific Plate motions, based on magnetic anomaly lineations (e.g., Lancelot and Larson, 1975), indicates that the oceanic crust beneath Sites 436 and 437 followed a 6700-km track from just south of the equator in the central Pacific during the Early Cretaceous to its present position (see Figure 5). The track has three main segments corresponding to the three principal changes in the direction of rotation of this region of the Pacific Plate. Over the past 40 m.y., the site location has been moving along a west-northwest line, relative to the present position of Hawaii, at a rate of 54 km/m.y. We notice from Figure 5 that Site 436 is 750 km west of Sites 303 and 304 (Lancelot and Larson, 1975); as a consequence it should have entered the high productivity zone associated with the Kuroshio Current 14 m.y. earlier than did Sites 303 and 304. From 70 to 40 m.y.B.P. the location of Sites 436 and 437 moved along a northerly track, and prior to 70 m.y.B.P. along a nearly northwesterly track.

Sites 436 and 437 were within a few degrees of the equator from 120 to 90 m.y.B.P. During that period the sea floor depth was between 2500 and 4500 meters; thus part of the time it was above the calcite-compensation depth (CCD), and carbonate deposition could have occurred on the newly formed basement.

OBJECTIVES

The principal objective at these sites was to obtain a complete stratigraphic section of the sedimentary layers on the oceanic crust thought to be underthrusting the

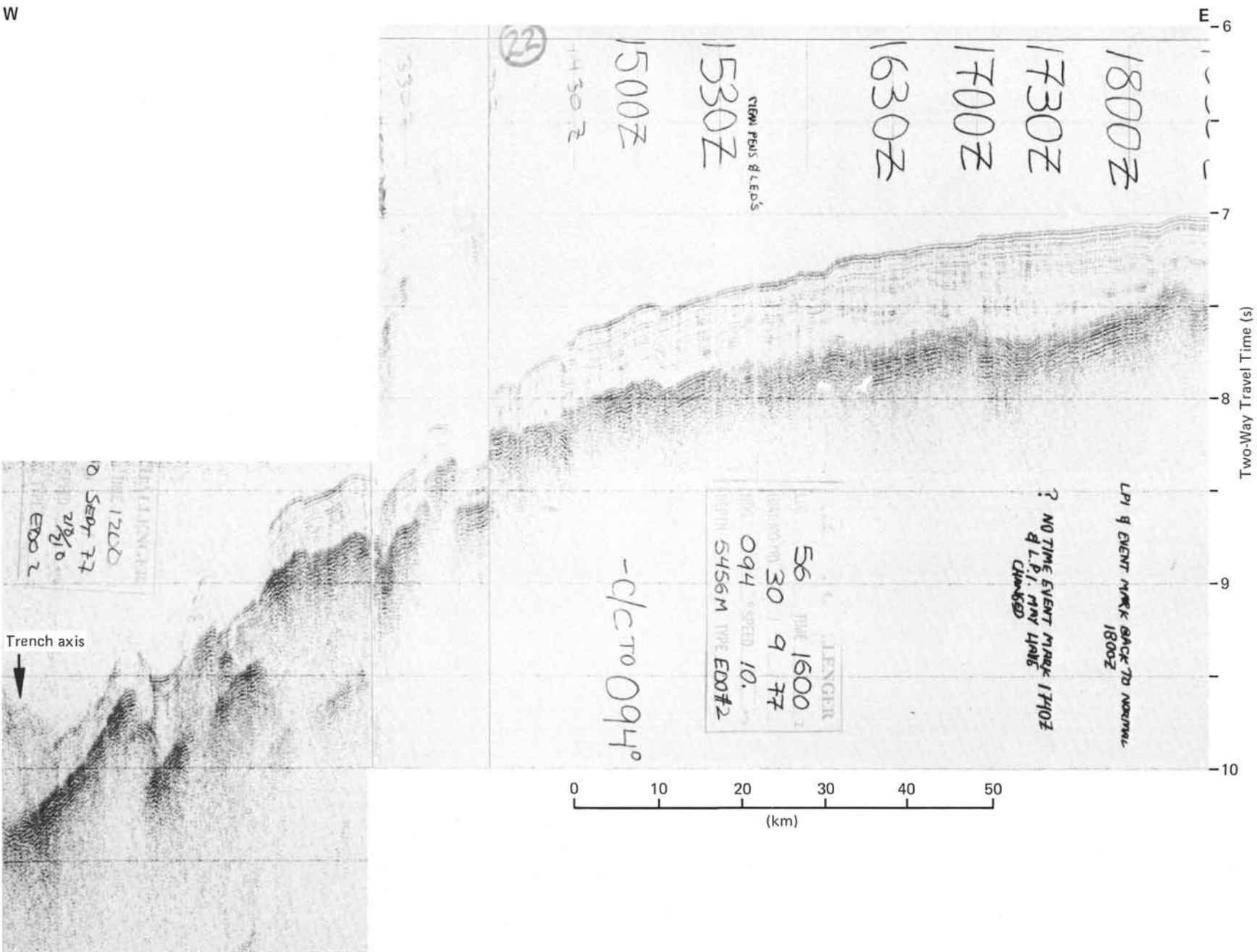


Figure 3. Glomar Challenger, DSDP Leg 56, seismic profile from the Japan Trench axis to the outer swell (1100-1830 Z, 30 September, 1977).

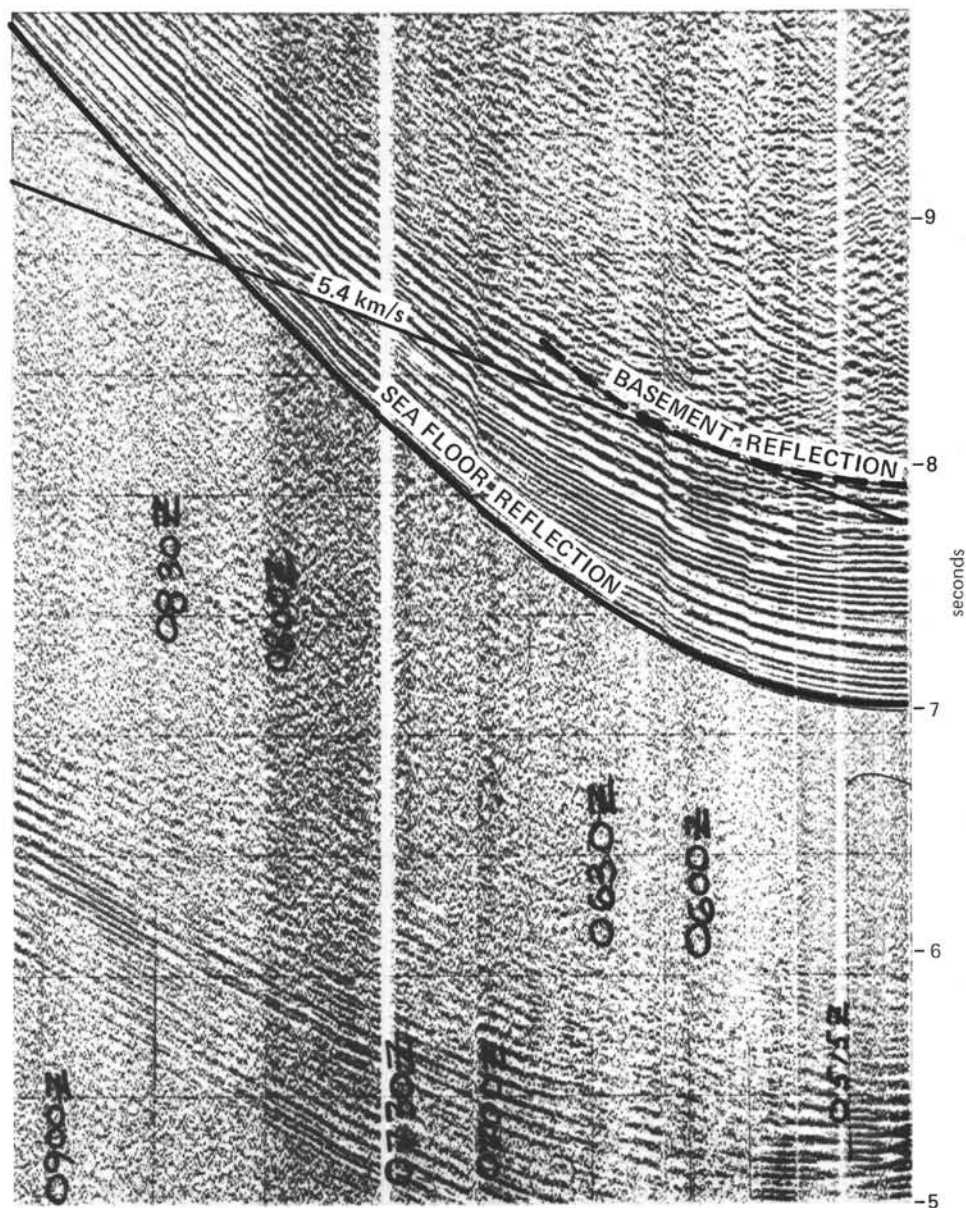


Figure 4. Record of Sonobuoy 2 at Site 436 from DSDP Leg 56.

continental crust of northern Honshu at the axis of the Japan Trench. It was expected that this site would provide a control section to compare with sediments in the accretionary prism.

The biostratigraphy and paleoenvironment stratigraphy of the sedimentary column are of great interest. The lower section of the column records the changing depositional environment from mid-oceanic ridge to sediment-starved deep oceanic environment. The Neogene section should provide a more complete record of surface water diatom populations and their variation as a result of changes in the main current systems and global temperature oscillations. A full record of ash falls through the Neogene is another important set of data that will define the history and composition of volcanism in northern Honshu.

In the Quaternary section, the occurrence of ice-rafted pebbles and other terrigenous debris give evidence of glacially induced cooling. More complete sampling of the upper sedimentary section at this site will reveal the biostratigraphy below the shifting front, between the warm Kuroshio Current and the cold Oyashio Current.

OPERATIONS

On 1 October we steamed to Site 436 on the outer ridge of the Japan Trench. Because a survey of the area near our primary target revealed a small knoll and an indistinct basement reflector, we decided to examine an alternate site 20 nautical miles to the northwest. In the second area, the basement was more clearly defined and there was little topographic relief. The first beacon mal-

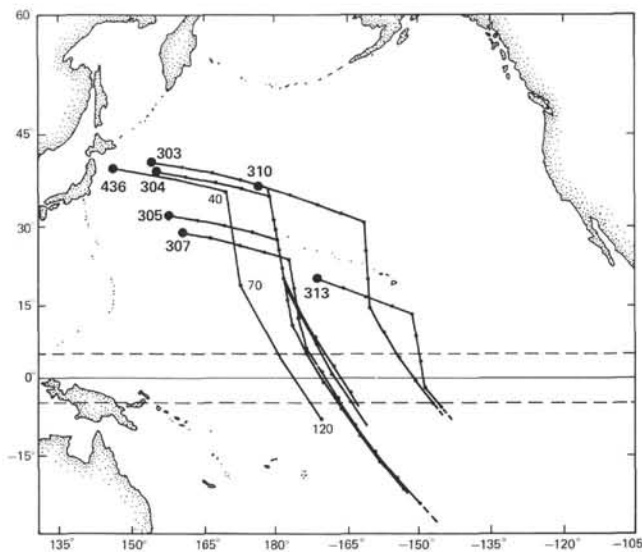


Figure 5. Location of Site 436, DSDP Leg 56, and its backtracked path through geologic time together with the paths of the Leg 32 sites from the northwest Pacific.

functioned, and we dropped a second at 1657 hours on 1 October. Bottom was felt at 5248 meters. Four days of fair weather allowed us to core to a depth of 397.5 meters sub-bottom, but near midnight on 4 October unexpectedly high winds (>50 knots) associated with a cold front forced us to pull the string above the mudline. Retrieval of pipe was slowed to one stand per hour, and we drifted several miles from Site 436.

Near noon on the following day the sea abated, and we decided to drop a new beacon and establish Site 437 rather than try to drag the pipe 8.7 km back to the original site. We recovered a few centimeters of sediments from a mudline core at Site 437, then initiated drilling with a center bit to reach the maximum sub-bottom depth at Site 436. However, forecasts of the passage of another front caused us to pull the pipe aboard without cutting a second core.

We steamed back to the beacon at the original location at Site 436, but the approach of Typhoon Gilda threatened to delay our arrival in Tokyo on 12 October. We departed the site for Tokyo at 2030 hours on 7 October 1977.

LITHOSTRATIGRAPHY

We distinguished three lithologic units at Site 436 (Figure 6): Unit 1, vitric diatomaceous silty clay and claystone; Unit 2, radiolarian diatomaceous claystone; and Unit 3, pelagic clay with chert and porcellanite. We subdivided Unit 1 into two sub-units on the basis of degree of lithification. Similarly, Unit 3 contains two sub-units differentiated by the presence or absence of chert and porcellanite in the pelagic clay. All contacts between successive units are gradational; thus boundaries are somewhat arbitrary. The upper diatomaceous sediments at this site are lithologically similar to those recovered at all other sites along the Japan Trench tran-

sect. In addition, the sequence at this site closely resembles the sedimentary sections penetrated at nearby Sites 303 and 304 (Leg 32), over 700 km east of Site 436 (Lancelot and Larson, 1975). More detailed descriptions follow.

Unit 1, Sub-unit 1A (Cores 436-1-436-26, 0-245.5 m sub-bottom, Holocene through Pliocene)

This sub-unit consists of soft, dusky yellowish-green to grayish-olive-green vitric diatomaceous silty clay. Clay content averages about 40 per cent, diatom frustules 20 per cent, and disseminated volcanic glass shards about 10 per cent. Radiolaria, sponge spicules, quartz, feldspar, pyrite, and heavy minerals occur in smaller, variable amounts. The average grain-size distribution is about 10 per cent sand, 30 per cent silt, and 60 per cent clay. Thin layers and patches of light gray volcanic ash occur intermittently throughout this sub-unit, notably in Cores 1, 6 to 10, 13, 14, 15, 20, and 23. Pumice fragments also occur sporadically.

Sedimentary structures are rare, probably because they have been obliterated by drilling. Ash layers are the most reliable indicators of bedding. None are more than several centimeters thick. Cores 12 to 18 are mottled, perhaps as a result of burrowing. The boundary between Sub-units 1A and 1B is gradational, assigned at the point where the degree of lithification increases noticeably.

Unit 1, Sub-unit 1B (Cores 436-27-436-33, 245.5-312 m sub-bottom, late Miocene)

As noted, this sub-unit differs from Sub-unit 1A mainly in degree of lithification. Composition and grain size are not significantly different. Cores 31 and 32 are brecciated by drilling. Core 33 contains distinct burrowed zones. The boundary with Unit 2 is transitional, marked by a gradual change in color from grayish-olive-green to dusky yellowish-brown and by an increase in the degree of dissolution of diatom frustules.

Unit 2 (Cores 436-34-436-38, 312-359.5 m sub-bottom, middle-upper Miocene)

Moderate yellowish-brown radiolarian diatomaceous claystone composes Unit 2. Clay is the dominant constituent, averaging about 72 per cent. Biogenic silica includes diatoms (10%), radiolarians (8%), and lesser amounts of sponge spicules. Volcanic glass averages 8 per cent. Sand-size crystals of rhodochrosite first appear in Core 24 (268 m sub-bottom), then again in Cores 31 through 40 (284-371 m sub-bottom). The grain-size distribution is about 5 per cent sand, 10 per cent silt, and 75 per cent clay. The apparent increase in radiolarians in this unit may be the result of progressive dissolution of diatom frustules. Layers and patches of light gray volcanic ash are less abundant in this unit than in the overlying sediments. Distinct burrowed and bioturbated zones are common in Core 38. Drilling-induced, horizontal (bedding parallel) fractures separate coherent blocks of claystone, each about 10 cm long. Other fractures or drilling breccia are absent. A gradual change in color from moderately yellowish-brown to light and

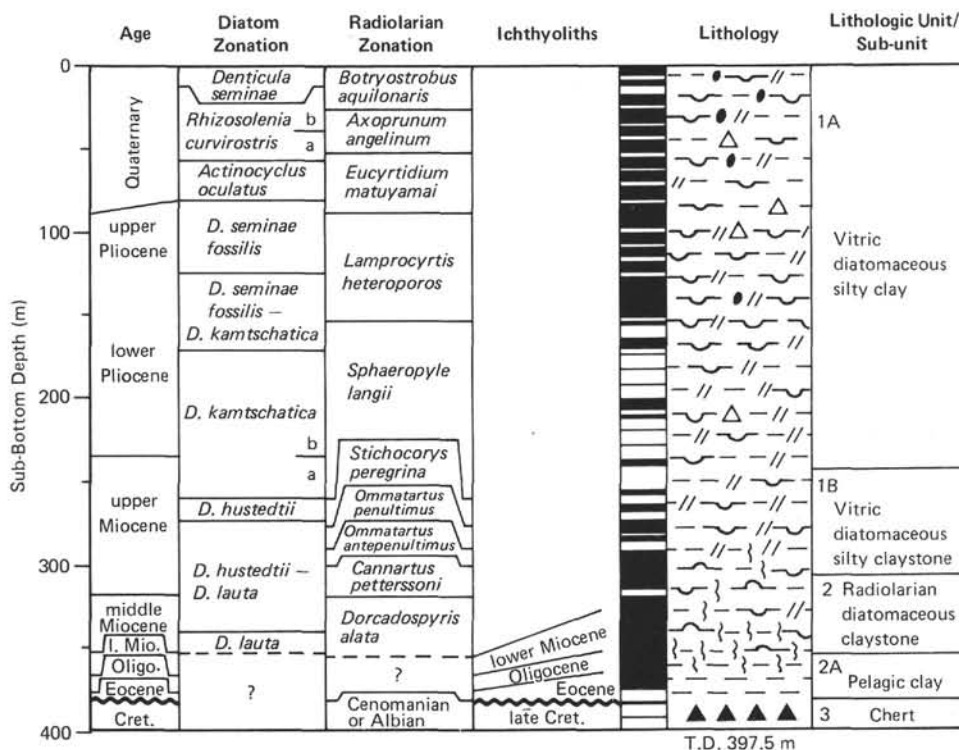


Figure 6. Lithologic and biostratigraphic zonation of the sedimentary section at Site 436.

moderate brown marks the boundary between Units 2 and 3. This transition occurs within the first 50 cm of Core 39.

Unit 3, Sub-unit 3A (Cores 436-39-436-41, 359.5-388.3 m sub-bottom, lower Miocene-Eocene)

Moderate brown to brownish-black pelagic clay composes this sub-unit. The sediment is almost entirely clay with abundant, small spherules of iron oxide and manganese oxide. Foraminiferal molds occur in the centers of some of these spherules. There is a manganese nodule 2 to 3 cm in diameter in Core 39. Light brown patches and lenses of montmorillonitic clay are scattered throughout the sub-unit. Biogenic siliceous components are rare, present mainly as partially dissolved tests of radiolarians. Prismatic crystals of clinoptilolite occur in Cores 39 (360-365 m sub-bottom) and 41. Grain-size analyses indicate an average of 97 per cent clay and about 3 per cent silt. Burrows are common throughout the sub-unit. Some of the light brown patches and lenses in this sediment may be altered volcanic ash. Laminations are not obvious, although they are preserved in the underlying chert and porcellanite. Quartz and opal-CT are the silica minerals in these siliceous rocks. Chalcedony-filled molds of radiolarians are common in the yellow quartzose cherts. These cherts are also veined and brecciated and sometimes show faint laminations. Pieces of unsilicified, clinoptilolite-bearing pelagic clay identical in color to these siliceous rocks occur in Core 42. These too are composed of quartz and opal-CT. Some pieces are laminated and contain silicified, light

brown, and reddish-brown patches or lenses. These hard siliceous rocks probably represent zones of silicification within the pelagic clay, as pieces of unsilicified pelagic clay also occur with these siliceous rocks. The difference in hardness most likely accounts for the poor recovery of pelagic clay in these two cores.

Petrology of Pebbles

Pebbles of altered dacite, vitric tuff, scoria, lithic wacke, and hornfels facies sandstone were collected from this site. The following is a description of igneous rock pebbles.

Dacite is the most common rock type of Site 436 pebbles. Sample 436-27-1, 37-39 cm, is hornblende dacite: phenocrystal plagioclase (1.2 mm) is euhedral and intensely altered to kaolinite; hornblende phenocrysts (0.4-1.2 mm) are entirely replaced by aggregates of chlorite, magnetite, and biotite. The groundmass with intersertal texture consists of oligoclase microlites (<0.15 mm) and anhedral quartz.

In Sample 436-15-1, 8-10 cm, of silicified dacite, mafic phenocrysts are wholly replaced by aggregates of epidote, chlorite, and quartz. The groundmass mainly composed of oligoclase microlites shows fluidal texture and is entirely silicified.

Sample 436-31-1, 1-3 cm, is hornblende-biotite-pyroxene dacite (Figure 7). Plagioclase phenocrysts (0.2 to 2.7 mm) are more or less altered to kaolinite. Hornblende and hypersthene phenocrysts are replaced by chlorite, augite by calcite, and biotite by chlorite and iron ores. The slightly silicified groundmass composed

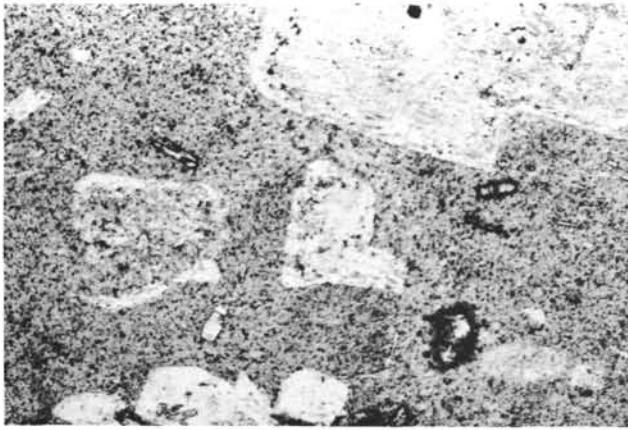


Figure 7. Photomicrograph of hornblende-biotite-pyroxene dacite (Sample 436-31-1, 1-3 cm). Bar scale equals 0.1 mm.

of oligoclase microlites (<0.03 mm) and glass shows hyalopilitic texture.

Sample 436-16-3, 86-87 cm, is biotite-hornblende dacite. Phenocrysts consist of quartz, plagioclase, green hornblende, and biotite; quartz is subhedral, ranging from 0.2 to 1 mm in size; plagioclase (about 0.3 mm) is mostly replaced by sericite and hornblende (about 0.2 mm) partly by epidote. The groundmass with hyalopilitic texture is subject to silicification and epidotization. Accessories include apatite and zircon.

Sample 436-17-1, 32-34 cm, is also intensely silicified dacite with quartz veinlets. Phenocryst plagioclase (0.3-0.6 mm) is wholly sericitized, and mafic minerals are replaced by magnetite. Vitreous groundmass is extremely silicified, and contains some recognizable oligoclase laths. Accessories consist of zircon and apatite.

Varieties of tuff include plagioclase vitric tuff (Samples 436-3-2, 98-99 cm; 436-31-1, 62-63 cm), augite-plagioclase vitric tuff (Samples 436-3-4, 6-9 cm; 436-4-6, 21-22 cm), and andesitic tuff (Sample 436-16-1, 4-6 cm). Scoria (Sample 436-14-2, 29-30 cm) with small amounts of augite and hypersthene microlites was also found.

BIOSTRATIGRAPHY

Introduction

A thick and unusually complete biostratigraphic section was cored at Site 436 (Figure 6). Microfossils are dominantly siliceous and are well preserved except for the lowermost cores. Calcareous microfossils are virtually absent.

Cores 1 through 38 (0-360 m) range from late Quaternary to middle Miocene in continuous sequence. Ice-raftering is recognized in the Pleistocene (Cores 1-5) from the presence of planktonic and calcareous benthonic foraminifers in association with pebbles. The Pliocene/Pleistocene boundary is placed between Core 9, Section 3, and Core 11, Section 1 (80-90 m). The early/late Pliocene boundary falls within the interval between Cores 15 and 17 (140-160 m) but is ill-defined owing to poor siliceous microfossil preservation. The Miocene/Plio-

cene boundary is located between Cores 24 and 25 (about 200 m) and the late/middle Miocene boundary near Core 34 (320 m).

Sediments between Cores 39 and 41, CC consist of dark pelagic clay which yields only zeolites, rare fish teeth, and small manganese micronodules bearing external molds of juvenile planktonic foraminifers. No ages were determined. The age of the oldest sediments cored is Cretaceous, based on scarce Albian-Cenomanian radiolarians from cherts in Core 41.

Diatoms

Diatoms are common to abundant in Cores 1 to 27, become increasingly less abundant in Cores 28 to 37, and are absent below Core 37.

Cores 1 and 2 represent the *Denticula seminae* Zone, and the top of the range of *Rhizosolenia curvirostris*, in Core 3, Section 2, marks the base of this zone (0.26 m.y. B.P.). Cores 3 and 7 lie in the *R. curvirostris* Zone, and the top occurrence of *Actinocyclus oculatus*, marking the base of this zone (0.9 m.y. B.P.), is in Core 7, Section 4. Cores 7 to 9 represent the *A. oculatus* Zone; the base of this zone (1.6-1.8 m.y.) approximates the Pliocene/Pleistocene boundary, and is based on the lowest occurrence of *Pseudoeunotia doliolus* and the highest occurrence of *Thalassiosira antiqua* (between Cores 9 and 10). Cores 10 to 14 have been assigned to the *D. seminae fossilis* Zone, although the top of occurrence of *D. kamtschatica*, marking the base of the zone, is difficult to locate because of reworking; it may be as high as Core 12, Section 5. Cores 12 to 19 were placed in the *D. seminae fossilis*-*D. kamtschatica* Zone. The early/late Pliocene boundary is in the lower portion of this zone but was not precisely located. The lowest occurrence of *D. seminae fossilis* was in Core 19 and was used to define the top of the *D. kamtschatica* Zone.

The Miocene/Pliocene boundary, based on the highest occurrence of *Rouxia californica*, is in Core 25. The lowest occurrence of *D. kamtschatica* in Core 28 marks the top of the *D. hustedtii* Zone, which extends from Cores 29 to 30. The highest occurrence of *D. lauta* in Core 30 marks the top of the *D. lauta*-*D. hustedtii* Zone. The lowest occurrence of *D. hustedtii* is in Core 37, Section 1, marking the top of the *D. lauta* Zone, which extends to the lower part of Core 37. No diatom remains were found in or below Core 38.

Radiolaria

Common to abundant, well-preserved radiolarians were recovered from Cores 1 through 39-1; they are not present between Cores 39-3 and 40 and are rare and poorly preserved in Cores 41 and 42.

In Cores 1 through 3, we recognized the latest Quaternary *Botryostrobus aquilonaris* Zone (0-0.4 m.y. B.P.). Cores 4 through 6 are assigned to the late Pleistocene *Axoprunum angelinum* Zone (0.4-0.9 m.y. B.P.) and Cores 7 through 10 to the early Pleistocene *Eucyrtidium matuyamai* Zone (0.9-1.8 m.y. B.P.). Cores 11 through 17 and 18 through 28 are assigned to the *Lamprocristis heteroporos* and *Sphaeropyle langii* zones, respectively. The *Cannartus pettersoni* Zone was recognized in Cores

33 through 34-3, and the middle/late Miocene boundary lies within or just below this interval. Cores 34-3 through 39-1 are assigned to the *Dorcadospyrus alata* Zone. Core 39-2 bears a few fragments of orosphaeridae radiolarians, but there is no indication of age.

The pale olive clay and cherts in Core 41 contain abundant but very poorly preserved radiolarians. The assemblage, including *Spongosaturnalis hueyi* group, *Hemicryptocapsa prepolyhedra*, and *Dictiomitra pseudomacrocephala* and lacking Cenozoic forms, suggests an Albian or Cenomanian age.

Foraminifera

Planktonic and calcareous, shelf-type benthonic foraminifers were recovered in association with pebbles from several samples in Cores 1 through 5. The depth of this site relative to the regional CCD (3500 m) requires a very rapid burial of calcareous material to prevent its dissolution, and ice-rafting in association with late Pleistocene climatic fluctuations provides a plausible mechanism.

Agglutinated benthonic foraminifers characterize surficial and subsurface Tertiary sediments at this site, including *Saccamina*, *Reophax*, *Cyclammina*, *Bathysiphon*, and *Martinottiella*, and the nonagglutinated siliceous species *Silicosigmoina splendida* described by Thompson in this volume. *Martinottiella* disappears at the top of Core 19 near the early/late Pliocene boundary.

External molds of small globigerinid or globorotaliid foraminifers were observed in small manganese micro-nodules from the otherwise fossil-poor pelagic clay between Cores 39 and 41. Nucleation of the manganese must have been rapid—otherwise the fragile foraminiferal tests would not have survived calcite dissolution at such depth during sedimentation of this interval.

Fecal Pellets

Four morphologically distinct types of fecal pellets were recovered between Cores 1 and 26. Because of the large proportion of detrital mineral matter in the pellets we assume burrowing sediment-eaters such as polychaetes or holothurians to be the producers. The fact that the greatest frequency of pellets occurs between peaks of volcanic ash layers may indicate that floods of volcanic debris disturbed the benthic ecology.

PHYSICAL PROPERTIES

At Site 436 we determined compressional sound velocity, wet bulk density, water content, porosity, undrained shear strength, and thermal conductivity. A summary of the shipboard techniques for determining these parameters is included in the introduction to this volume, and a more detailed discussion is presented by Boyce (1976).

Generally high core recovery allowed frequent determinations of velocity and of wet bulk density with the GRAPE. Gravimetric techniques on numerous samples gave good quality determinations of density, porosity, and water content throughout the hole; excellent agreement is seen between these data and the interpretative

values obtained from the continuous GRAPE data. Data for physical properties are presented in Appendix II (this volume), and plots with depth of velocity, density and porosity are shown on the Site 436 Site Summary Chart (back pocket, this volume). Table 1 shows averages of velocity, density, and porosity for each lithologic unit.

Velocity

Velocity values generally increase with depth in the first 40 cores, ranging from 1.5 km/s at the top to 1.65 km/s near the bottom. In Sub-unit 3B only scattered chert was recovered, and no formation velocity can be estimated. The changes in velocity correlate well with lithologic changes. Consolidation of recovered sediment with sub-bottom depth in lithologic Units 1A and 1B is indicated by a gradual increase in the velocity from about 1.53 km/s to 1.60 km/s. An increase in the velocity to about 1.64 km/s corresponds with the change to lithologic Unit 2. The transition from Unit 2 to Sub-unit 3A (pelagic clay) is accompanied by a significant decrease in velocity to about 1.61 km/s. Velocities were taken on several porcellanite and chert samples; two ranges of values were found, averaging around 2.6 km/s (eight porcellanite samples) and 4.8 km/s (two chert samples).

Numerous ash layers are present in the upper 300 meters of the hole; 17 velocity determinations gave an average value of 1.64 km/s, which is substantially higher than the average of all values. This suggests that the faint seismic reflectors within the sedimentary section (see Figure 2) are from ash-rich layers within an otherwise uniform section.

Velocity measurements were made on samples both parallel and perpendicular to the bedding to determine if any velocity anisotropy is present. Half of these determinations are in the vitric diatomaceous claystone of Sub-unit 1B, the rest in the radiolarian diatomaceous claystone and pelagic clay of Unit 2 and Sub-unit 3A. Eight of 14 pairs in Sub-unit 1B show a slightly higher velocity parallel to the bedding (0.016 ± 0.005 km/s), 2 indicate an opposite anisotropy (0.013 ± 0.001 km/s), and 4 are inconclusive. Of 14 measurements in Unit 2 and Sub-unit 3A, 11 indicate a higher velocity parallel to bedding (0.045 ± 0.021 km/s); 3 are inconclusive. These results indicate that there is only a slight anisotropy in the vitric diatomaceous claystone but that a well-defined anisotropy is developed in the radiolarian

TABLE 1
Correlation of Physical Property Data with Lithology at Site 436

Lithologic Unit/Sub-unit	Depth Interval (m)	Interval Velocity (km/s)	Density (Mg/m ³)	Porosity (%)	Cumulative Two-Way Travel Time (s)
1A	0-245.5	1.53 ± 0.02	1.39 ± 0.6	72 ± 4	0.320
1B	245.5-312	1.60 ± 0.03	1.44 ± 0.04	74 ± 2	0.404
2	312.0-359.5	1.63 ± 0.03	1.50 ± 0.05	72 ± 3	0.462
3A	359.5-378.5	1.61 ± 0.03	1.68 ± 0.05	65 ± 2	0.486
3B	378.5-397.5	—	—	—	—

Note: Values for velocity, density, and porosity are averages of measured values over each lithologic unit. The two-way travel time is calculated from the interval velocity and indicates the seismic reflection time to the base of the lithologic unit.

diatomaceous claystone and pelagic clay, with velocity parallel to the bedding about 3 per cent faster in each case.

Several velocity intervals appear to be present in the hole; these intervals correlate well to changes in lithology and are discussed further under the section on correlation with seismic reflection data. The interval velocities shown assume that 5 per cent of the section is composed of ash layers with a velocity of 1.65 km/s.

Wet Bulk Density

Wet bulk density increases gradually throughout the first 350 meters of the hole, from about 1.4 to 1.5 Mg/m³. A more rapid increase to about 1.7 Mg/m³ occurs at the base of Unit 2 and in Sub-unit 3A, corresponding to increased amounts of pelagic clay. In general, the density appears to reflect primarily increasing consolidation with depth throughout most of the hole, except in the pelagic clay, where the increased density reflects the abrupt change in lithology.

Density measurements were made on five ash units but show considerable scatter; the average is 1.45 ± 0.15 Mg/m³, or slightly lower than that of the surrounding sediment. There is excellent agreement between the gravimetric data and the continuous and two-minute GRAPE data.

Porosity and Water Content

Both porosity and water content are also relatively uniform. Porosity is around 70 per cent and decreases to around 55 per cent in the pelagic clay. Water content is around 50 per cent throughout the upper 300 meters, decreasing to 37 per cent in the brown clay. Again the agreement between the GRAPE and gravimetric porosity data is excellent.

Shear Strength

Shear strength determinations were all made with the CI-600 Torvane apparatus. The data show considerable scatter but generally increase from around 6 kPa at the surface to a maximum measured value of around 65 kPa at 200 meters. Measurements were discontinued below 213 meters when cracking of the sediment indicated lack of cohesion. The deep ocean sediments appear to have somewhat greater shear strength than the inner trench wall sediments at Site 435, although the difference may reflect primarily fracturing of sediment through degassing at Site 435. A plot and discussion of the shear strength values is included in Carson and Bruns (this volume).

Thermal Conductivity

The excellent percentage of core recovery at Site 436 allowed numerous good quality measurements of thermal conductivity to be made over the complete core section. The measured values are plotted versus depth in Figure 8. The needle probe observations (triangles) show slightly more variation than the QTM observations, suggesting that the random error associated with the QTM measurements is less. The QTM values are somewhat higher in the upper 60 meters than in the sec-

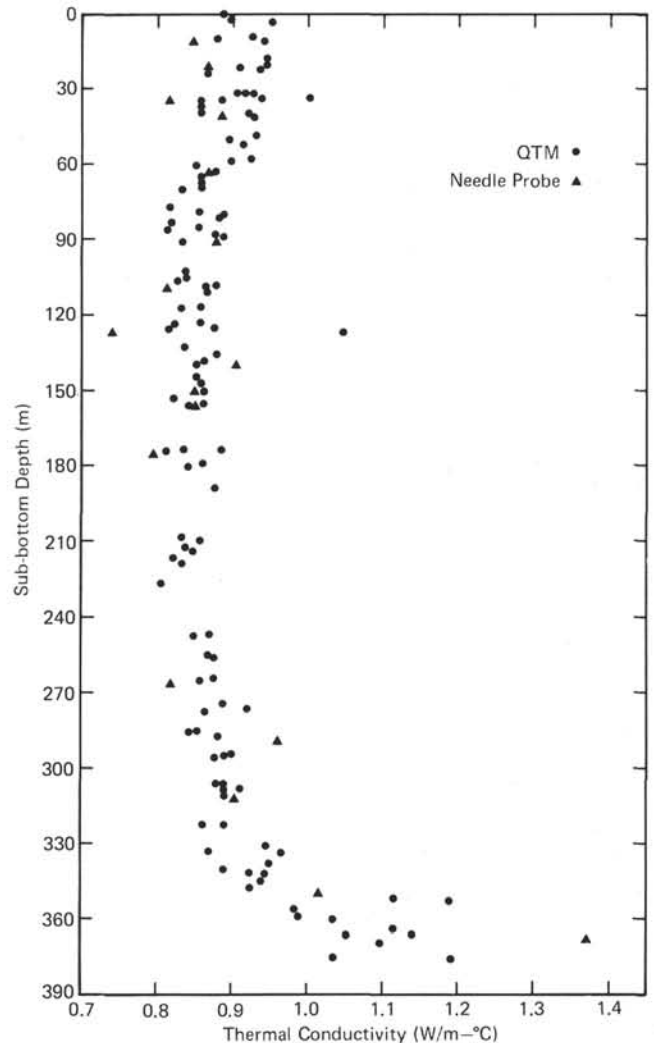


Figure 8. *Thermal conductivity versus sub-bottom depth, Site 436.*

tion between 60 and 260 meters. The needle probe observations, on the other hand, show uniform values from the surface to 280 meters. The QTM measurements in the upper 60 meters may be biased to higher values because of systematic errors in measurement technique. These errors are discussed in the Introduction and Explanatory Notes (this volume). However, values at 435 were also higher in the upper 60 meters of sediment.

The thermal conductivity appears only slightly sensitive to the increasing lithification of the sediments with depth. The diatomaceous ooze becomes increasingly firm at a depth of about 200 meters and at 250 meters can be classed as mudstone—in this interval the conductivity does not increase at all. Below 250 meters, conductivity increases significantly and in the dark brown manganese-rich clay near the bottom of the hole gives relatively high values (1.0–1.3 W/m-°C). The increase correlates with a decrease in water content in the zeolitic clays and, to a lesser extent, with the composition of the sediment.

Discussion

Physical properties at Site 436 are remarkably uniform, with the slight changes in the upper 330 meters due primarily to consolidation. Major changes occur in the bottom 70 meters of the hole and are due to the decreasing abundance of biogenic silica, increasing clay content, and diagenetic changes of the sediment. Major changes in physical properties probably occur in the chert-rich sediments of Cores 41 and 42, but recovery was inadequate to study these changes.

CORRELATION WITH SEISMIC REFLECTION DATA

The major lithologic units can be recognized in the acoustic stratigraphy of single-channel seismic records. Figure 2 shows the seismic reflection record obtained by the *Glomar Challenger* passing over Site 436. Table 1 gives the lithologic units and interval velocity values used to calculate two-way reflection times to lithologic boundaries. The upper 0.1 second of the record is obscured by bubble reverberations. The increase in frequency of closely spaced reflectors in the Pliocene and late Miocene section may result from increasing ash content. The tan pelagic sediments are represented by a transparent zone. The chert shows a strong though discontinuous reflector. Deeper sediments were not sampled.

GEOCHEMISTRY

Site 436 was drilled in 5248 meters of water on the seaward side of the Japan Trench to a sub-bottom depth of 397.5 meters. The top 300 meters of sediment were primarily diatomaceous with interbedding volcanic ash layers. A layer of brownish-black clay at 350 to 380 meters covered a chert bed at hole bottom.

Interstitial Water

A major accomplishment at this site was obtaining five *in situ* water samples using a sampler designed by Ross Barnes (see *Initial Reports* Volume 47, Part 2, for description of apparatus) from sub-bottom depths of 90 to 330 meters. This is the greatest depth at which the sampler has been used successfully and the first time that an attempt was made to obtain samples at regular intervals.

Ordinarily, interstitial water is squeezed from sediment after the core has been brought on deck. During the time between cutting the core at depth and squeezing pore water in the laboratory, ions can equilibrate between water and sediment so that the interstitial water chemistry obtained may not represent the geochemistry *in situ*. Pressure and temperature differences as well as sea water drilling fluid contamination can exaggerate these effects. The *in situ* water sampler eliminates these problems because it is shoved into the sediment at the bottom of the hole. Interstitial water is then taken, sealed, and brought to the surface.

Because the interstitial water ions are the "soup" in which sediment diagenesis takes place, obtaining valid

analyses on samples taken at *in situ* temperatures and pressures is valuable to understanding the geochemistry and chemical diagenesis in sea floor sediments.

The results of analyses of both laboratory-squeezed and *in situ* interstitial water are shown in Figure 9. Figure 9 shows that alkalinity was high (nine times that of sea water) from 35 to 80 meters and then gradually decreased to hole bottom. However, its level throughout the hole remained at least twice that of surface sea water values. This parameter provided a convenient way to monitor proper functioning of the *in situ* sampler. As Figure 9 shows, the *in situ* samples have the same decreasing trend with depth as the laboratory samples. However, the *in situ* samples show about 2 meq/l more alkalinity than the laboratory samples. Two other unsuccessful attempts to use the *in situ* sampler were made at 65 meters and 141 meters. Low alkalinity showed these samples to be sea water.

Calcium shows an increase with depth, whereas magnesium decreases. This type of trend has been observed at other DSDP sites with similar deposition rates (about 5 cm/10³ years, 0–200 m) (Sayles and Manheim, 1975). Salinity and chlorinity are both higher at depth than at the surface. Similar trends have been observed at other sites containing volcanic debris (Sayles and Manheim, 1975). *In situ* water values generally show the same trends as the normal samples, with the values of *in situ* water generally showing a greater difference from those of surface water.

All chemical parameters for Core 40 (378 m) from Site 436 are anomalous in comparison to the rest of the hole. The sediment is a brownish-black clay which first appears, with a dramatic sediment color change, in Core 39. Small manganese nodules and fish teeth are evident in the sediment. The deposition rate has been estimated to be lower here than in the rest of the hole. Interstitial water values show a drop in both pH and alkalinity. These changes may be related to mineral diagenesis, because salinity, chlorinity, magnesium, and calcium all increase. In particular, calcium rises to a value of twice that seen anywhere else in this hole. It may be significant that these changes occur just above a chert layer.

We found one peculiarity in the interstitial water analysis of calcium in some of the samples that may be relevant to the presence of other unanalyzed metal ions: An "interference" was noted periodically, particularly in Core 40. Using the method of Tsunogai, Nishimura, and Nakaya (1968), the presence of calcium is indicated by a color change from pink to colorless upon titration with ethylene bis (oxyethylenenitrile) tetra-acetic acid (EGTA) in the presence of 2,2'-ethane-diyldene dinitrilodiphenol (GHA) indicator. In our analysis a yellow color formed in the mixture before titration, interfering with detection of the color change. Because we know diphenols to be prone to oxidation by such agents as transition metals to give quinones, which are usually colored (see, for example, Fieser and Fieser, 1961), and because there is other evidence of extensive manganese in this sediment the presence of manganese in one of its higher oxidation states is consistent with the interference.

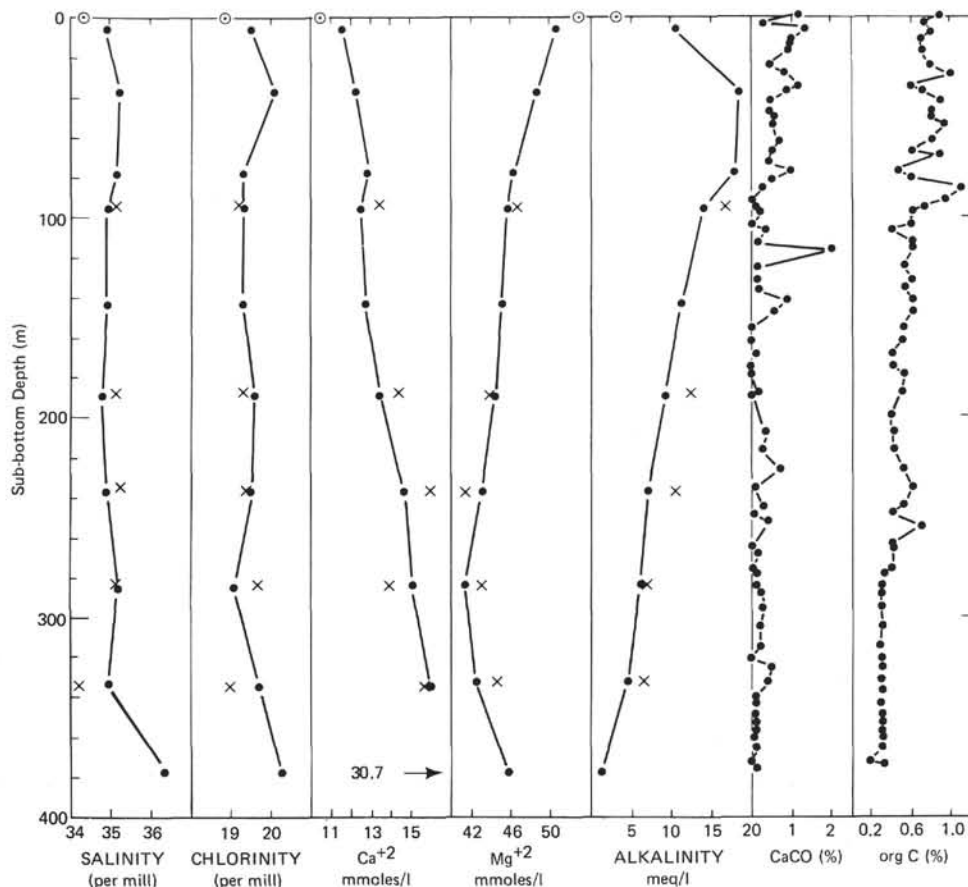


Figure 9. Interstitial water analysis (alkalinity, chlorinity, salinity, and calcium and magnesium) and sediment organic carbon and calcium carbonate. (× = in situ water samples, ● = normal samples, and ○ = surface sea water.)

Organic Chemistry

No methane was detected in Hole 436. Only a few cores (at about 200–300 m) showed any gas pressure upon standing. The Carle gas chromatograph indicated that this gas consisted of air or air enriched with nitrogen. The total absence of methane is puzzling, because Holes 434 and 435, which have very similar lithologies, contained biogenic methane. The deposition rate in this hole (about 5 cm/1000 yr at 0–200 m and about 2.5 cm/1000 yr at 250–300 m) is comparable to that found in the upper sections of the other two holes. Organic carbon content (Figure 9) from 0 to 200 meters is lower (0.4%–0.8%) than at the other sites and drops to below 0.4 per cent in Core 11, at about 100 meters. This is about the depth at which CH_4 production usually begins in other DSDP sites. Thus, absence of CH_4 is probably due to insufficient carbon for microbial growth. The carbon may have been used up by sulfate-reducing bacteria in the top 100 meters, so that sulfate reduction never yields to deeper bacterial methane production. The presence of pyrite throughout this hole—particularly as black bands below volcanic ash beds—the decrease of organic carbon with depth, and the high interstitial water alkalinity values are all consistent with the occurrence of microbial reduction of sulfate to sulfide through

the hole. In addition, the organic matter below 100 meters may be more reworked and refractory and not as good for a microbial diet as material in Holes 434 and 435. This seems unlikely in the top part of the holes, because both organic input (diatoms) and deposition rates are comparable for the three sites. However, fecal pellets and manganese-encrusted fish teeth are common in the top 100 meters of Hole 436 (see Thompson and Whelan, this volume). The source of the fecal pellets is unknown but could be burrowing bottom feeders, such as benthic worms. The presence of the burrowers and small manganese nodules indicates a more oxic depositional environment, which should result in more refractory organic material.

Pyrolysis-fluorescence data are plotted versus organic carbon in Figure 10. The fluorescence is low and shows considerable scatter. Qualitatively, these values are diagnostic of refractory organic material (see Ryan and von Rad, 1979, for description of the technique, and Site 434 chapter, this volume, for further description of the meaning of the data).

REFERENCES

- Boyce, R. E., 1976. Definitions and laboratory techniques of compressional sound velocity parameters and wet-water

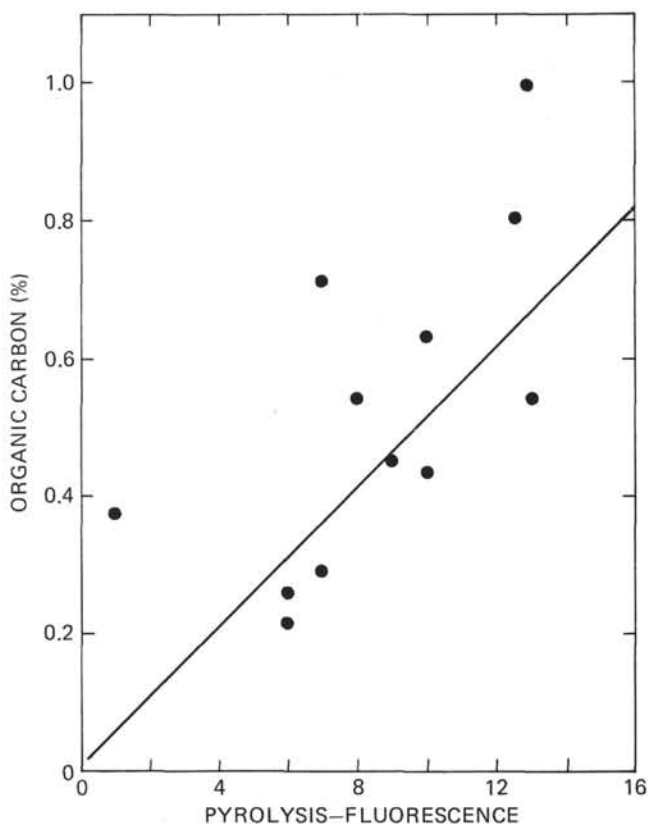


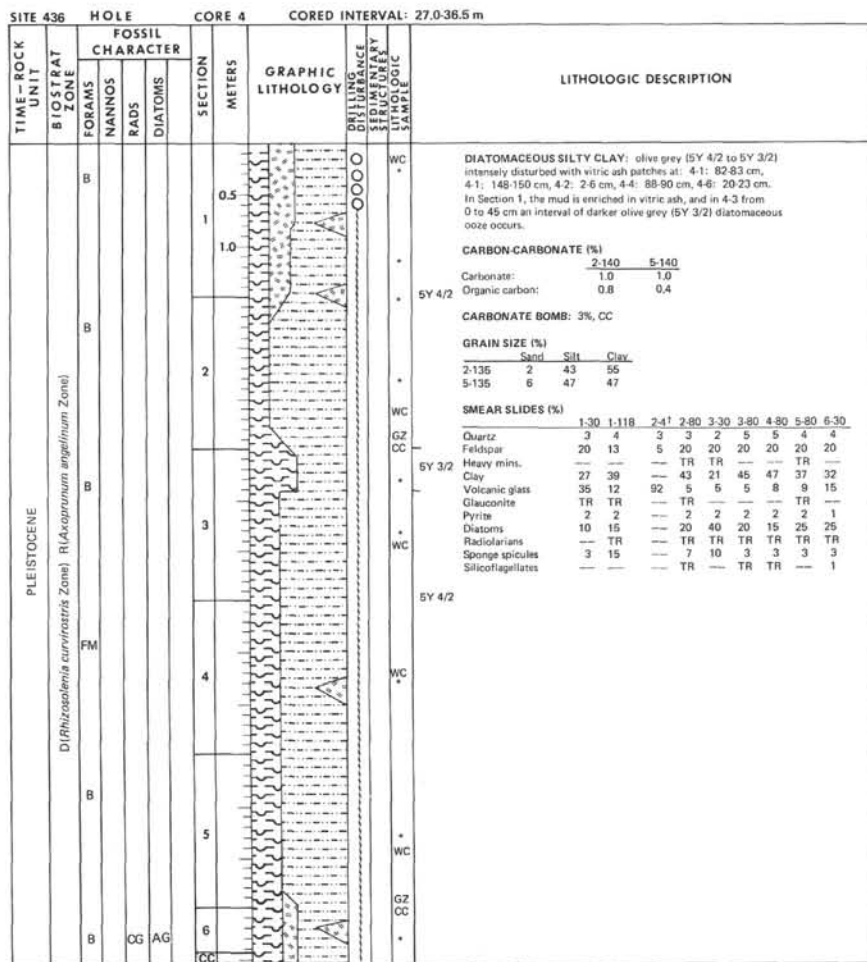
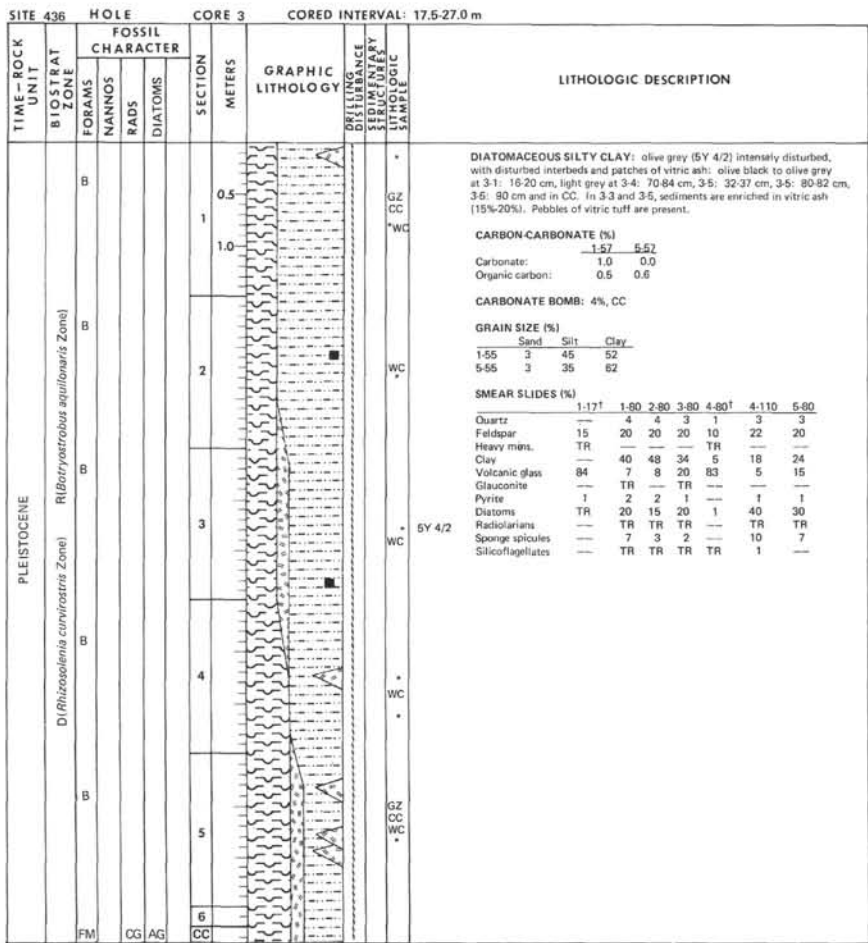
Figure 10. Organic carbon pyrolysis-fluorescence versus organic carbon content for Hole 436. (Pyrolysis-fluorescence is measured in fluorescence units per 3 ml of solvent per 0.1 g of sediment.)

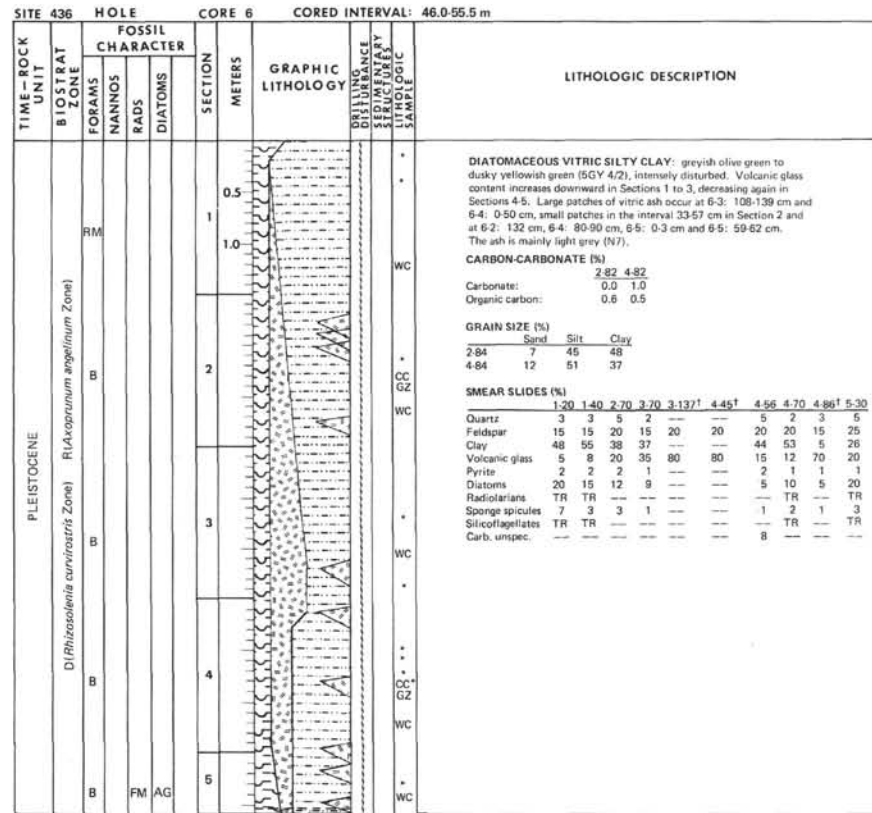
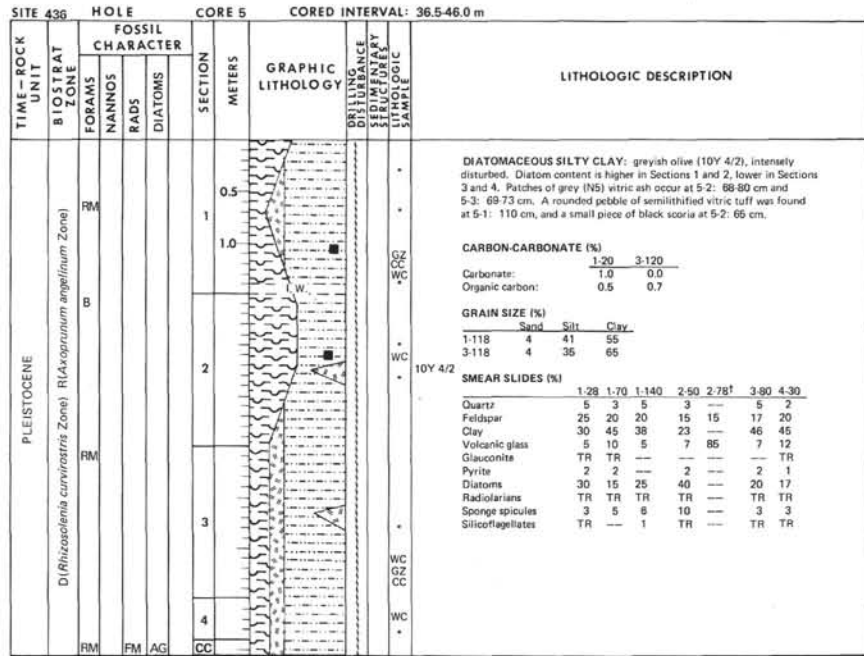
content, wet-bulk density, and porosity parameters by gravimetric and gamma ray attenuation techniques. In Schlanger, S. O., Jackson, E. D., et al., *Init. Repts. DSDP*, 33: Washington (U.S. Govt. Printing Office), 931-958.

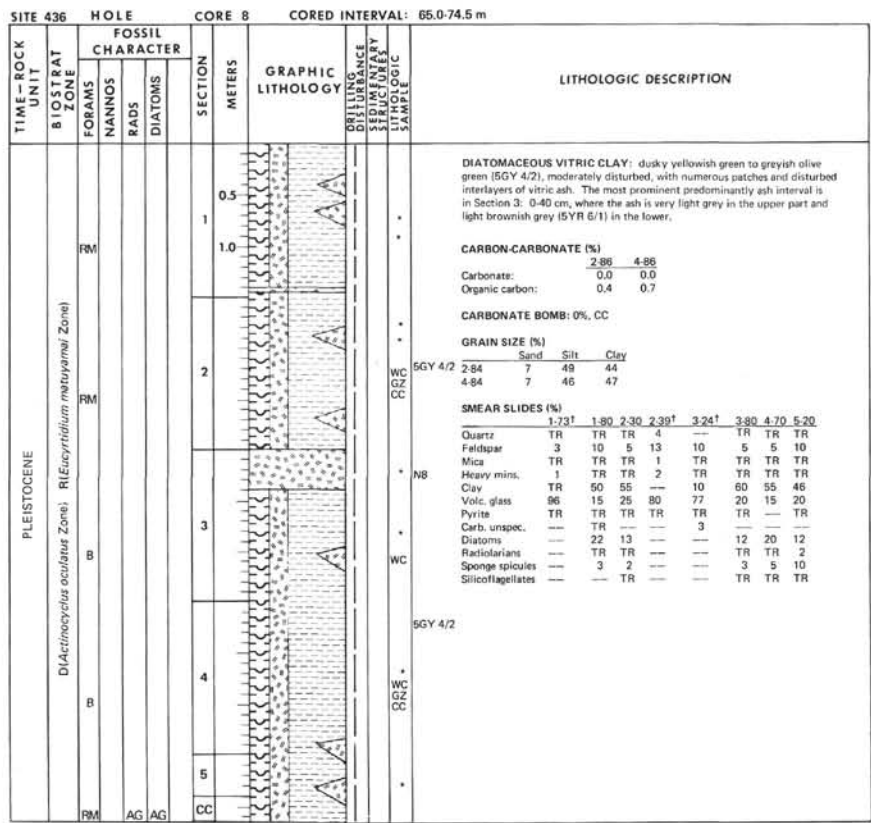
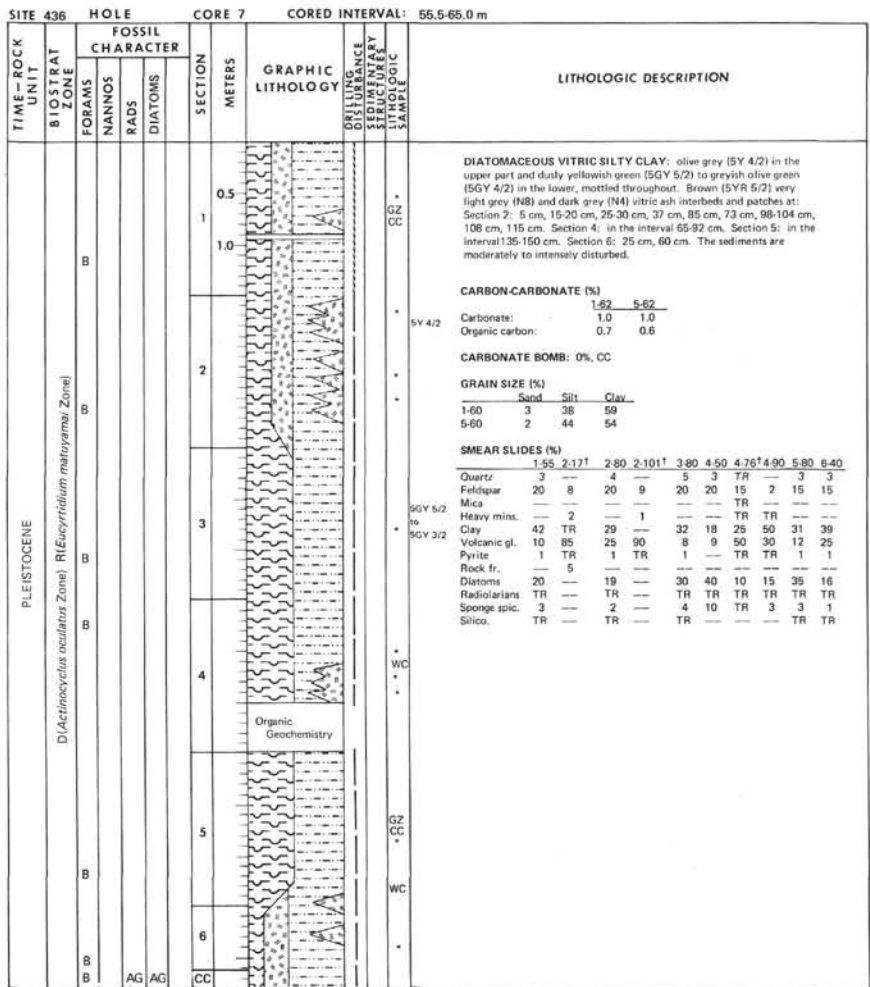
- Fieser, L. F., and Fieser, M., 1961. *Advanced Organic Chemistry*: New York (Reinhold), pp. 845-851.
- Hilde, T. W. C., Isezaki, N., and Wageman, J. M., 1976. Mesozoic sea-floor spreading in the North Pacific. *Geophys. Monogr. 19*, Amer. Geophys. Union, 205-226.
- Honza, E. (Ed.), 1977. Geological investigation of Japan and southern Kuril Trench and slope areas. GH-76-2 Cruise. *Geol. Surv. Japan, Cruise Rept.*, 7, 1-127.
- Lancelot, Y., and Larson, R. L., 1975. Sedimentary and tectonic evolution of the northwestern Pacific. In Larson, R. L., Moberly, R., et al., *Init. Repts. DSDP*, 32: Washington (U.S. Govt. Printing Office), 38.
- Larson, R. L., and Chase, C. G., 1972. Late Mesozoic evolution of the Western Pacific Ocean. *Geol. Soc. Amer. Bull.*, 83, 3627-3644.
- Nasu, N., and Kobayashi, K., 1980. *Preliminary Report of the Hokuho Maru Cruise KH-77-1 (IPOD Site Survey)*. Ocean Research Institute, University of Tokyo.
- Ryan, W. B. F., and von Rad, U., 1979. Site 397. In Ryan, W. B. F., von Rad, U., et al., *Init. Repts. DSDP*, 47, Pt. 1: Washington (U.S. Govt. Printing Office), 17-218.
- Sayles, F. L., and Manheim, F. T., 1975. Interstitial solutions and diagenesis in deeply buried marine sediments: Results from the Deep Sea Drilling Project. *Geochim. et Cosmochim. Acta*, 39, 103-127.
- Tsunogai, S., Nishimura, M., and Nakaya, S., 1968. Complexometric titration of calcium in the presence of larger amounts of magnesium. *Talanta*, 15, 385.
- Uyeda, S., Vacquier, V., Yasui, M., Sclater, J., Saito, T., Lawson, J., Watanabe, T., Dixon, F., Silver, E., Fukas, Y., Sud, K., Nishikawa, M., and Tanaka, T., 1967. Results of geomagnetic survey during the cruise of R/V *Argo* in the Western Pacific, 1966, and the compilation of magnetic charts of the same area. *Earthquake Research Institute Bull.* (Tokyo University), 45, 799-814.
- Watts, A. B., and Talwani, M., 1974. Gravity anomalies seaward of deep sea trenches and their tectonic implications. *Geophys. J.*, 36, 57-90.

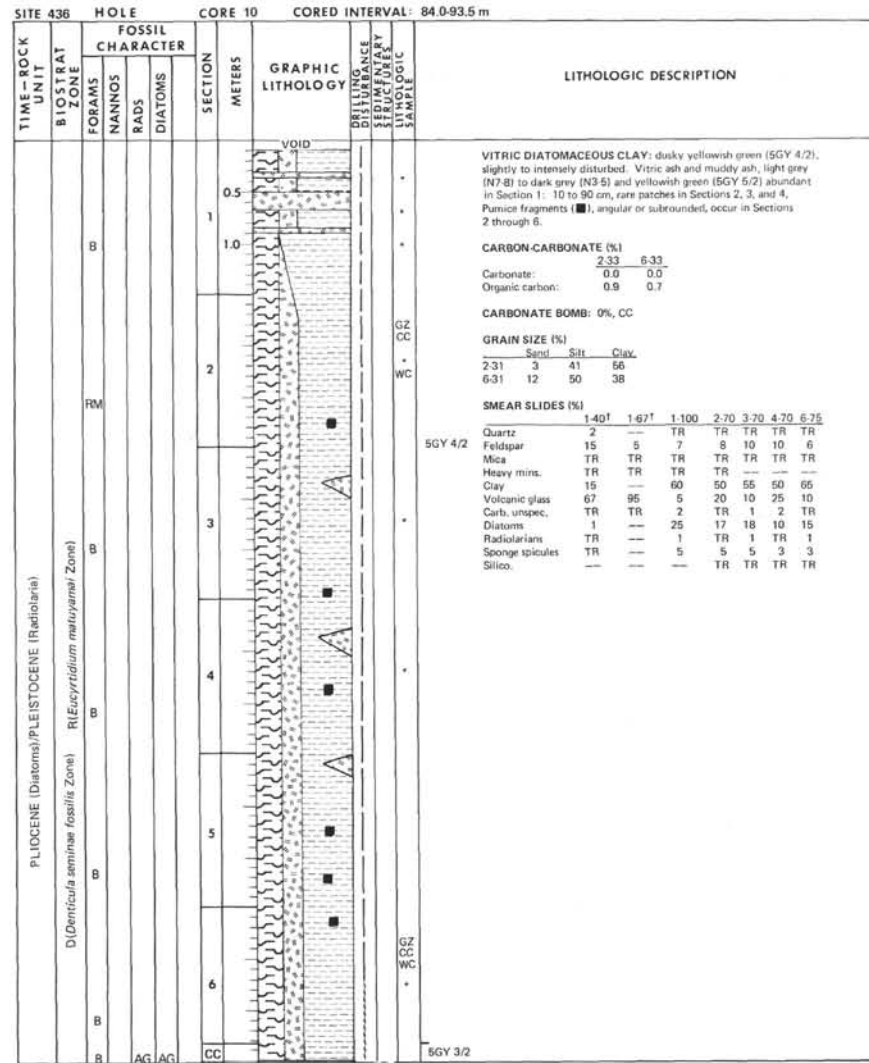
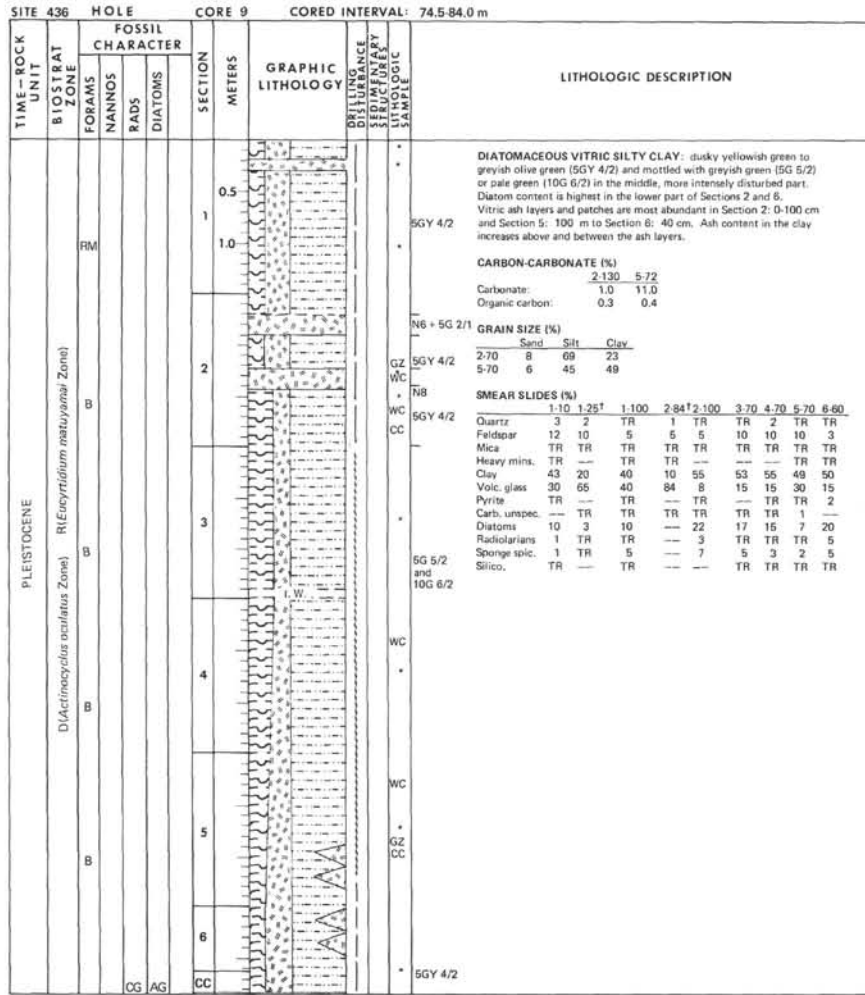
SITE 436		HOLE		CORE 1		CORED INTERVAL: 0.0-8.0 m																																																																																																																																																																						
TIME-ROCK UNIT	BIOSTRAT ZONE	FOSSIL CHARACTER			SECTION METERS	GRAPHIC LITHOLOGY	LITHOLOGIC DESCRIPTION																																																																																																																																																																					
		FORAMS	NANNOS	RADS				DIATOMS																																																																																																																																																																				
PLEISTOCENE	R (<i>Botryostrobus equilonaris</i> Zone)	B			0.5		<p>VITRIC DIATOMACEOUS SILTY CLAY AND DIATOMACEOUS SILTY CLAY: olive grey, (5Y 4/2) to light olive grey, slightly disturbed in Sections 3 through 5, with several vitric ash interbeds and patches at: 1-2: 18-21 cm, 1-2: 82-85 cm, 1-3: 103-105 cm, 1-4: 20 cm, 1-4: 109-111 cm, 1-4: 128-142 cm, 1-5: 14-20 cm, 1-5: 39-46 cm, 1-5: 81-87 cm, 1-5: 100-112 cm. The ash is mainly light grey (NB-N7), in some patches it is olive black or greenish black (pyritized). Both boundaries of ash interbeds are usually sharp.</p> <p>CARBON-CARBONATE (%)</p> <table border="1"> <tr> <td></td> <td>1-52</td> <td>3-52</td> </tr> <tr> <td>Carbonate:</td> <td>1.0</td> <td>0.0</td> </tr> <tr> <td>Organic carbon:</td> <td>0.7</td> <td>0.5</td> </tr> </table> <p>CARBONATE BOMB: 4%, CC</p> <p>GRAIN SIZE (%)</p> <table border="1"> <tr> <td></td> <td>Sand</td> <td>Silt</td> <td>Clay</td> </tr> <tr> <td>1-50</td> <td>4</td> <td>44</td> <td>52</td> </tr> <tr> <td>3-50</td> <td>7</td> <td>52</td> <td>41</td> </tr> </table> <p>SMEAR SLIDES (%)</p> <table border="1"> <tr> <td></td> <td>1-70</td> <td>2-21</td> <td>2-70</td> <td>2-82</td> <td>3-70</td> <td>3-105</td> <td>4-40</td> <td>4-110</td> <td>4-133</td> <td>5-60</td> <td>5-87</td> </tr> <tr> <td>Quartz</td> <td>7</td> <td>4</td> <td>5</td> <td>2</td> <td>1</td> <td>3</td> <td>7</td> <td>1</td> <td>2</td> <td>2</td> <td>5</td> </tr> <tr> <td>Feldspar</td> <td>20</td> <td>8</td> <td>20</td> <td>20</td> <td>25</td> <td>20</td> <td>20</td> <td>—</td> <td>8</td> <td>20</td> <td>20</td> </tr> <tr> <td>Mica</td> <td>—</td> <td>TR</td> <td>—</td> <td>—</td> <td>TR</td> <td>—</td> <td>—</td> <td>—</td> <td>—</td> <td>—</td> <td>—</td> </tr> <tr> <td>H. mins.</td> <td>—</td> <td>TR</td> <td>TR</td> <td>TR</td> <td>—</td> <td>—</td> <td>—</td> <td>—</td> <td>TR</td> <td>—</td> <td>—</td> </tr> <tr> <td>Clay</td> <td>46</td> <td>—</td> <td>41</td> <td>25</td> <td>55</td> <td>34</td> <td>36</td> <td>—</td> <td>—</td> <td>44</td> <td>33</td> </tr> <tr> <td>Volc. g.</td> <td>7</td> <td>87</td> <td>7</td> <td>40</td> <td>7</td> <td>30</td> <td>15</td> <td>88</td> <td>—</td> <td>12</td> <td>30</td> </tr> <tr> <td>Pyrite</td> <td>1</td> <td>1</td> <td>—</td> <td>2</td> <td>1</td> <td>2</td> <td>2</td> <td>1</td> <td>1</td> <td>2</td> <td>3</td> </tr> <tr> <td>Diatoms</td> <td>15</td> <td>—</td> <td>20</td> <td>8</td> <td>9</td> <td>8</td> <td>15</td> <td>—</td> <td>—</td> <td>12</td> <td>5</td> </tr> <tr> <td>Radiolar.</td> <td>TR</td> <td>—</td> <td>TR</td> <td>—</td> <td>—</td> <td>TR</td> <td>TR</td> <td>—</td> <td>—</td> <td>—</td> <td>—</td> </tr> <tr> <td>Sponge s.</td> <td>5</td> <td>—</td> <td>7</td> <td>2</td> <td>3</td> <td>3</td> <td>5</td> <td>—</td> <td>—</td> <td>8</td> <td>4</td> </tr> <tr> <td>Silico.</td> <td>TR</td> <td>—</td> <td>TR</td> <td>TR</td> <td>TR</td> <td>TR</td> <td>TR</td> <td>—</td> <td>—</td> <td>TR</td> <td>—</td> </tr> </table>		1-52	3-52	Carbonate:	1.0	0.0	Organic carbon:	0.7	0.5		Sand	Silt	Clay	1-50	4	44	52	3-50	7	52	41		1-70	2-21	2-70	2-82	3-70	3-105	4-40	4-110	4-133	5-60	5-87	Quartz	7	4	5	2	1	3	7	1	2	2	5	Feldspar	20	8	20	20	25	20	20	—	8	20	20	Mica	—	TR	—	—	TR	—	—	—	—	—	—	H. mins.	—	TR	TR	TR	—	—	—	—	TR	—	—	Clay	46	—	41	25	55	34	36	—	—	44	33	Volc. g.	7	87	7	40	7	30	15	88	—	12	30	Pyrite	1	1	—	2	1	2	2	1	1	2	3	Diatoms	15	—	20	8	9	8	15	—	—	12	5	Radiolar.	TR	—	TR	—	—	TR	TR	—	—	—	—	Sponge s.	5	—	7	2	3	3	5	—	—	8	4	Silico.	TR	—	TR	TR	TR	TR	TR	—	—	TR	—
			1-52	3-52																																																																																																																																																																								
		Carbonate:	1.0	0.0																																																																																																																																																																								
		Organic carbon:	0.7	0.5																																																																																																																																																																								
			Sand	Silt	Clay																																																																																																																																																																							
1-50	4	44	52																																																																																																																																																																									
3-50	7	52	41																																																																																																																																																																									
	1-70	2-21	2-70	2-82	3-70	3-105	4-40	4-110	4-133	5-60	5-87																																																																																																																																																																	
Quartz	7	4	5	2	1	3	7	1	2	2	5																																																																																																																																																																	
Feldspar	20	8	20	20	25	20	20	—	8	20	20																																																																																																																																																																	
Mica	—	TR	—	—	TR	—	—	—	—	—	—																																																																																																																																																																	
H. mins.	—	TR	TR	TR	—	—	—	—	TR	—	—																																																																																																																																																																	
Clay	46	—	41	25	55	34	36	—	—	44	33																																																																																																																																																																	
Volc. g.	7	87	7	40	7	30	15	88	—	12	30																																																																																																																																																																	
Pyrite	1	1	—	2	1	2	2	1	1	2	3																																																																																																																																																																	
Diatoms	15	—	20	8	9	8	15	—	—	12	5																																																																																																																																																																	
Radiolar.	TR	—	TR	—	—	TR	TR	—	—	—	—																																																																																																																																																																	
Sponge s.	5	—	7	2	3	3	5	—	—	8	4																																																																																																																																																																	
Silico.	TR	—	TR	TR	TR	TR	TR	—	—	TR	—																																																																																																																																																																	
				1.0	VOID																																																																																																																																																																							
				2																																																																																																																																																																								
				3																																																																																																																																																																								
				4																																																																																																																																																																								
				5																																																																																																																																																																								

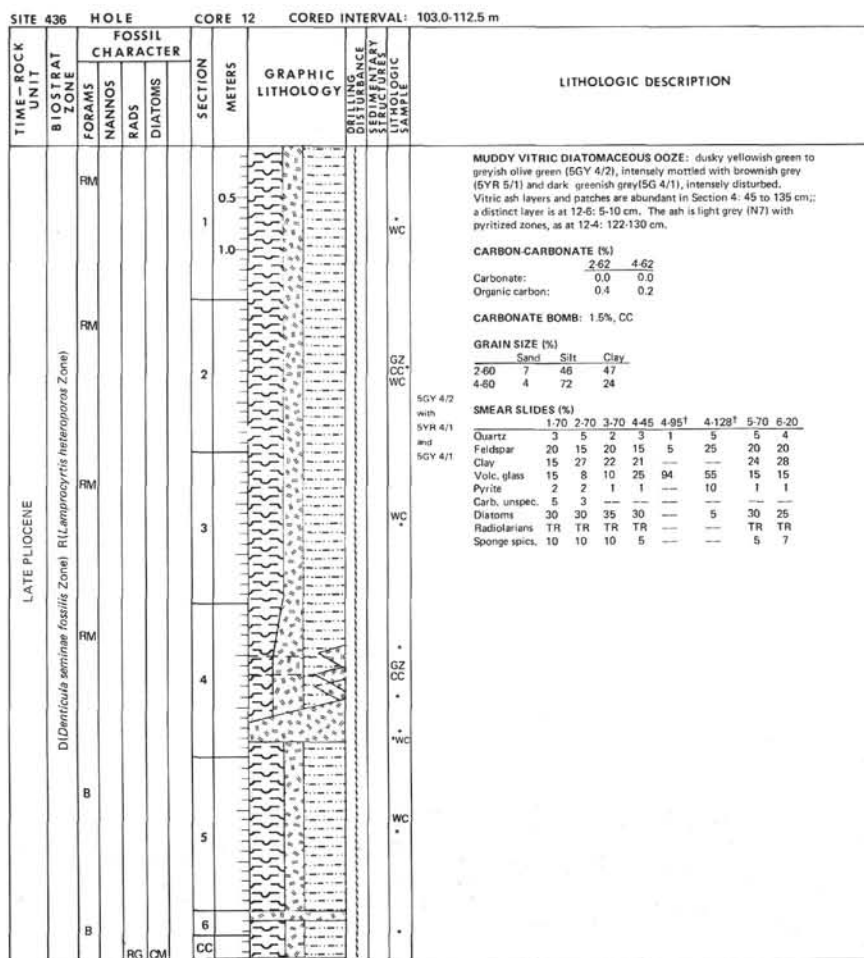
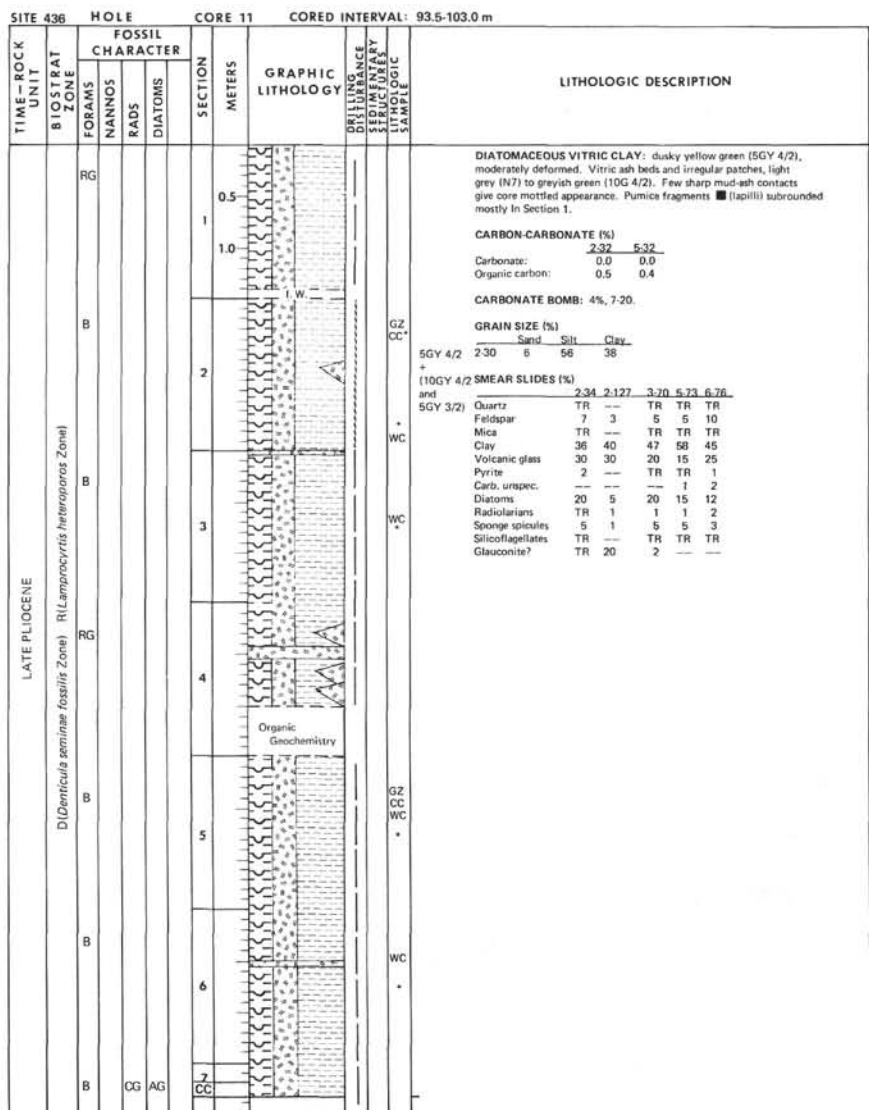
SITE 436		HOLE		CORE 2		CORED INTERVAL: 3.0-17.5 m																																																																																																																						
TIME-ROCK UNIT	BIOSTRAT ZONE	FOSSIL CHARACTER			SECTION METERS	GRAPHIC LITHOLOGY	LITHOLOGIC DESCRIPTION																																																																																																																					
		FORAMS	NANNOS	RADS				DIATOMS																																																																																																																				
PLEISTOCENE	R (<i>Botryostrobus equilonaris</i> Zone)	B			0.5		<p>MUDDY DIATOMACEOUS OOZE: olive grey (5Y 4/2), intensely disturbed, with greenish black (5G 2/1) spots and patches, which contain abundant pyrite. Sponge spicules are abundant in Sections 2 and 3. A rounded pebble of a dark lithic wacke rich in pyrite was found at 2-2: 57 cm. The interval 82-110 is greyish olive green (5GY 4/2).</p> <p>CARBON-CARBONATE (%)</p> <table border="1"> <tr> <td></td> <td>1-82</td> <td>3-12</td> </tr> <tr> <td>Carbonate:</td> <td>1.0</td> <td>1.0</td> </tr> <tr> <td>Organic carbon:</td> <td>0.6</td> <td>0.5</td> </tr> </table> <p>GRAIN SIZE (%)</p> <table border="1"> <tr> <td></td> <td>Sand</td> <td>Silt</td> <td>Clay</td> </tr> <tr> <td>1-80</td> <td>10</td> <td>38</td> <td>52</td> </tr> <tr> <td>3-10</td> <td>5</td> <td>48</td> <td>47</td> </tr> </table> <p>SMEAR SLIDES (%)</p> <table border="1"> <tr> <td></td> <td>1-61</td> <td>1-65</td> <td>1-99</td> <td>2-50</td> <td>2-70</td> <td>3-50</td> <td>3-90</td> </tr> <tr> <td>Quartz</td> <td>3</td> <td>3</td> <td>2</td> <td>7</td> <td>3</td> <td>5</td> <td>3</td> </tr> <tr> <td>Feldspar</td> <td>16</td> <td>20</td> <td>15</td> <td>25</td> <td>20</td> <td>15</td> <td>20</td> </tr> <tr> <td>Heavy mins.</td> <td>—</td> <td>—</td> <td>—</td> <td>TR</td> <td>—</td> <td>—</td> <td>—</td> </tr> <tr> <td>Clay</td> <td>9</td> <td>27</td> <td>20</td> <td>23</td> <td>14</td> <td>27</td> <td>25</td> </tr> <tr> <td>Volcanic glass</td> <td>4</td> <td>8</td> <td>8</td> <td>TR</td> <td>7</td> <td>10</td> <td>15</td> </tr> <tr> <td>Glaucinite</td> <td>—</td> <td>—</td> <td>—</td> <td>TR</td> <td>—</td> <td>—</td> <td>—</td> </tr> <tr> <td>Pyrite</td> <td>25</td> <td>2</td> <td>—</td> <td>5</td> <td>1</td> <td>2</td> <td>2</td> </tr> <tr> <td>Diatoms</td> <td>40</td> <td>35</td> <td>35</td> <td>35</td> <td>35</td> <td>30</td> <td>35</td> </tr> <tr> <td>Radiolarians</td> <td>TR</td> <td>TR</td> <td>TR</td> <td>TR</td> <td>TR</td> <td>TR</td> <td>TR</td> </tr> <tr> <td>Sponge spicules</td> <td>3</td> <td>5</td> <td>20</td> <td>5</td> <td>20</td> <td>10</td> <td>10</td> </tr> <tr> <td>Silicoflagellates</td> <td>—</td> <td>TR</td> <td>TR</td> <td>—</td> <td>TR</td> <td>1</td> <td>—</td> </tr> </table>		1-82	3-12	Carbonate:	1.0	1.0	Organic carbon:	0.6	0.5		Sand	Silt	Clay	1-80	10	38	52	3-10	5	48	47		1-61	1-65	1-99	2-50	2-70	3-50	3-90	Quartz	3	3	2	7	3	5	3	Feldspar	16	20	15	25	20	15	20	Heavy mins.	—	—	—	TR	—	—	—	Clay	9	27	20	23	14	27	25	Volcanic glass	4	8	8	TR	7	10	15	Glaucinite	—	—	—	TR	—	—	—	Pyrite	25	2	—	5	1	2	2	Diatoms	40	35	35	35	35	30	35	Radiolarians	TR	Sponge spicules	3	5	20	5	20	10	10	Silicoflagellates	—	TR	TR	—	TR	1	—						
			1-82	3-12																																																																																																																								
		Carbonate:	1.0	1.0																																																																																																																								
Organic carbon:	0.6	0.5																																																																																																																										
	Sand	Silt	Clay																																																																																																																									
1-80	10	38	52																																																																																																																									
3-10	5	48	47																																																																																																																									
	1-61	1-65	1-99	2-50	2-70	3-50	3-90																																																																																																																					
Quartz	3	3	2	7	3	5	3																																																																																																																					
Feldspar	16	20	15	25	20	15	20																																																																																																																					
Heavy mins.	—	—	—	TR	—	—	—																																																																																																																					
Clay	9	27	20	23	14	27	25																																																																																																																					
Volcanic glass	4	8	8	TR	7	10	15																																																																																																																					
Glaucinite	—	—	—	TR	—	—	—																																																																																																																					
Pyrite	25	2	—	5	1	2	2																																																																																																																					
Diatoms	40	35	35	35	35	30	35																																																																																																																					
Radiolarians	TR	TR	TR	TR	TR	TR	TR																																																																																																																					
Sponge spicules	3	5	20	5	20	10	10																																																																																																																					
Silicoflagellates	—	TR	TR	—	TR	1	—																																																																																																																					
				1.0																																																																																																																								
				2																																																																																																																								
				3																																																																																																																								

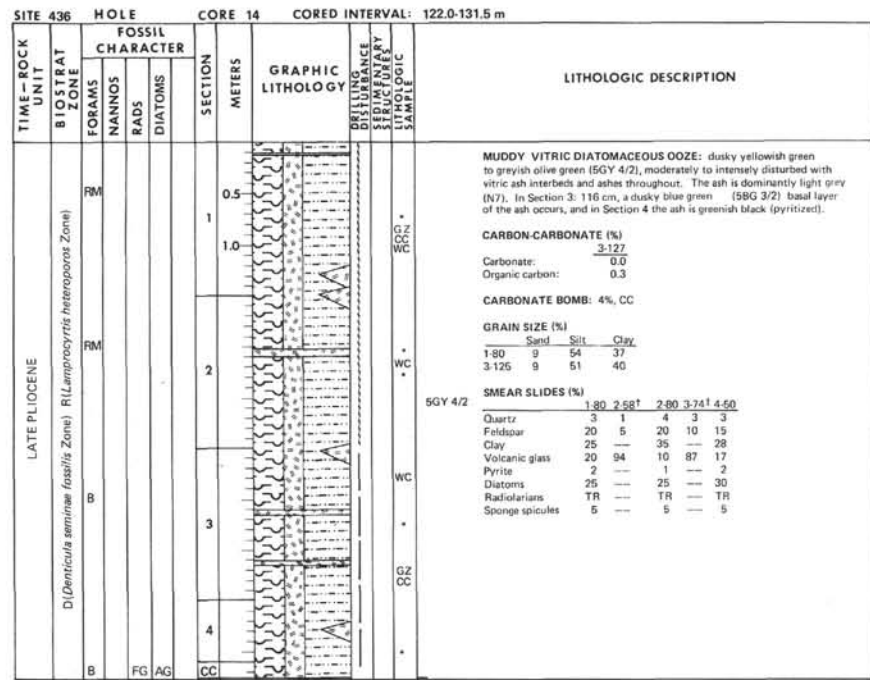
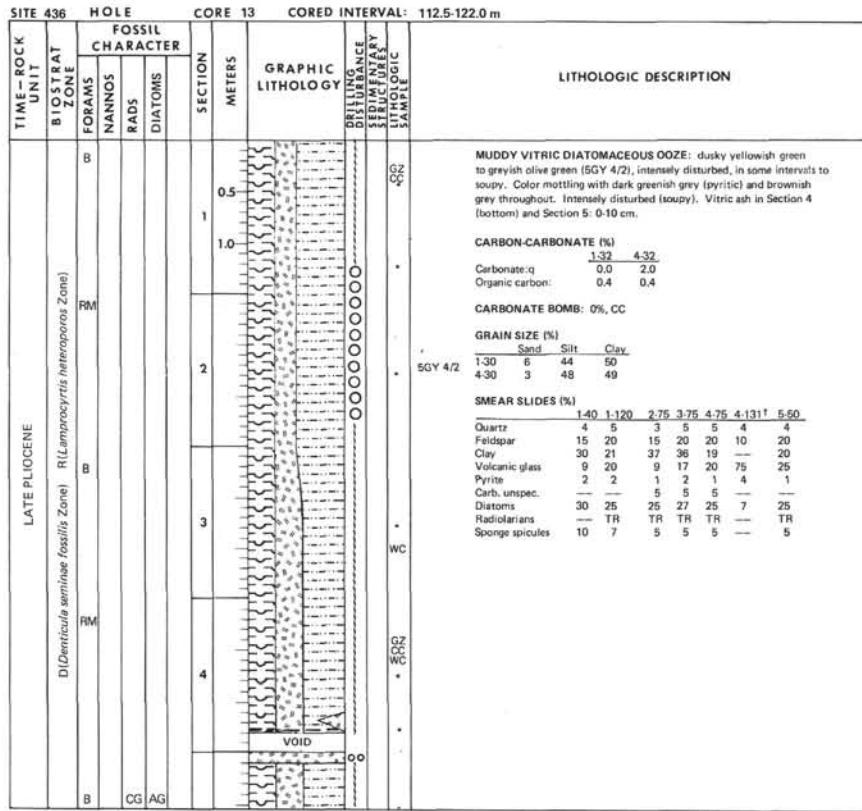


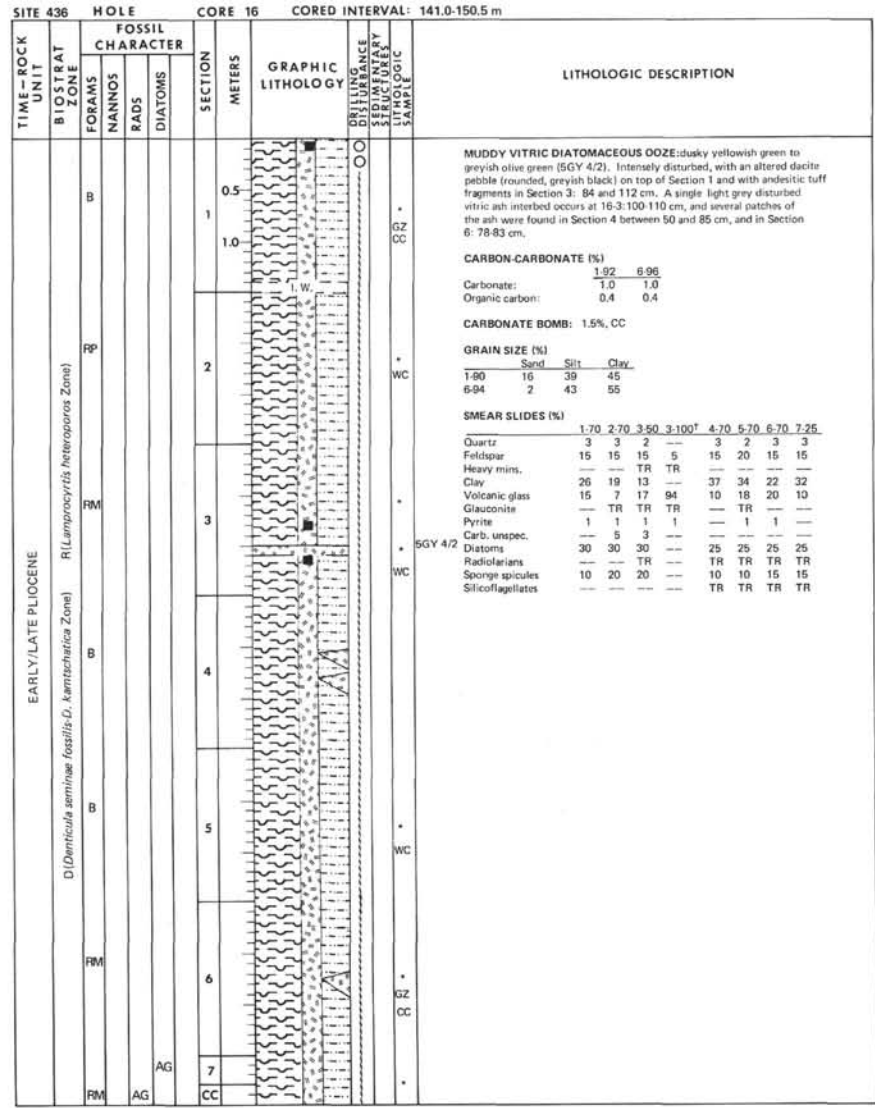
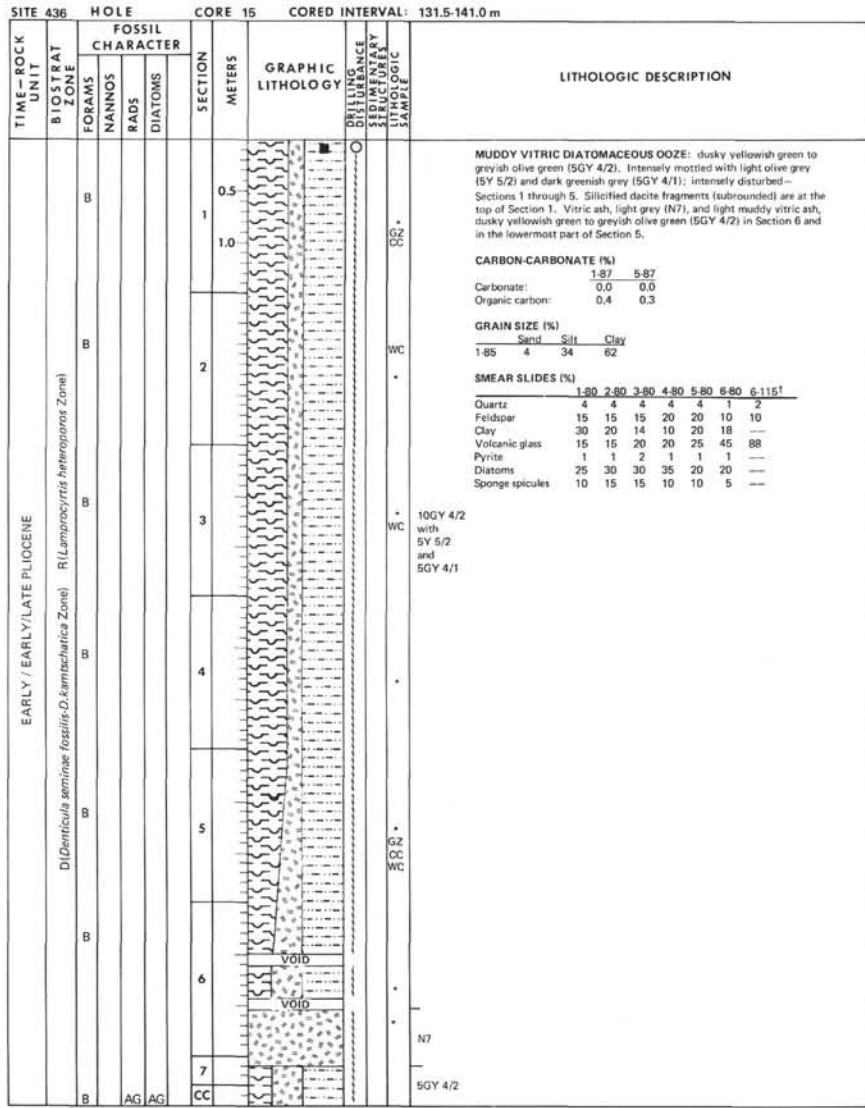


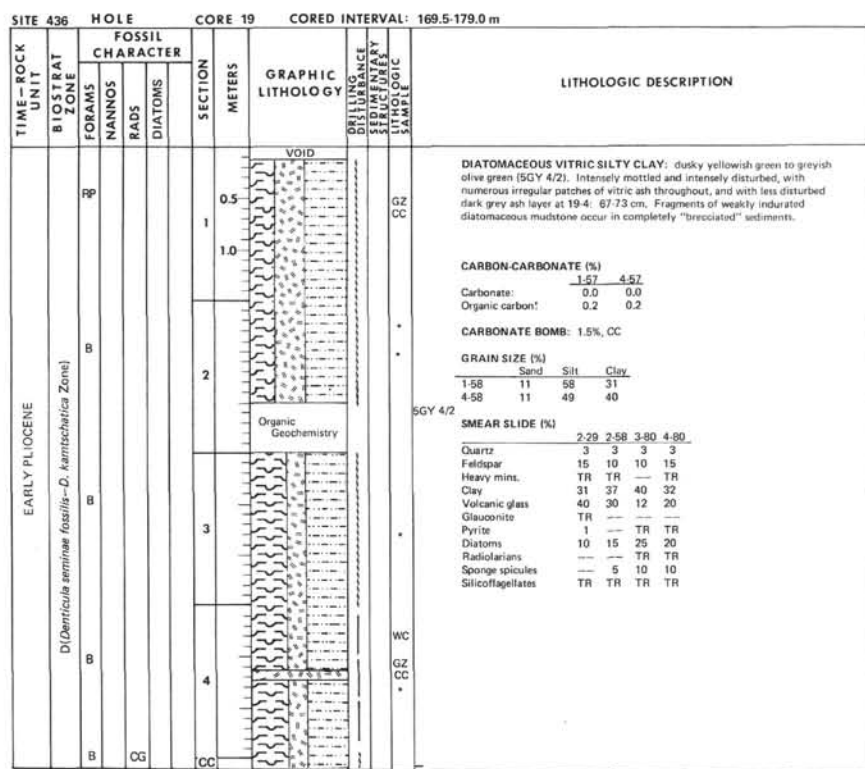
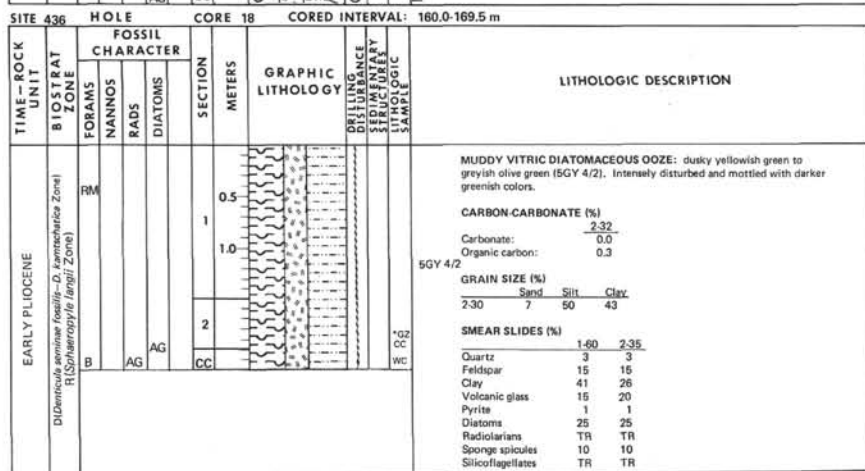
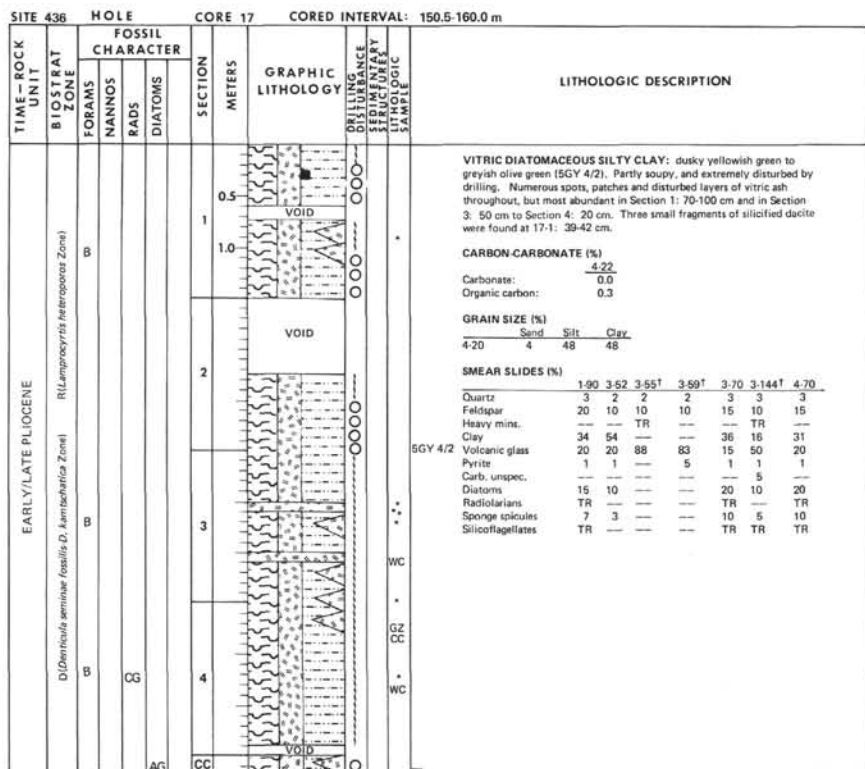


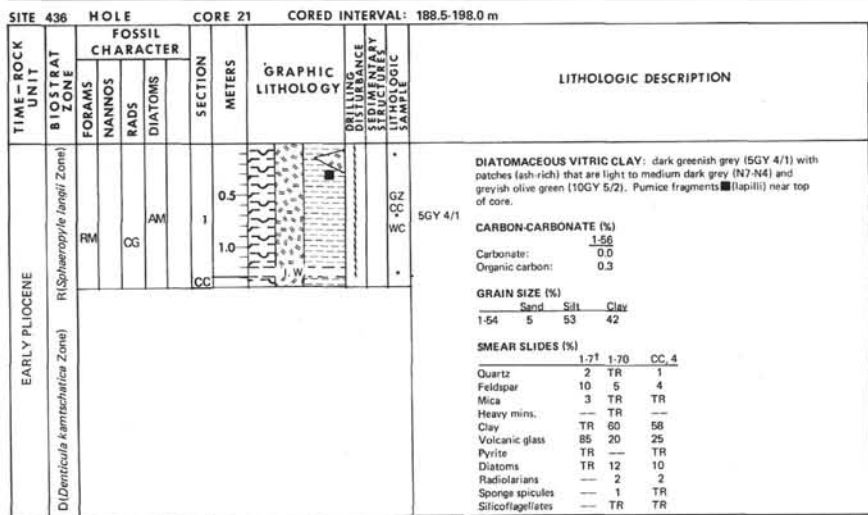
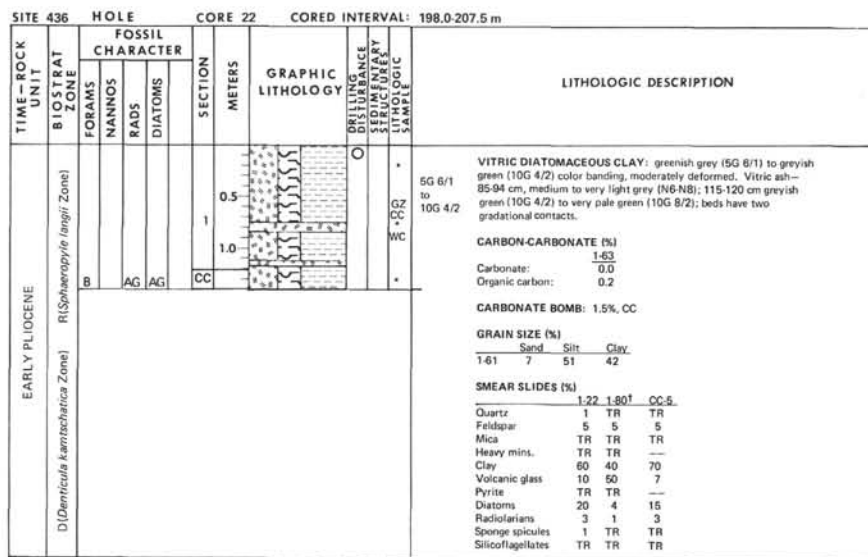
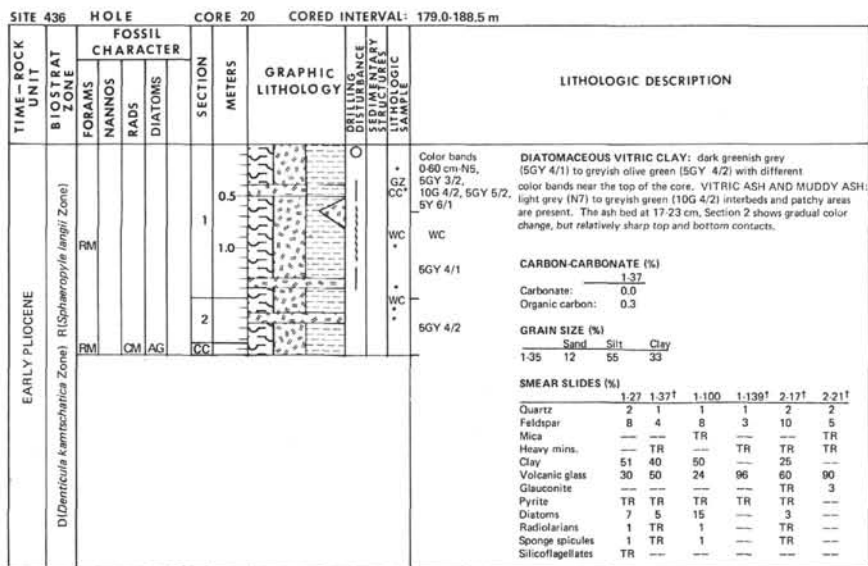


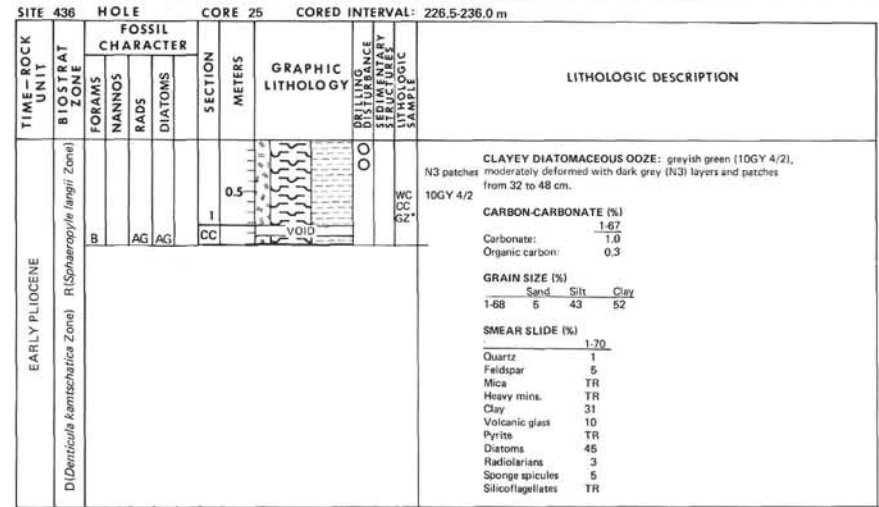
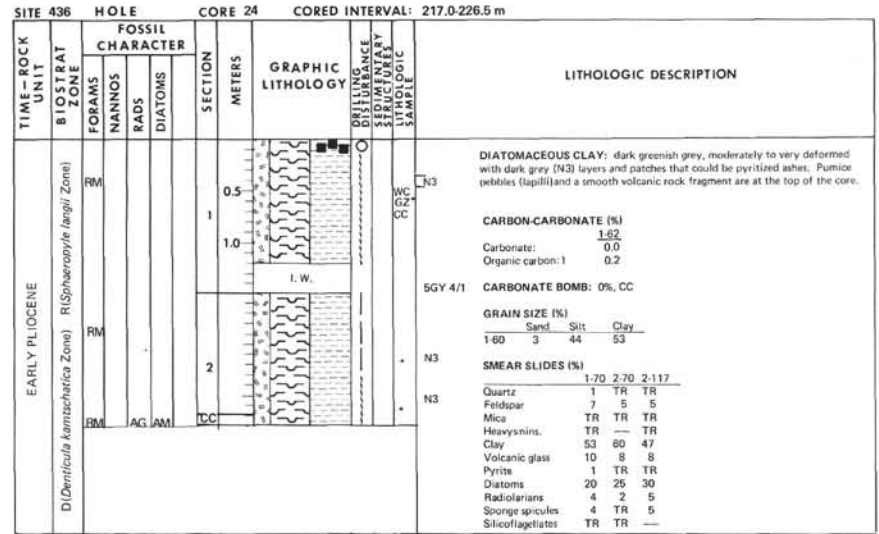
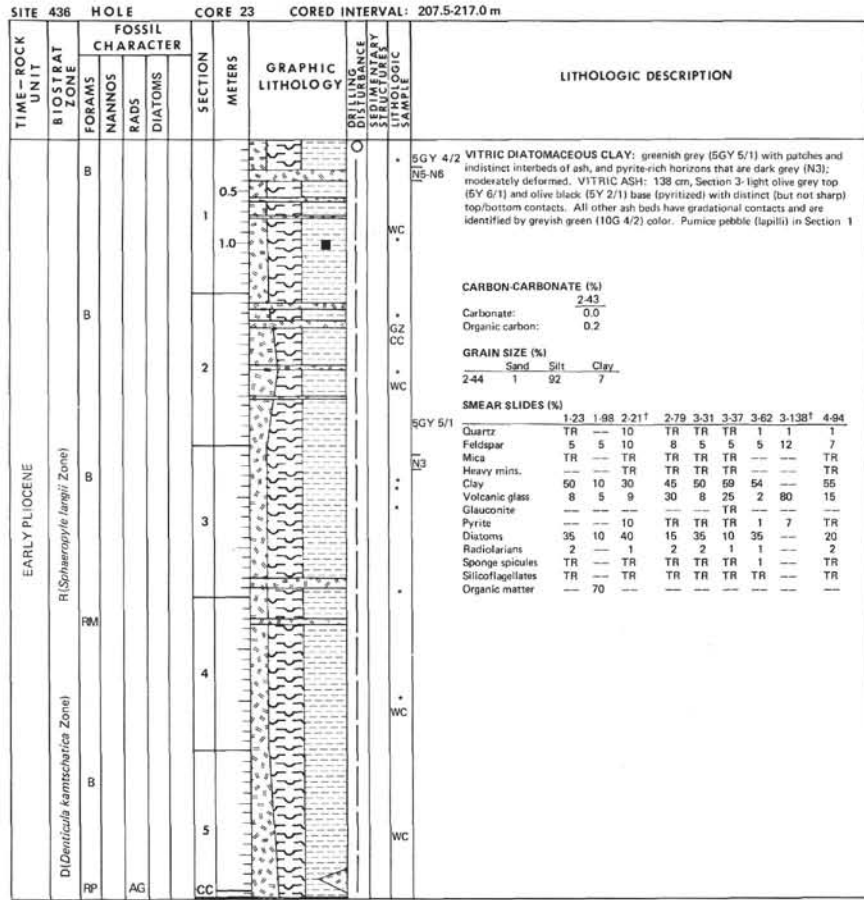










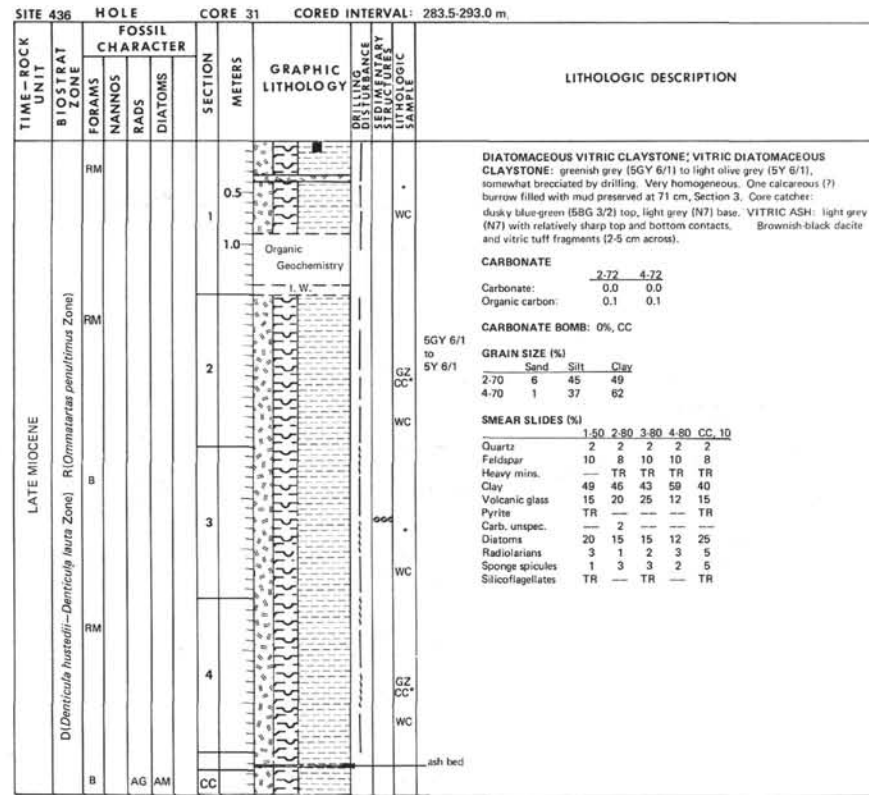
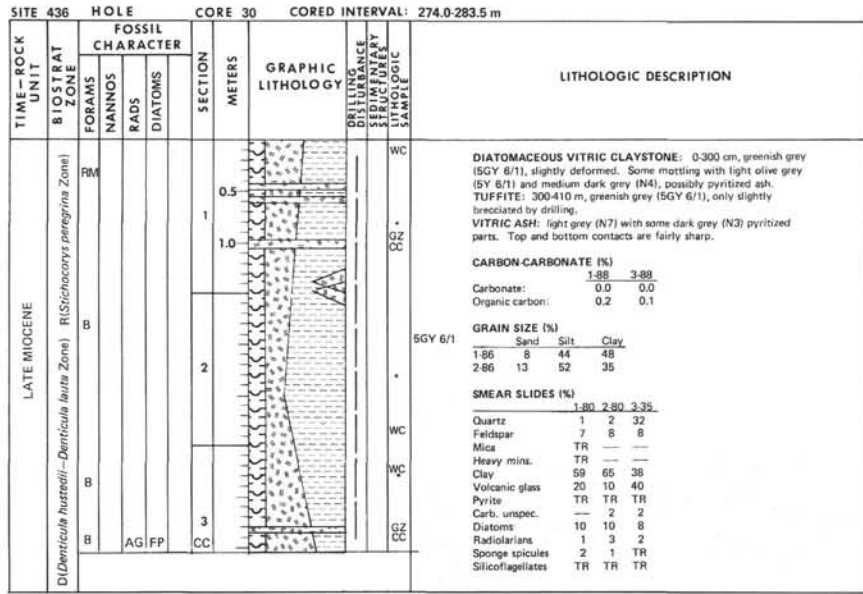


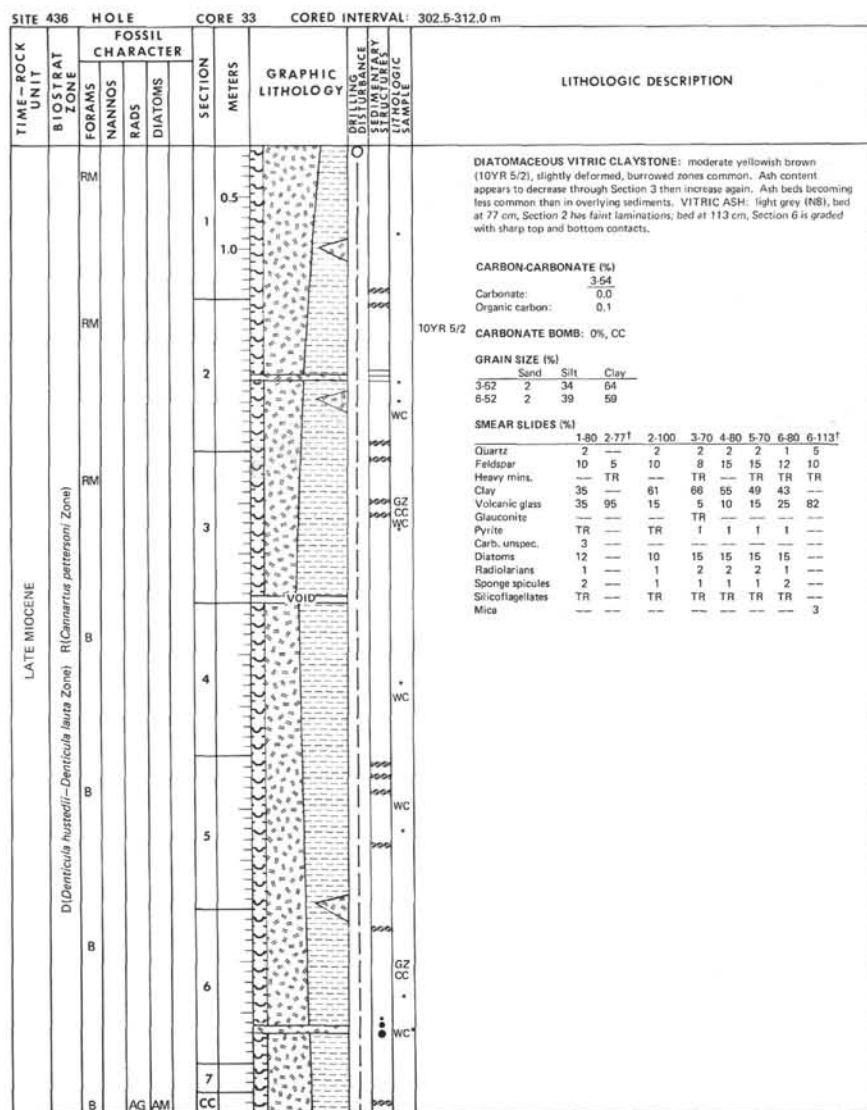
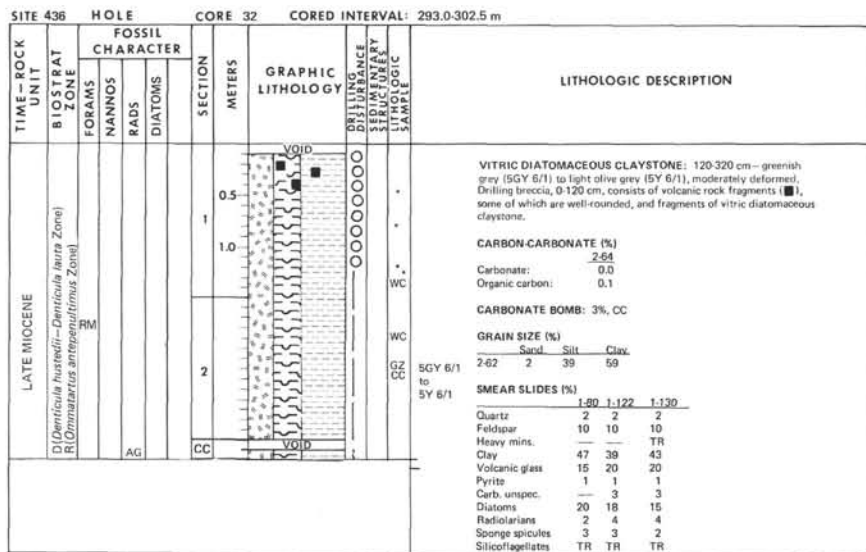
SITE 436		HOLE			CORE 26		CORED INTERVAL: 236.0-245.5 m			
TIME-ROCK UNIT	BIOSTRAT ZONE	FOSSIL CHARACTER			SECTION METERS	GRAPHIC LITHOLOGY	DRILLING DISTURBANCE	SEDIMENTARY STRUCTURE	LITHOLOGIC SAMPLE	LITHOLOGIC DESCRIPTION
		FORAMS	NANNOS	RADS						
LATE MIOGENE	R(Sphaeropyle langii Zone)	B		AG AG	0.5				5G 5/1 to 5G 4/1	CLAYEY ASH grades downward to DIATOMACEOUS CLAY: greenish grey (5G 5/1) to dark greenish grey (5G 4/1), very deformed. Ash-rich patch at 16 cm. CARBON-CARBONATE (%) Carbonate: 1.27 Organic carbon: 0.0 0.4 CARBONATE BOMB: 0%, CC GRAIN SIZE (%) Sand Silt Clay 1-25 1 35 64 SMEAR SLIDES (%) 1-16 1-40 Quartz 2 2 Feldspar 7 10 Clay 49 44 Volcanic glass 32 8 Pyrite 1 1 Carb. unsp. — 5 Diatoms 9 30 Radiolarians TR TR Sponge spicules TR TR Silicoflagellates TR TR

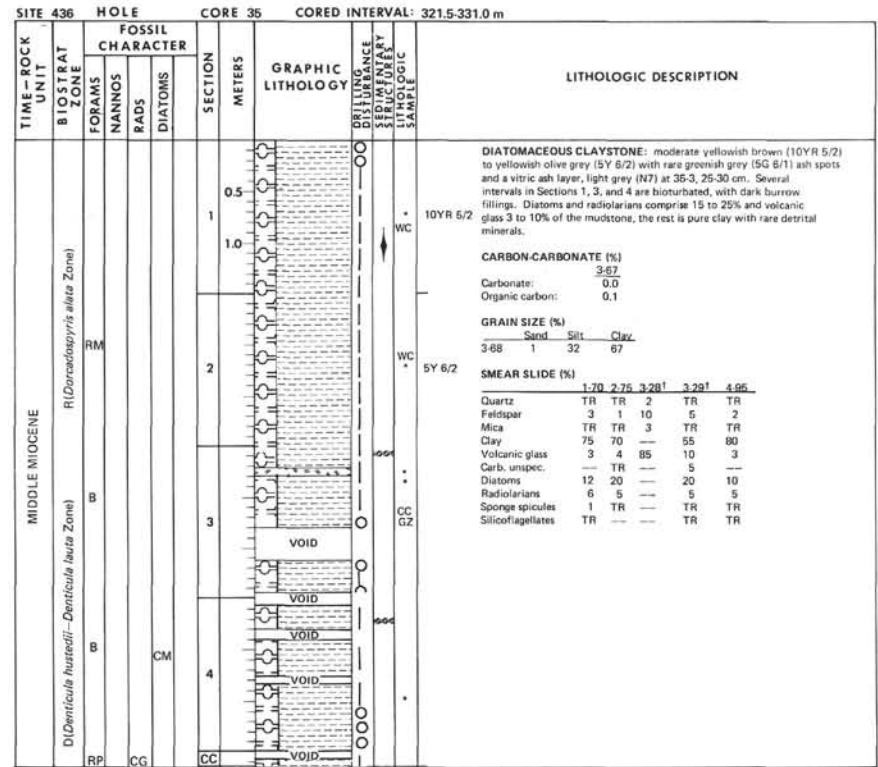
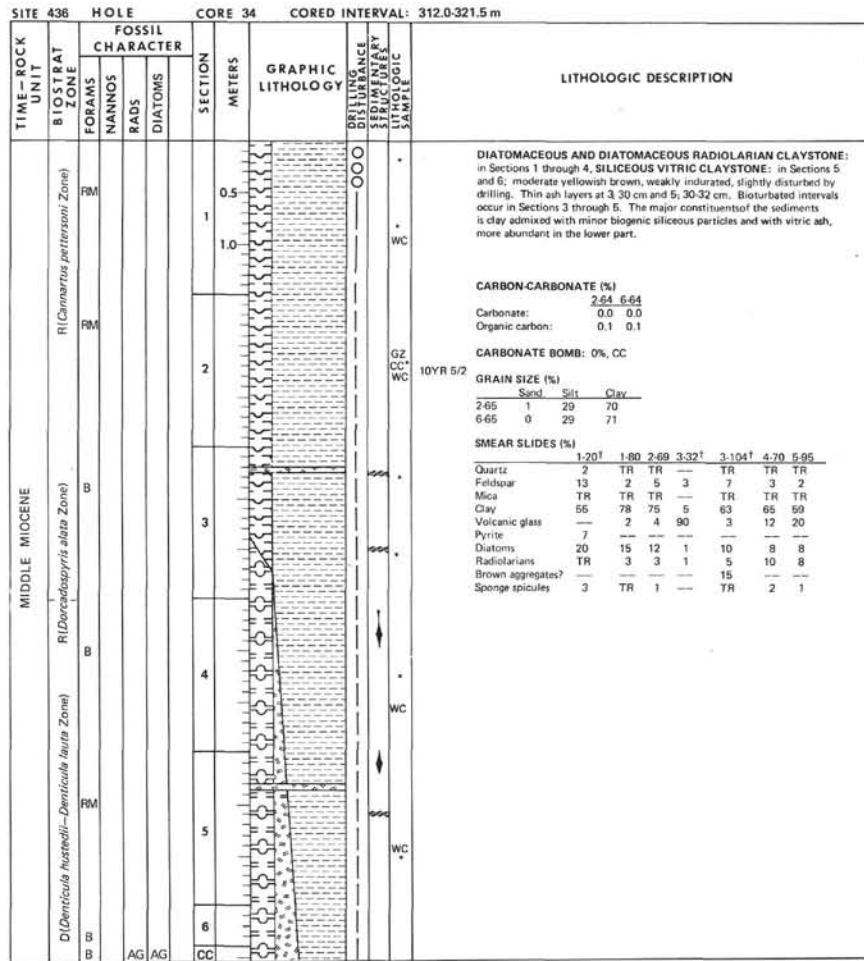
SITE 436		HOLE			CORE 28		CORED INTERVAL: 255.0-264.5 m			
TIME-ROCK UNIT	BIOSTRAT ZONE	FOSSIL CHARACTER			SECTION METERS	GRAPHIC LITHOLOGY	DRILLING DISTURBANCE	SEDIMENTARY STRUCTURE	LITHOLOGIC SAMPLE	LITHOLOGIC DESCRIPTION
		FORAMS	NANNOS	RADS						
LATE MIOGENE	R(Sphaeropyle langii Zone)	B		AG AM	1.0				5G 6/1 with 5G 6/1 mottling	CLAYSTONE: greenish grey (5G 6/1) with light olive grey mottling (5G 6/1). Deformation is slight to moderate except near top of core. Secondary pyrite stains (?) resembling cross-beds at 43-45 cm. 35-68 cm; brownish black (5YR 2/1) concretion about 2.5 x 2.0 cm. CARBON-CARBONATE (%) Carbonate: 1.82 Organic carbon: 0.0 0.5 CARBONATE BOMB: 0%, CC GRAIN SIZE (%) Sand Silt Clay 1-80 2 38 60 smeared slides (%) 1-40 1-73 Quartz 2 3 Feldspar 15 12 Clay 65 66 Volcanic glass 5 8 Pyrite 1 TR Carb. unsp. 3 2 Diatoms 8 8 Radiolarians TR TR Sponge spicules 1 1 Silicoflagellates TR TR

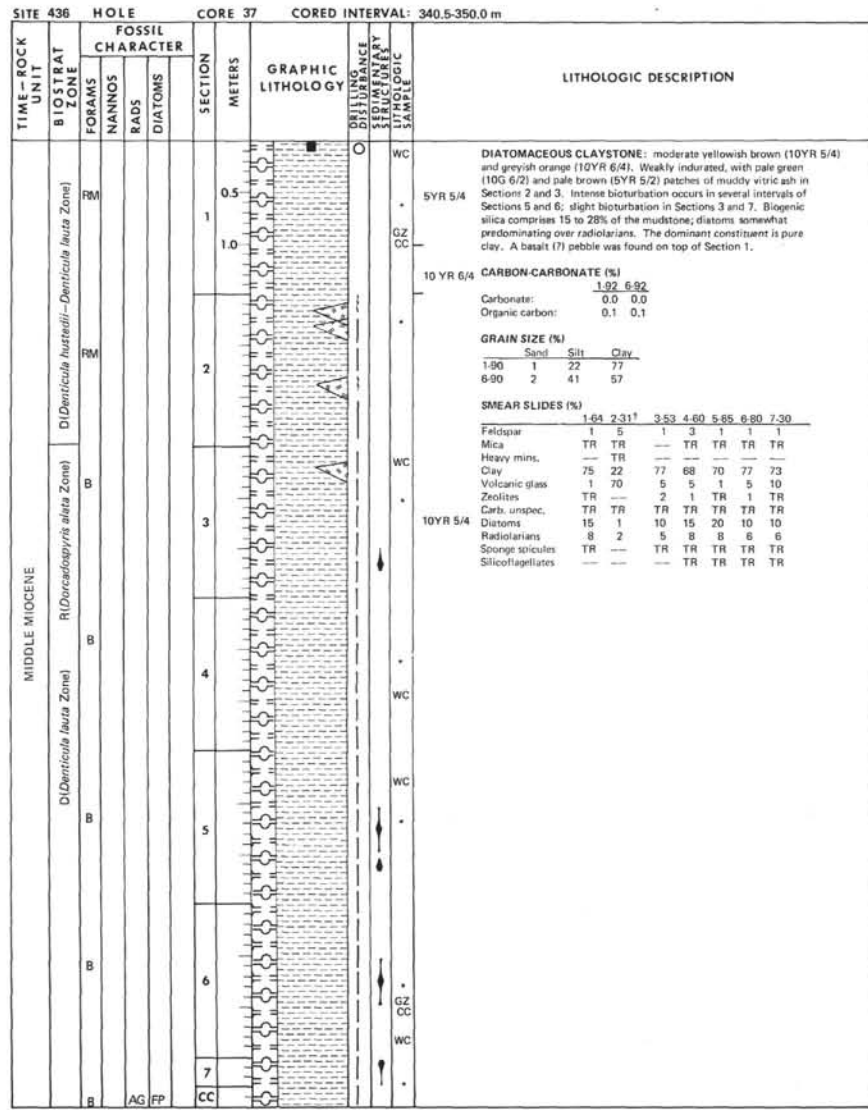
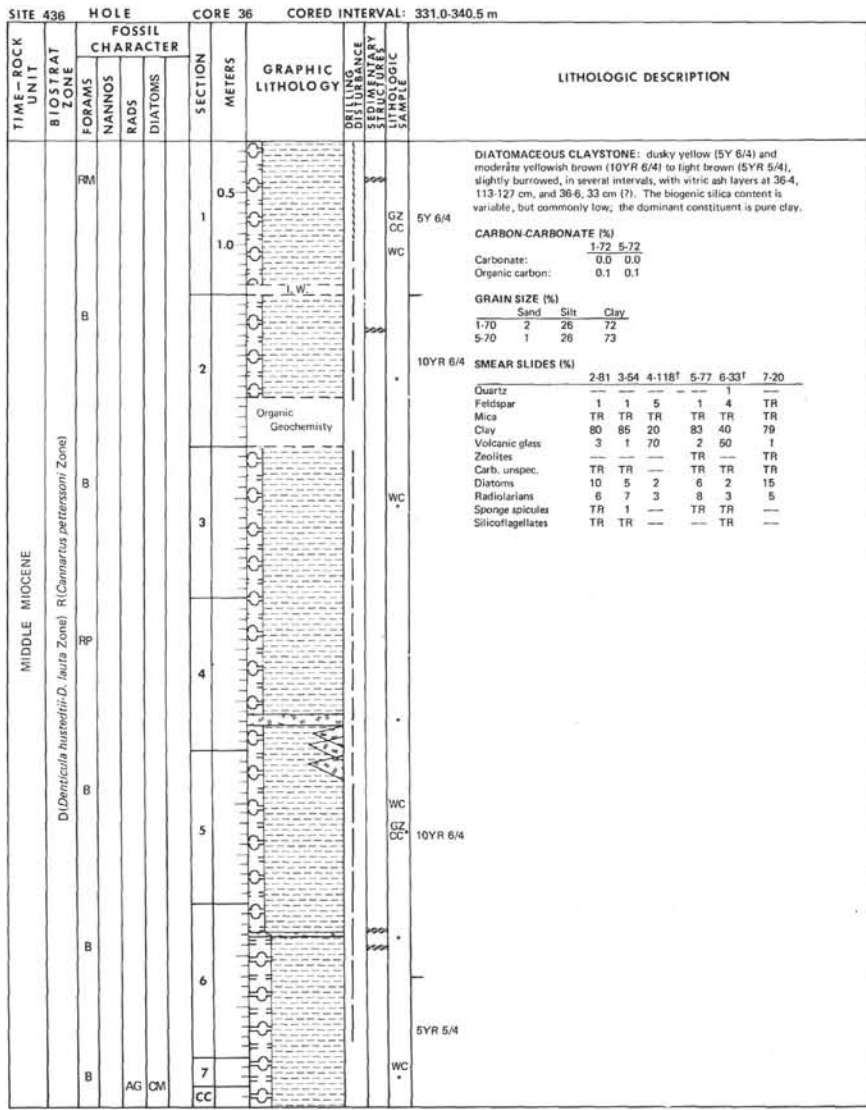
SITE 436		HOLE			CORE 27		CORED INTERVAL: 245.5-255.0 m			
TIME-ROCK UNIT	BIOSTRAT ZONE	FOSSIL CHARACTER			SECTION METERS	GRAPHIC LITHOLOGY	DRILLING DISTURBANCE	SEDIMENTARY STRUCTURE	LITHOLOGIC SAMPLE	LITHOLOGIC DESCRIPTION
		FORAMS	NANNOS	RADS						
LATE MIOGENE	R(Sphaeropyle langii Zone)	B		AG	1.0				5G 5/1	DIATOMACEOUS VITRIC SILTY CLAY AND CLAYSTONE: 0-300 cm, dark greenish grey (5G 5/1), slightly deformed, with parts becoming harder, more lithified. (First occurrence of semi-lithified units). VITRIC ASH: light grey (N7), some pyritized with gradational top and bottom contacts. Ash rich layer at 74-75 cm. Section 1 is brownish black (5YR 2/1). Silicified hornblende dacite. CARBON-CARBONATE(%) Carbonate: 1.69 3.38 Organic carbon: 0.0 0.0 0.3 0.2 GRAIN SIZE (%) Sand Silt Clay 1-70 5 41 54 3-38 B 38 54 SMEAR SLIDES (%) 1-40 1-75† 1-140 2-80 3-40 Quartz 3 — 2 — 2 3 Feldspar 15 3 15 10 10 Heavy mins. — TR TR — — Clay 53 63 44 45 44 Volcanic glass 15 17 25 25 5 Pyrite 1 10 1 TR 1 Carb. unsp. 3 — 3 3 2 Diatoms 10 7 10 15 30 Radiolarians TR — TR — — Sponge spicules TR — TR TR 5 Silicoflagellates TR — TR — —

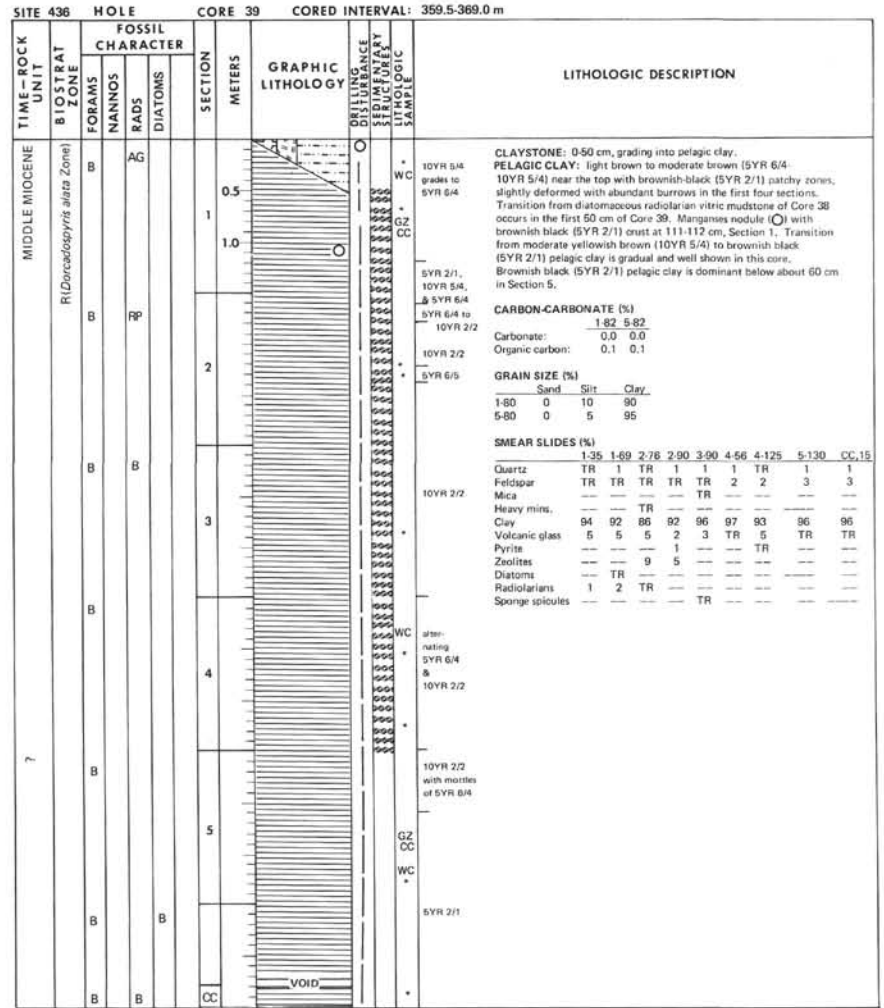
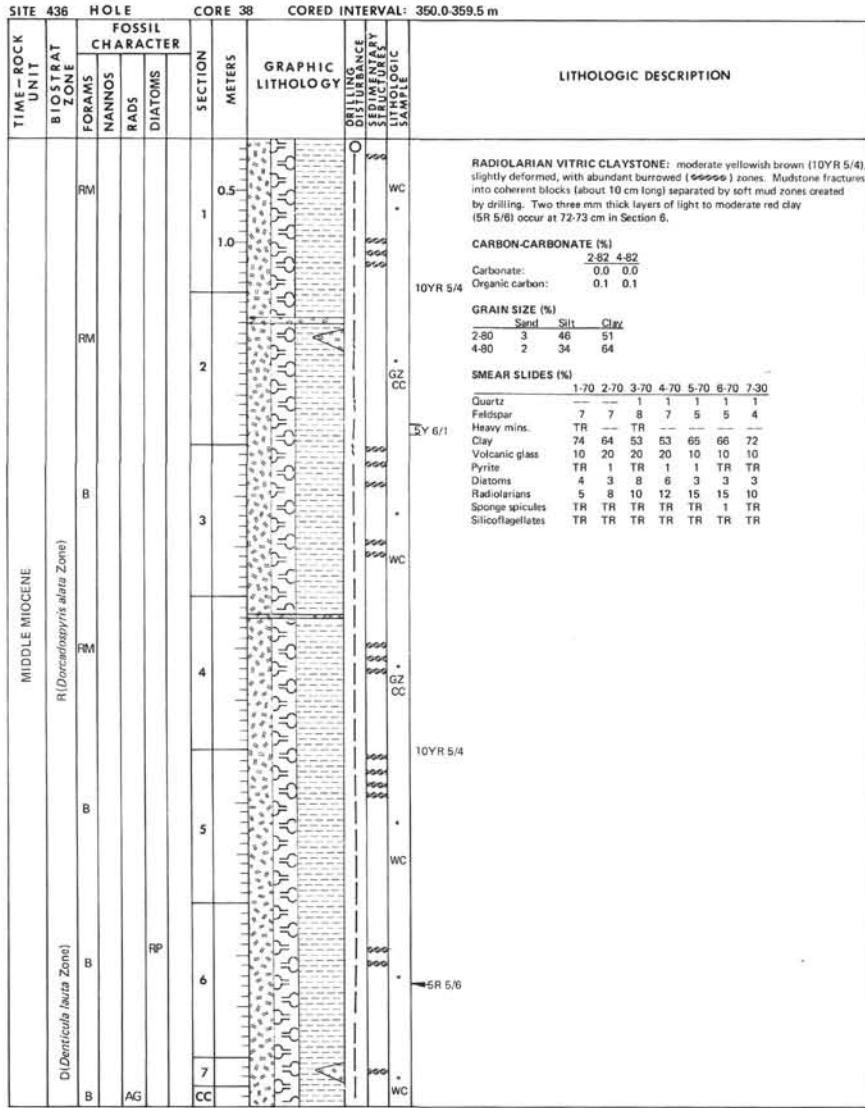
SITE 436		HOLE			CORE 29		CORED INTERVAL: 264.5-274.0 m			
TIME-ROCK UNIT	BIOSTRAT ZONE	FOSSIL CHARACTER			SECTION METERS	GRAPHIC LITHOLOGY	DRILLING DISTURBANCE	SEDIMENTARY STRUCTURE	LITHOLOGIC SAMPLE	LITHOLOGIC DESCRIPTION
		FORAMS	NANNOS	RADS						
LATE MIOGENE	R(Sichonyx peregrina Zone)	RM		AG OM	2.0				5G 5/1 to 5G 6/1	DIATOMACEOUS CLAYSTONE: greenish grey (5G 6/1) to dark greenish grey (5G 5/1), slightly to moderately deformed. Some dark concretionary or concentric banding at 34-38 cm. VITRIC ASH: light grey (N7) to very light grey (N8). Ash at 104-120 cm is medium dark grey (N4), pyritized and deformed by drilling. CARBON-CARBONATE (%) Carbonate: 1.44 2.44 Organic carbon: 0.0 0.0 0.2 0.2 GRAIN SIZE (%) Sand Silt Clay 1-42 5 44 51 2-42 5 42 53 SMEAR SLIDES (%) 1-30 1-70† 1-118† 1-140 2-85† Quartz 2 3 — 2 3 Feldspar 10 10 — 10 2 Heavy mins. — TR TR TR — Clay 60 — — 70 — Volcanic glass 8 87 90 9 96 Pyrite TR TR 10 TR TR Diatoms 15 TR — 9 — Radiolarians TR — — TR — Sponge spicules 5 TR — TR — Silicoflagellates TR — — TR —

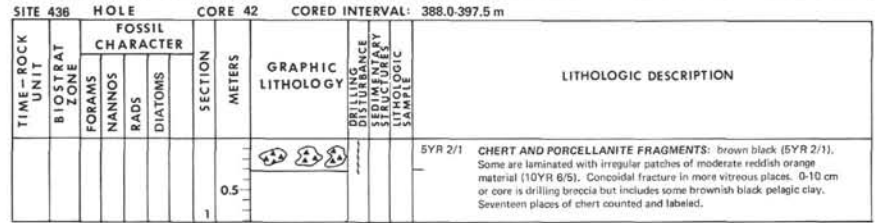
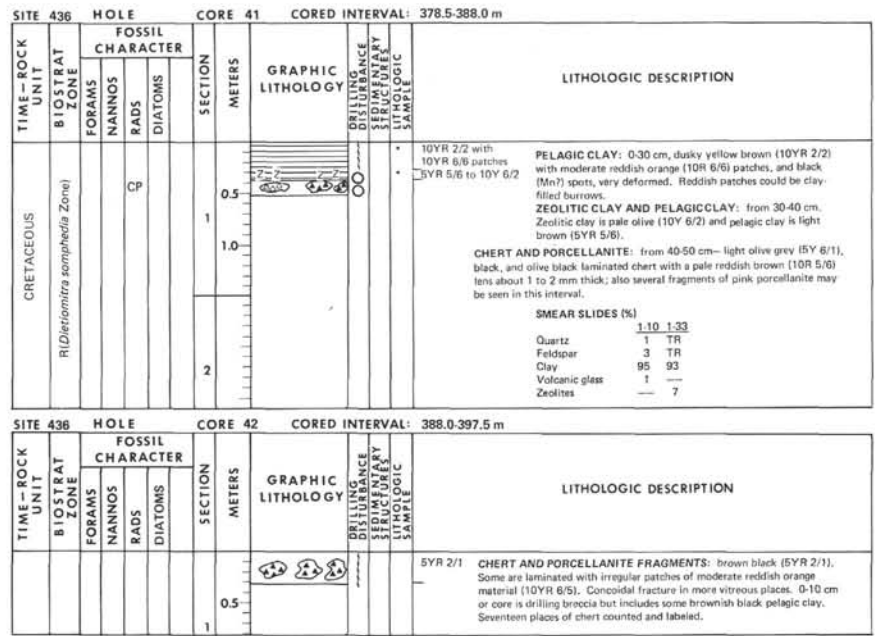
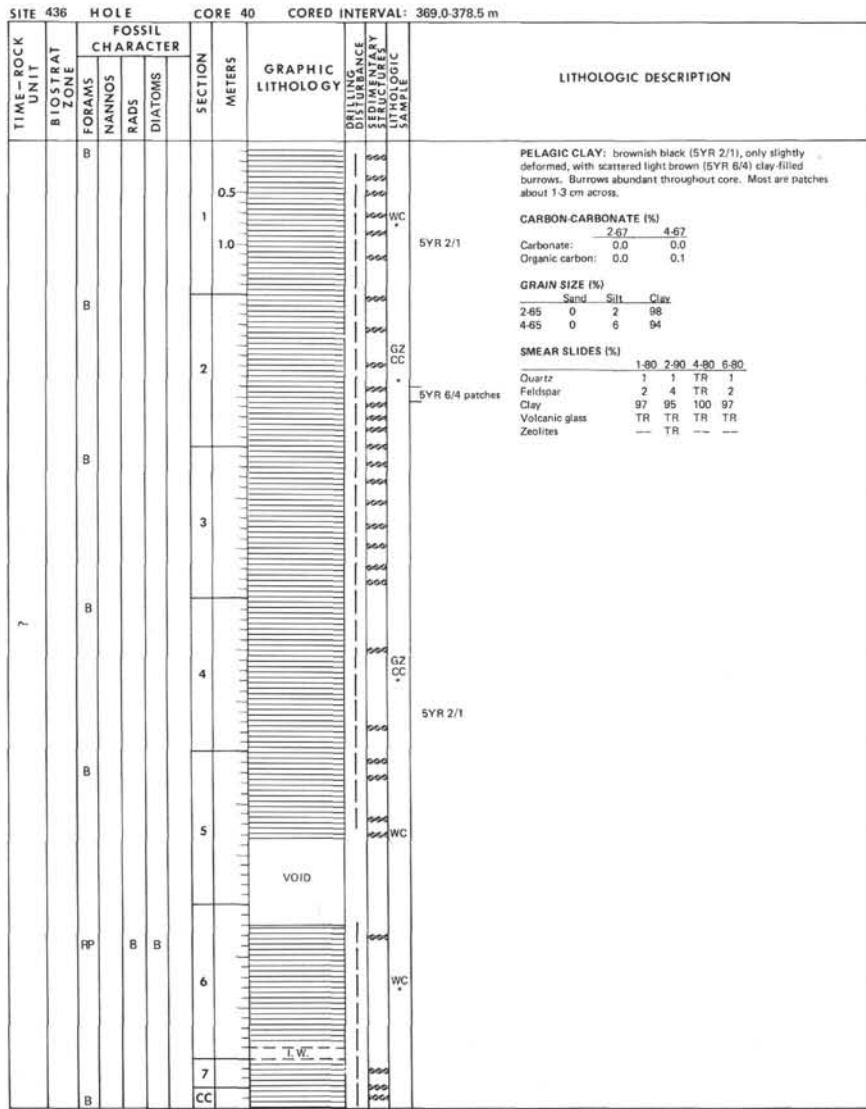




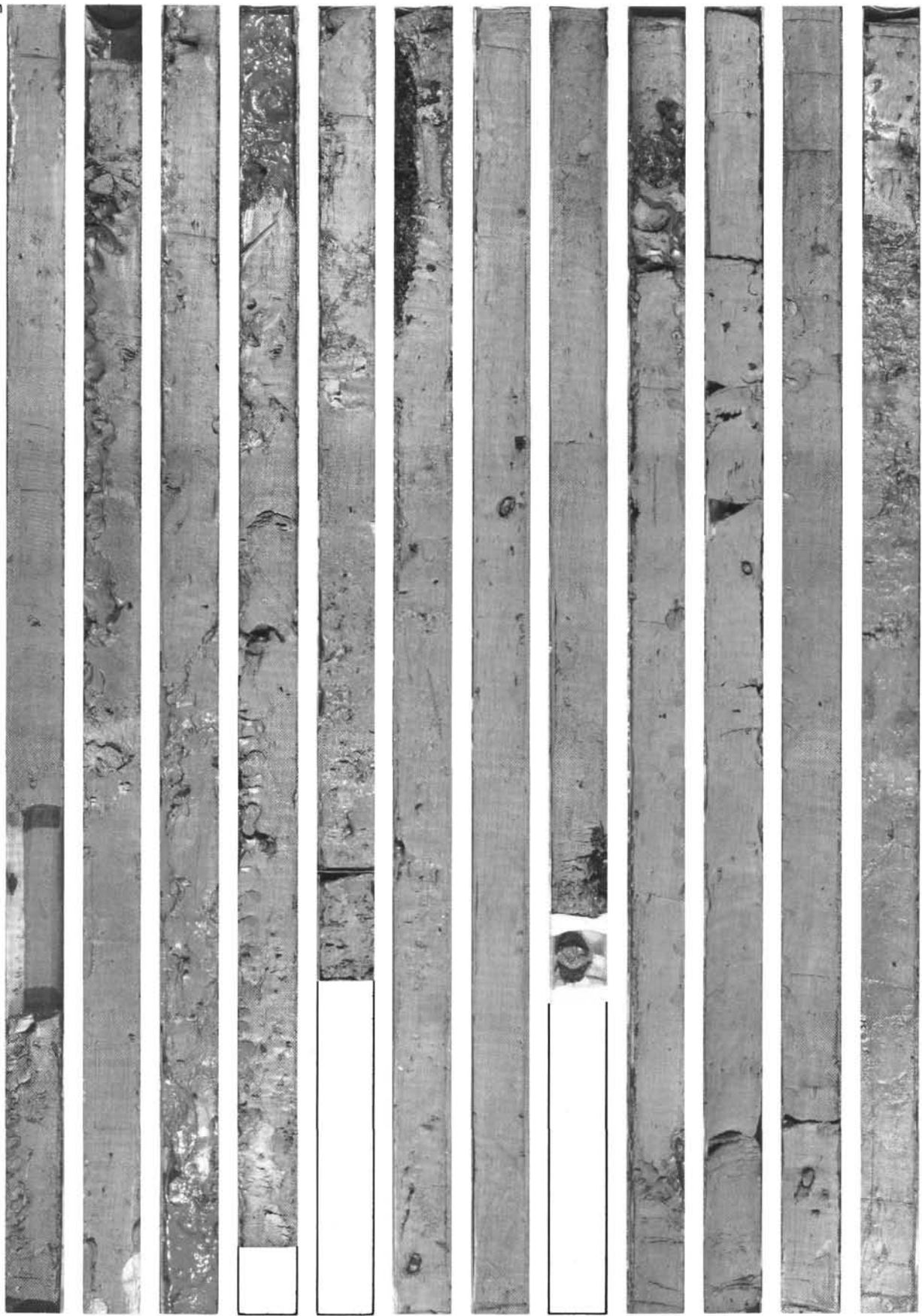
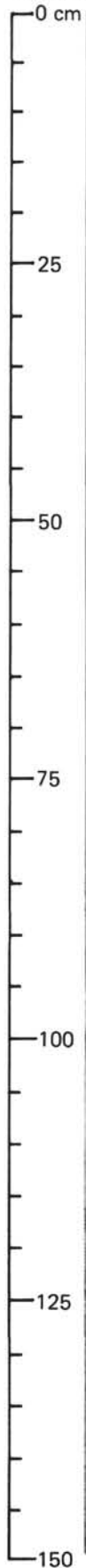






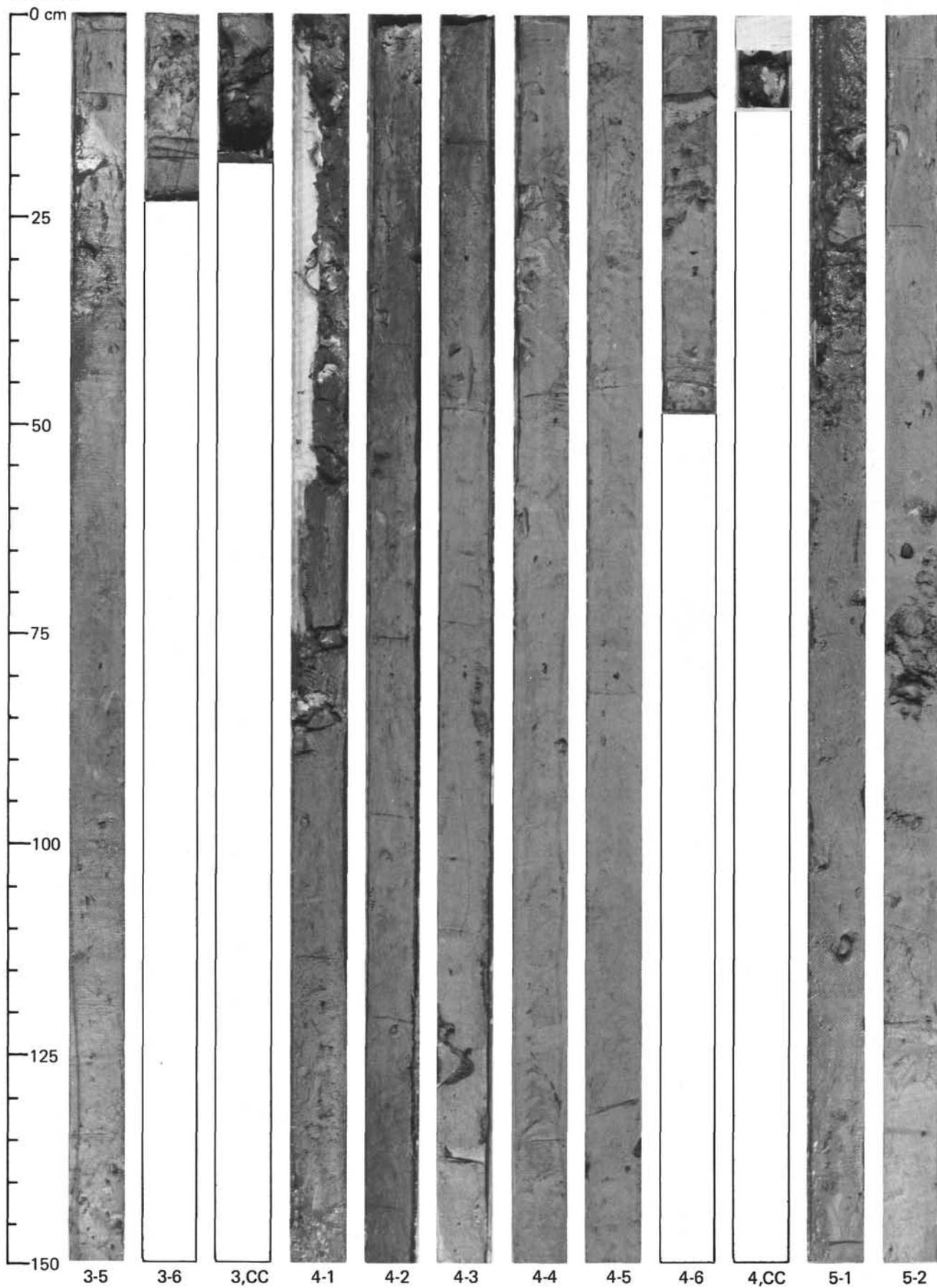


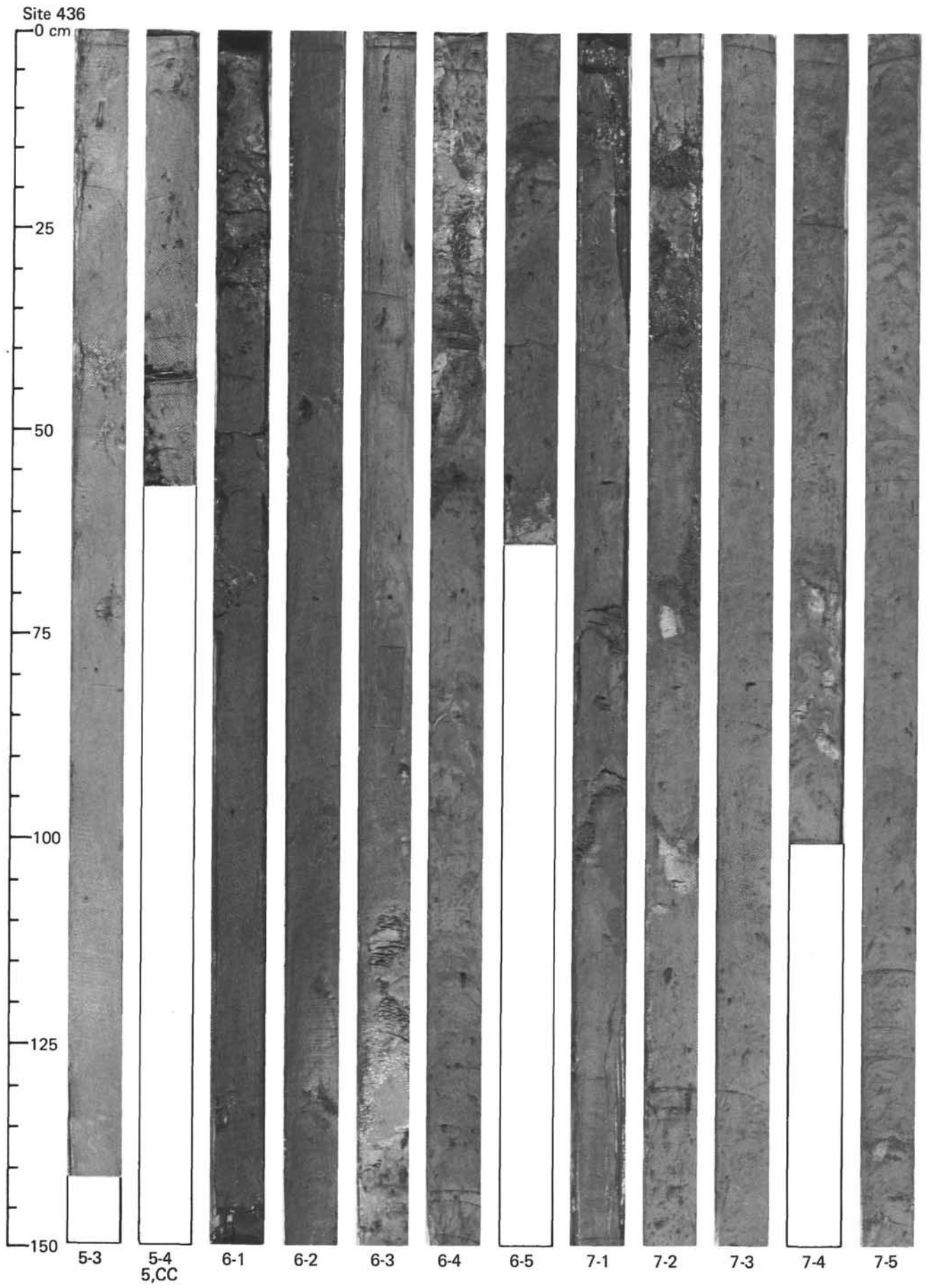
Site 436

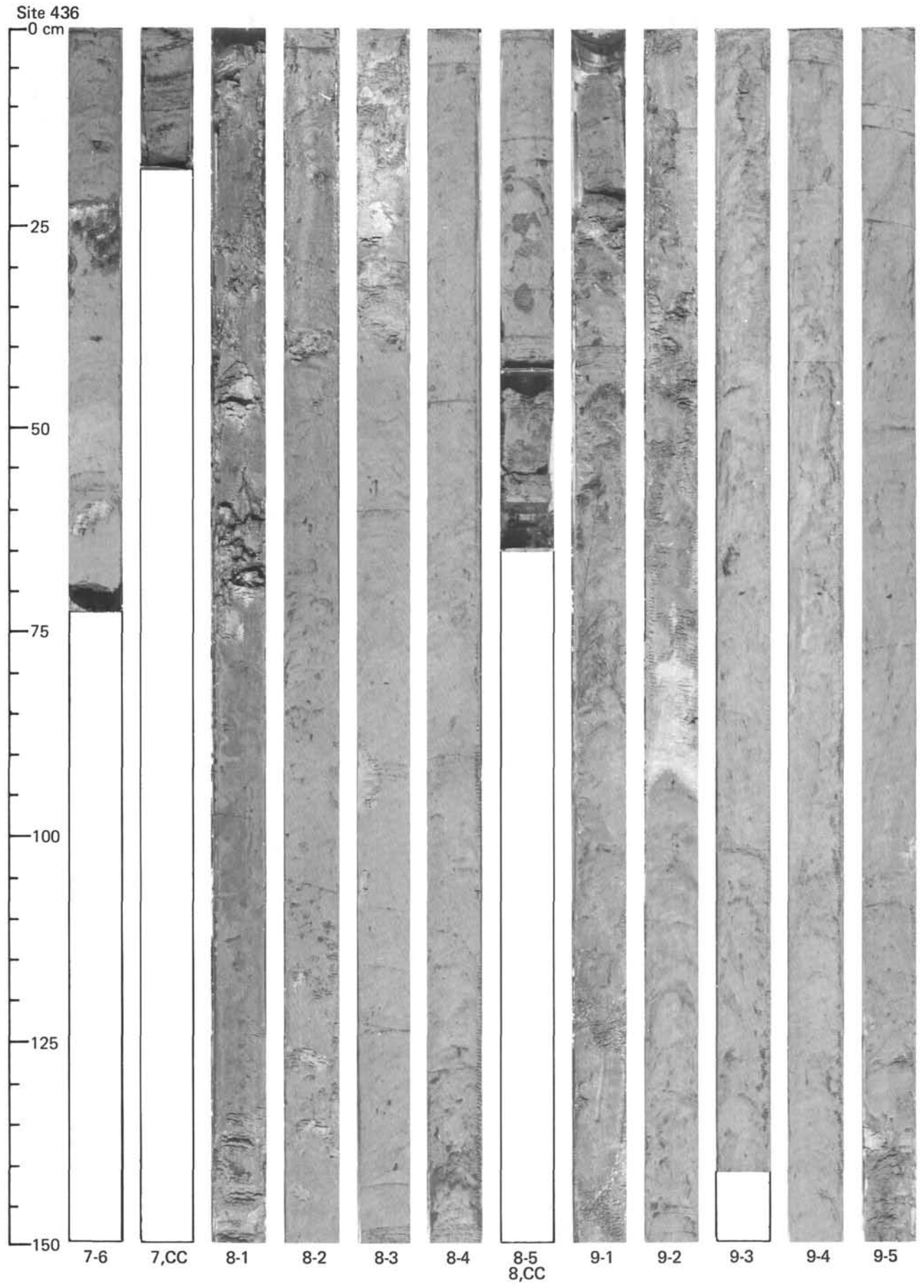


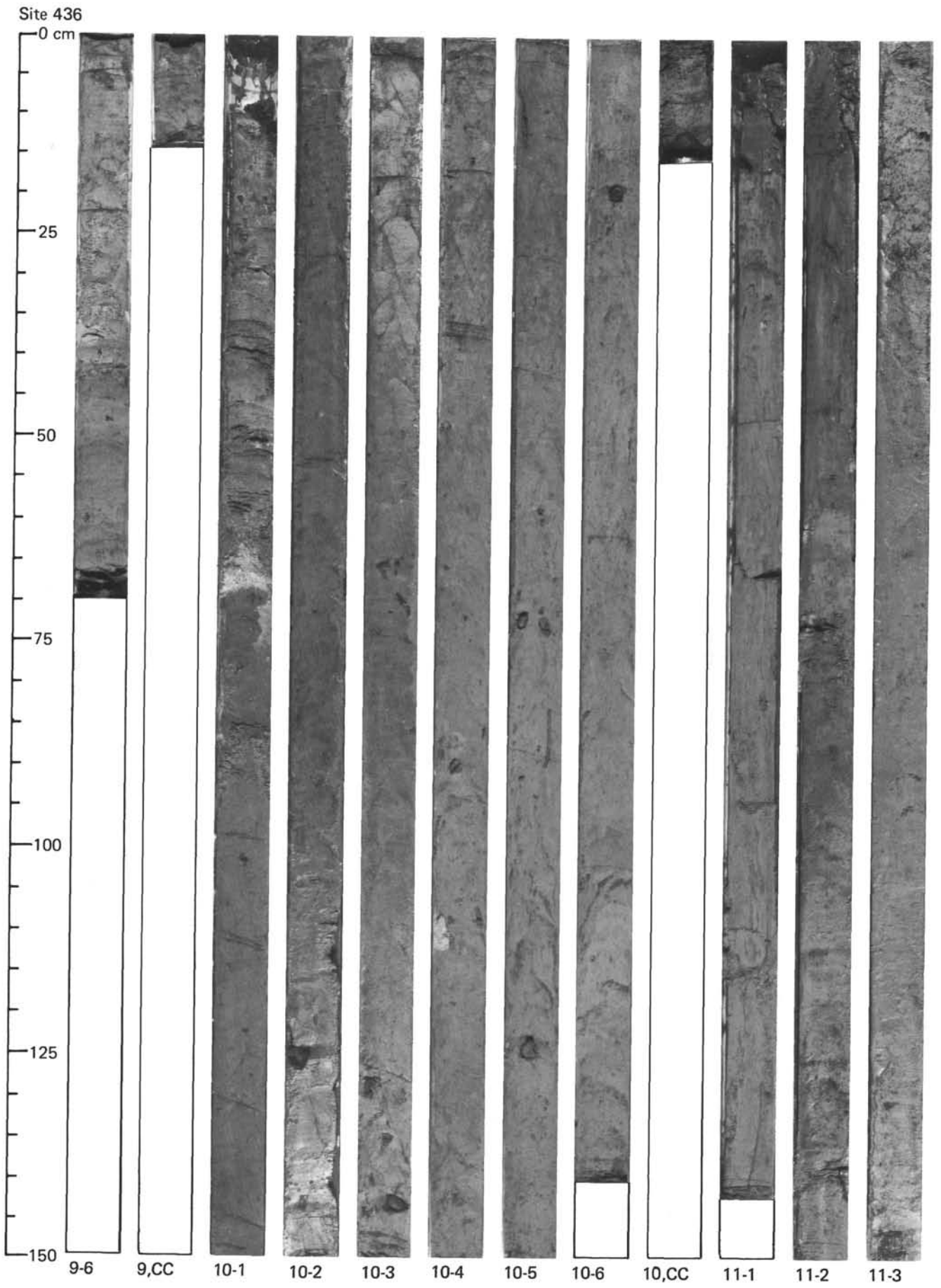
1-1 1-2 1-3 1-4 1-5 2-1 2-2 2-3 3-1 3-2 3-3 3-4
1,CC 2,CC

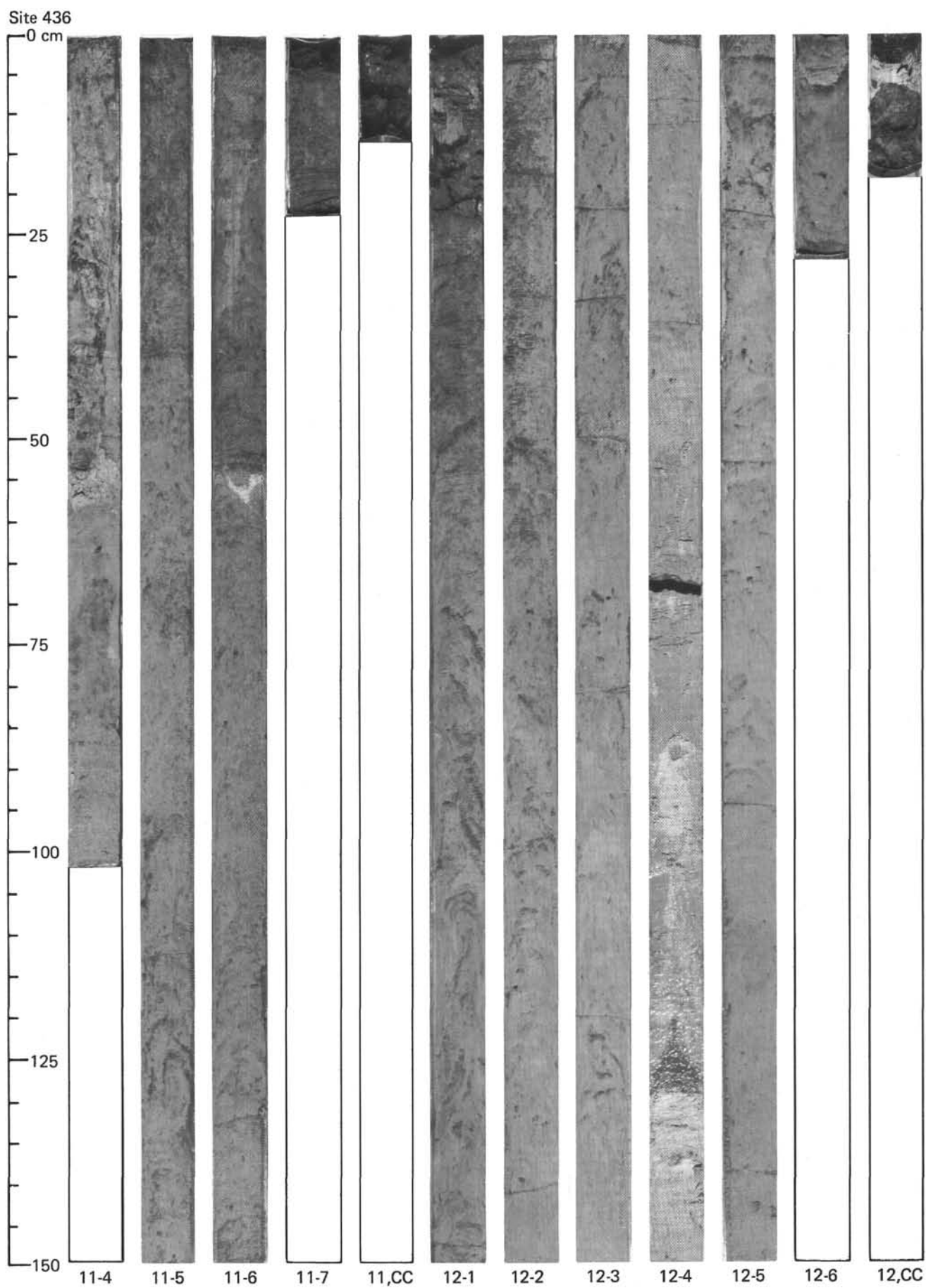
Site 436

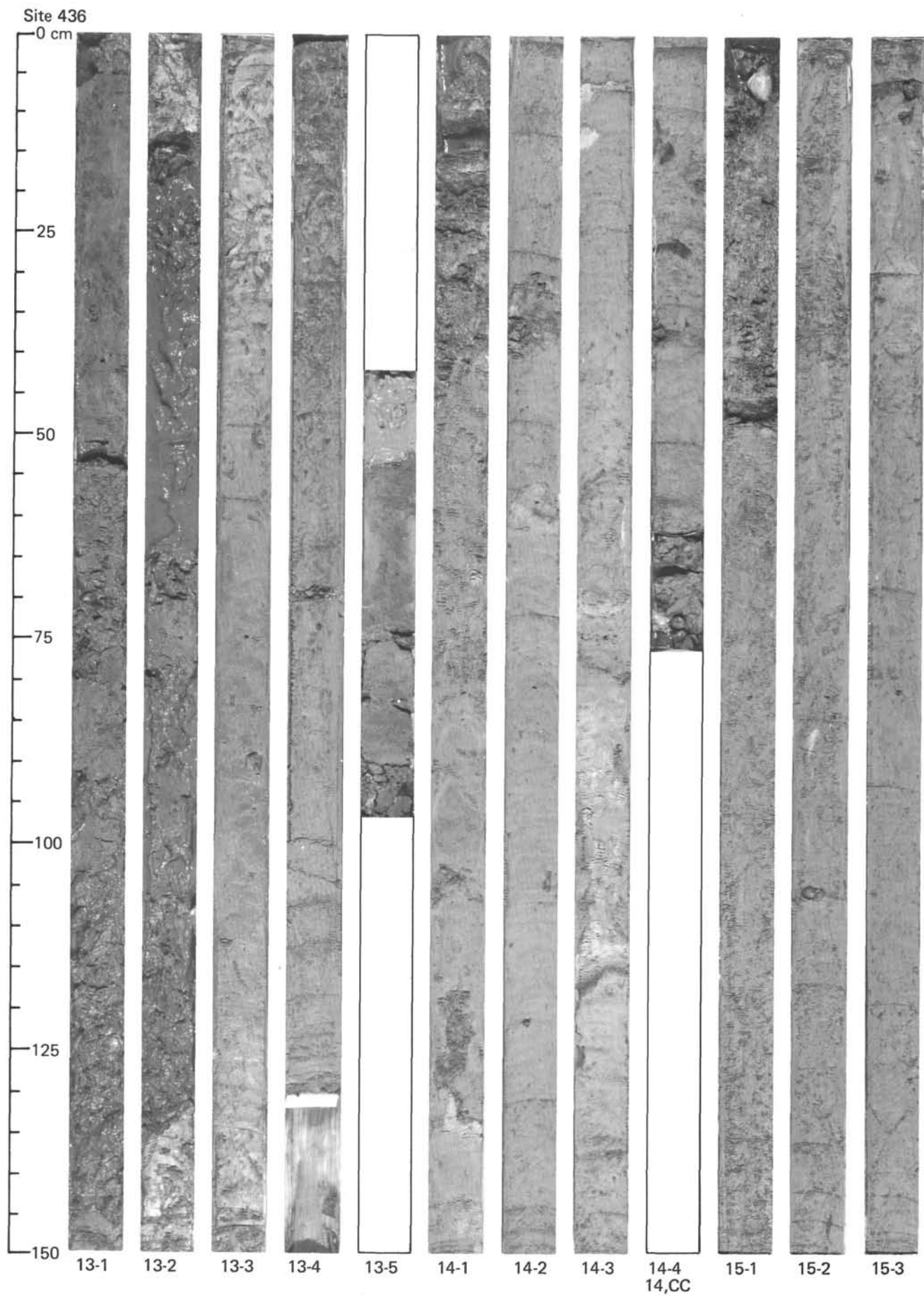




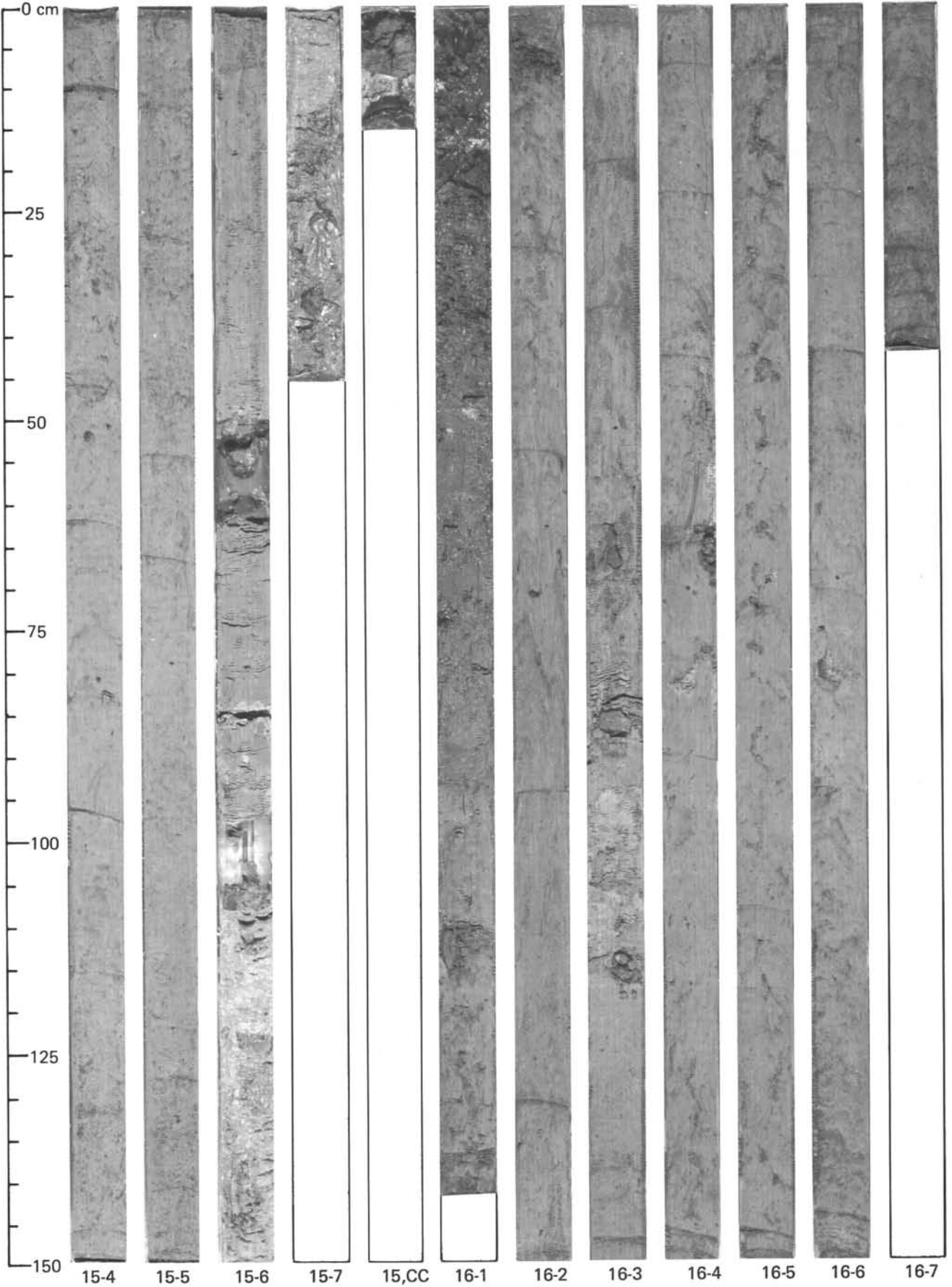


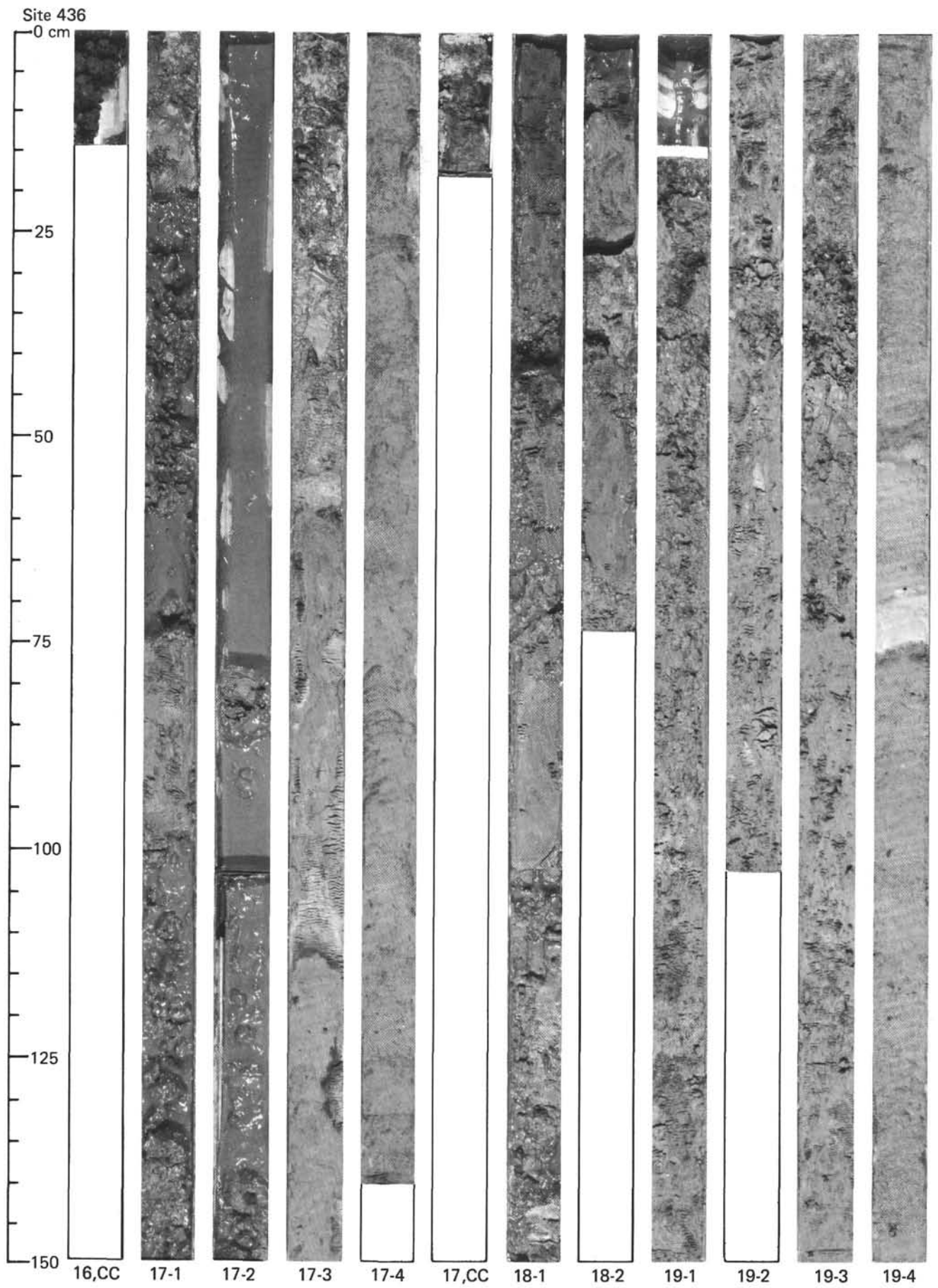


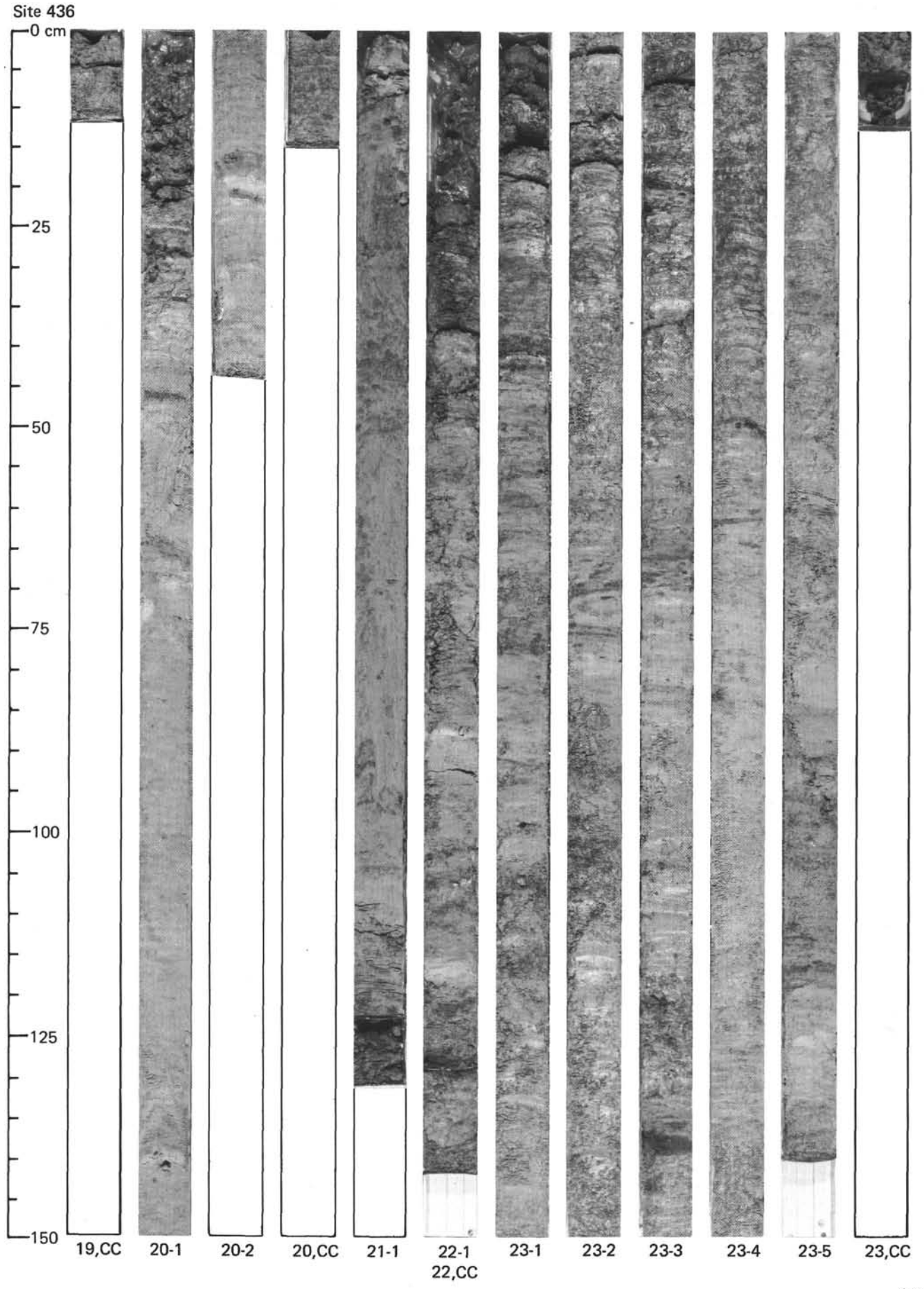


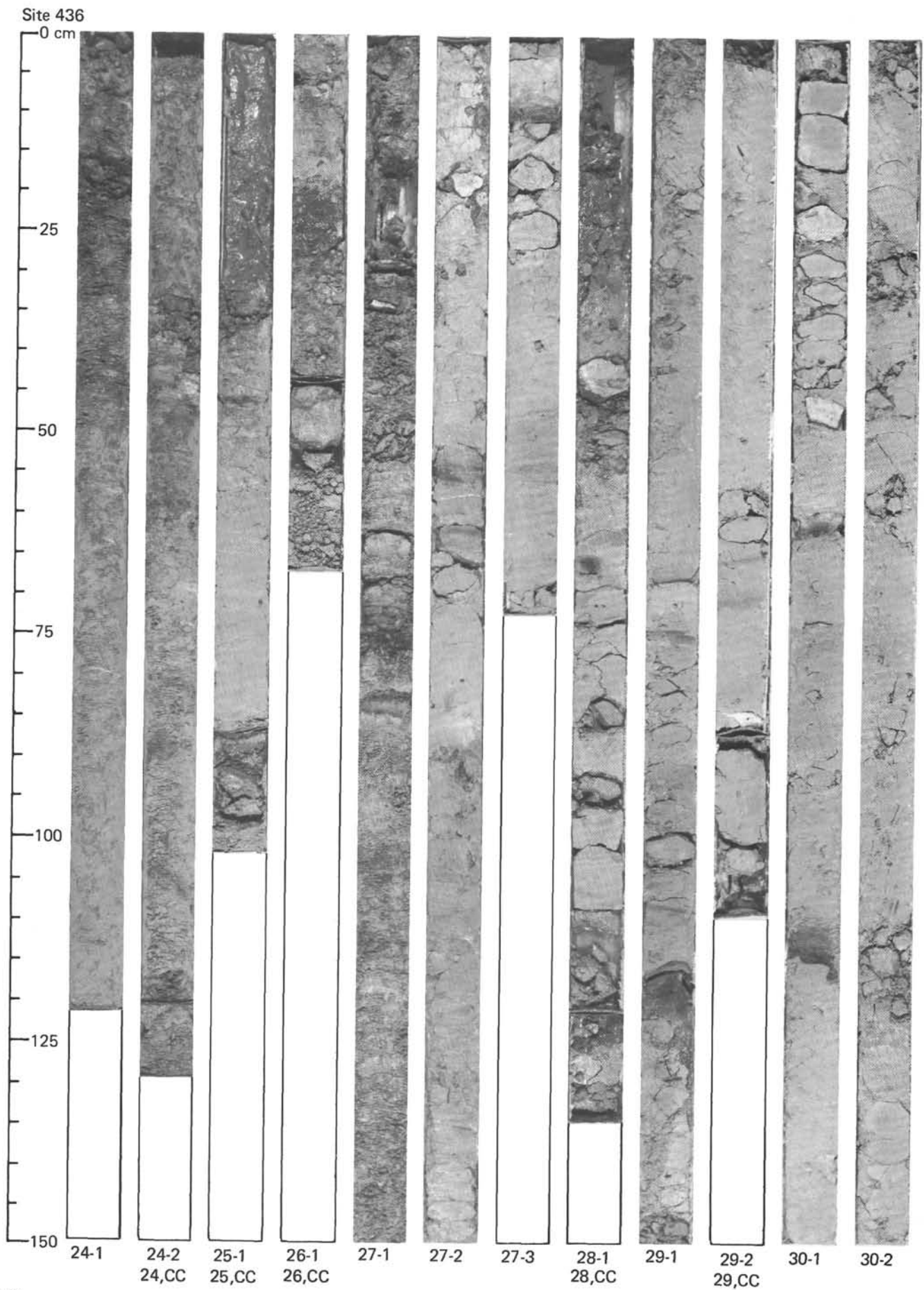


Site 436

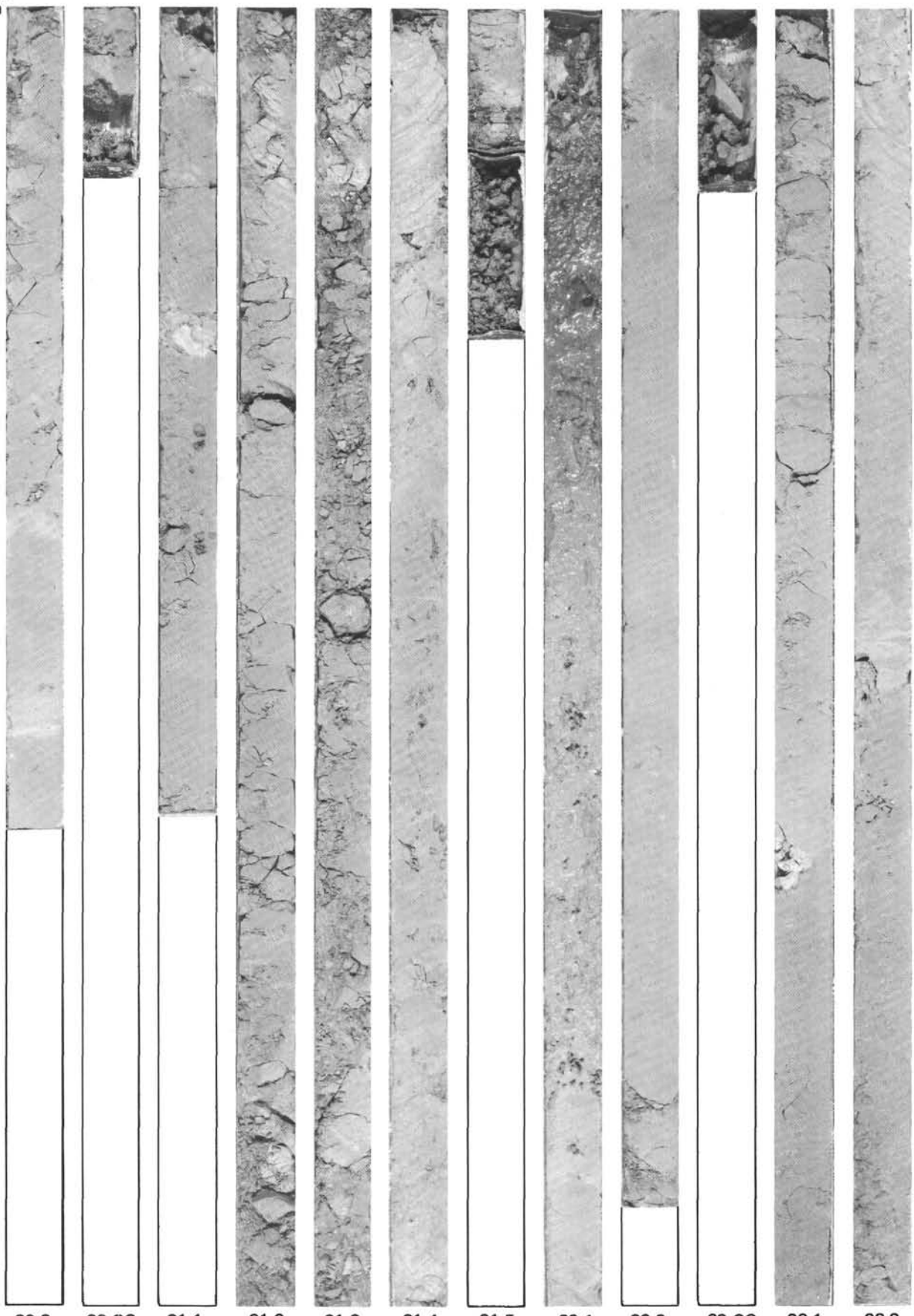
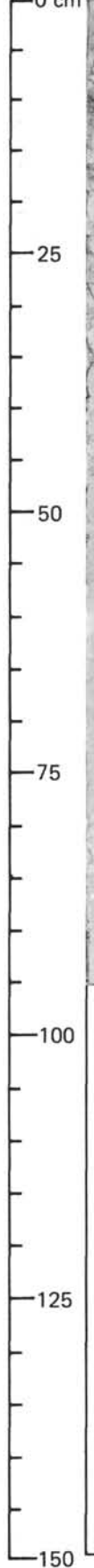




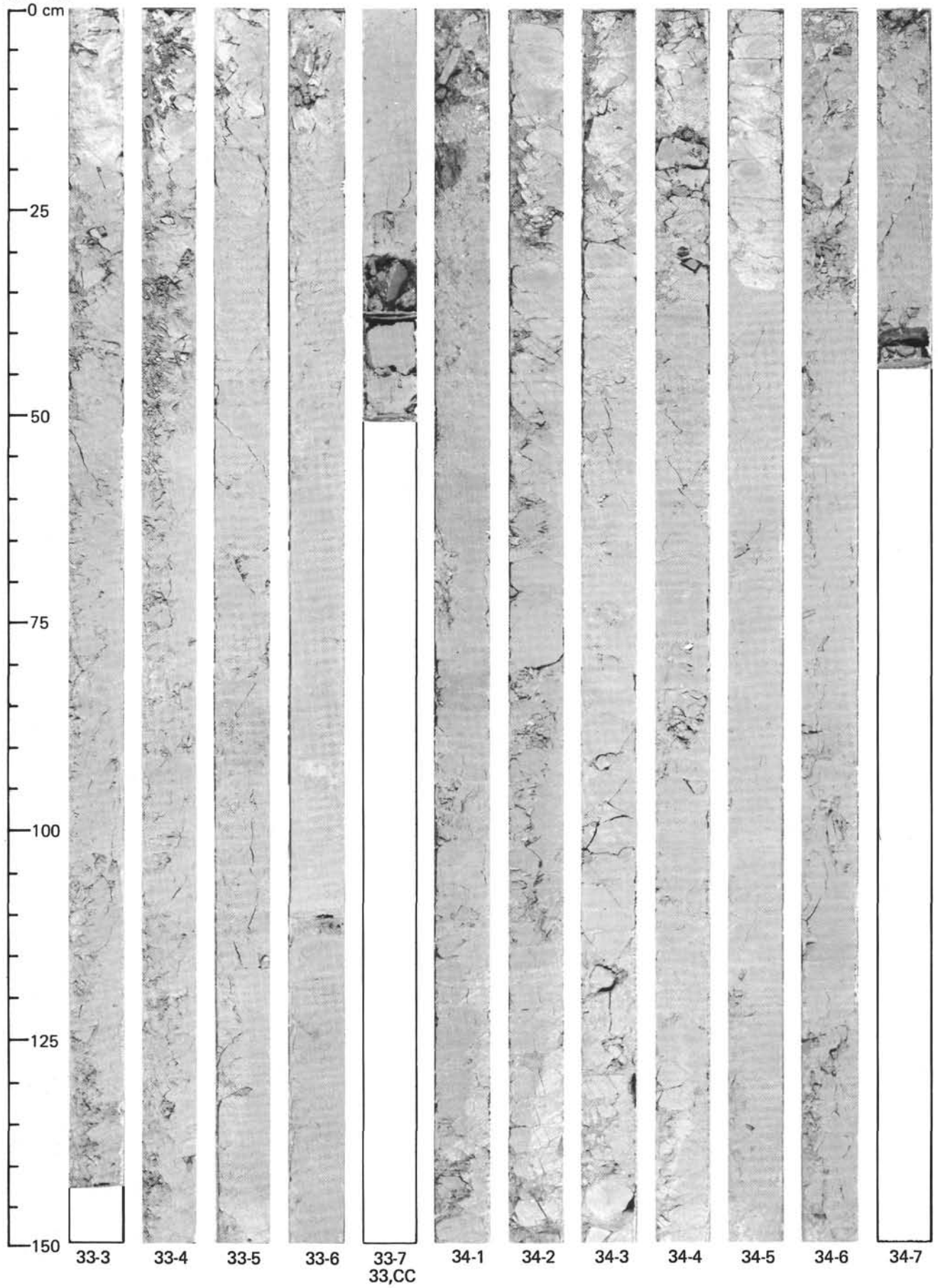




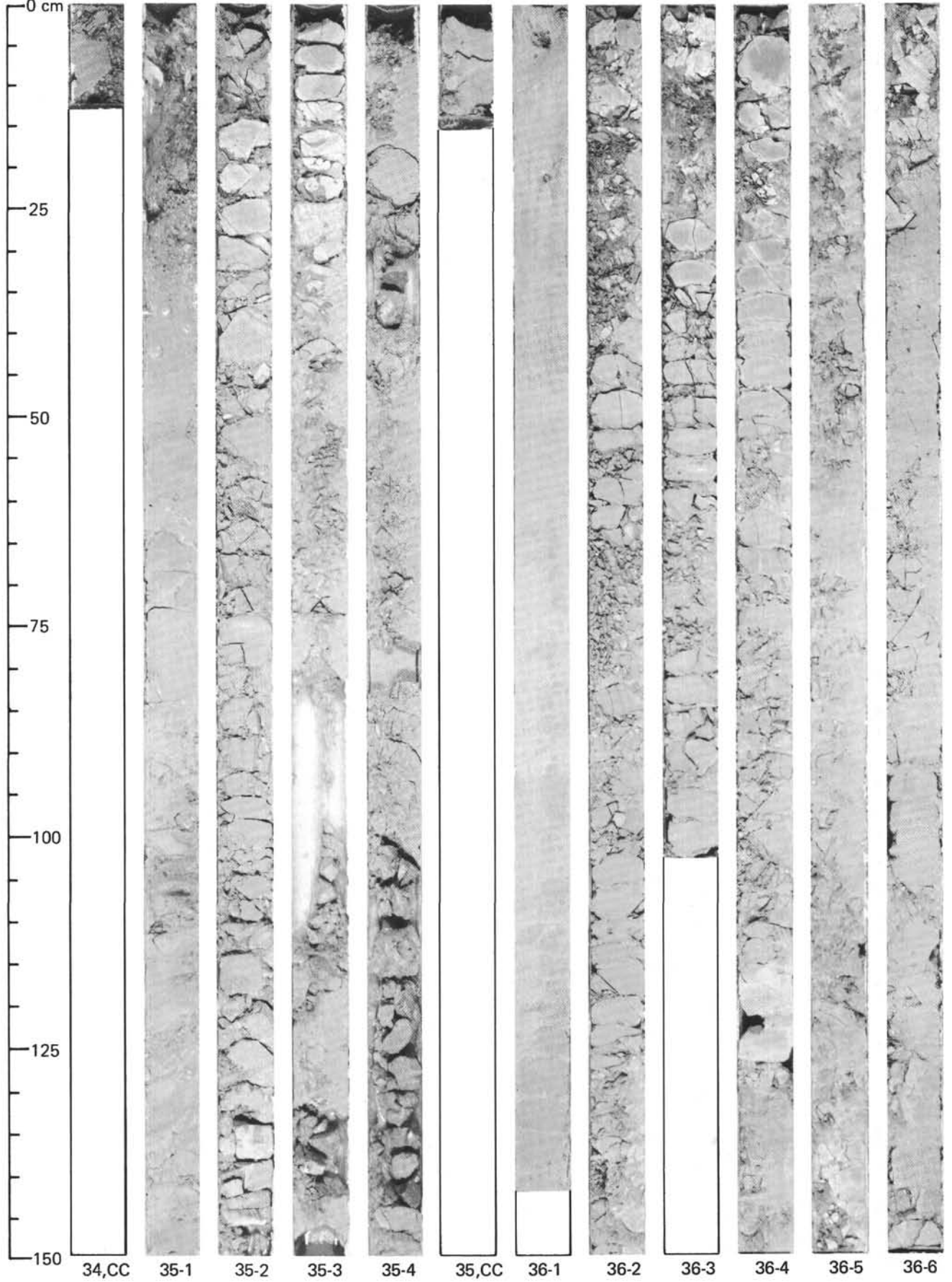
Site 436



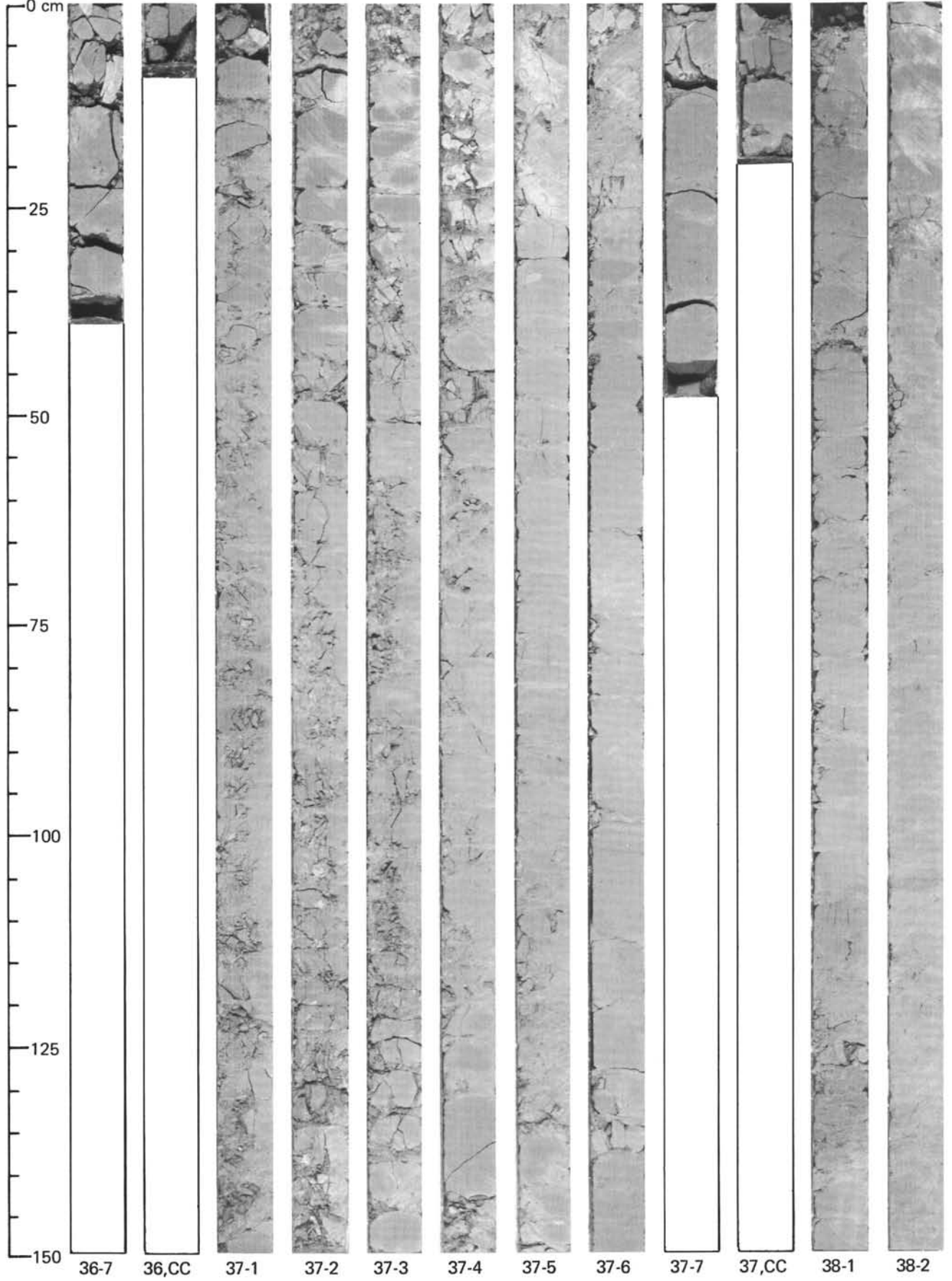
Site 436



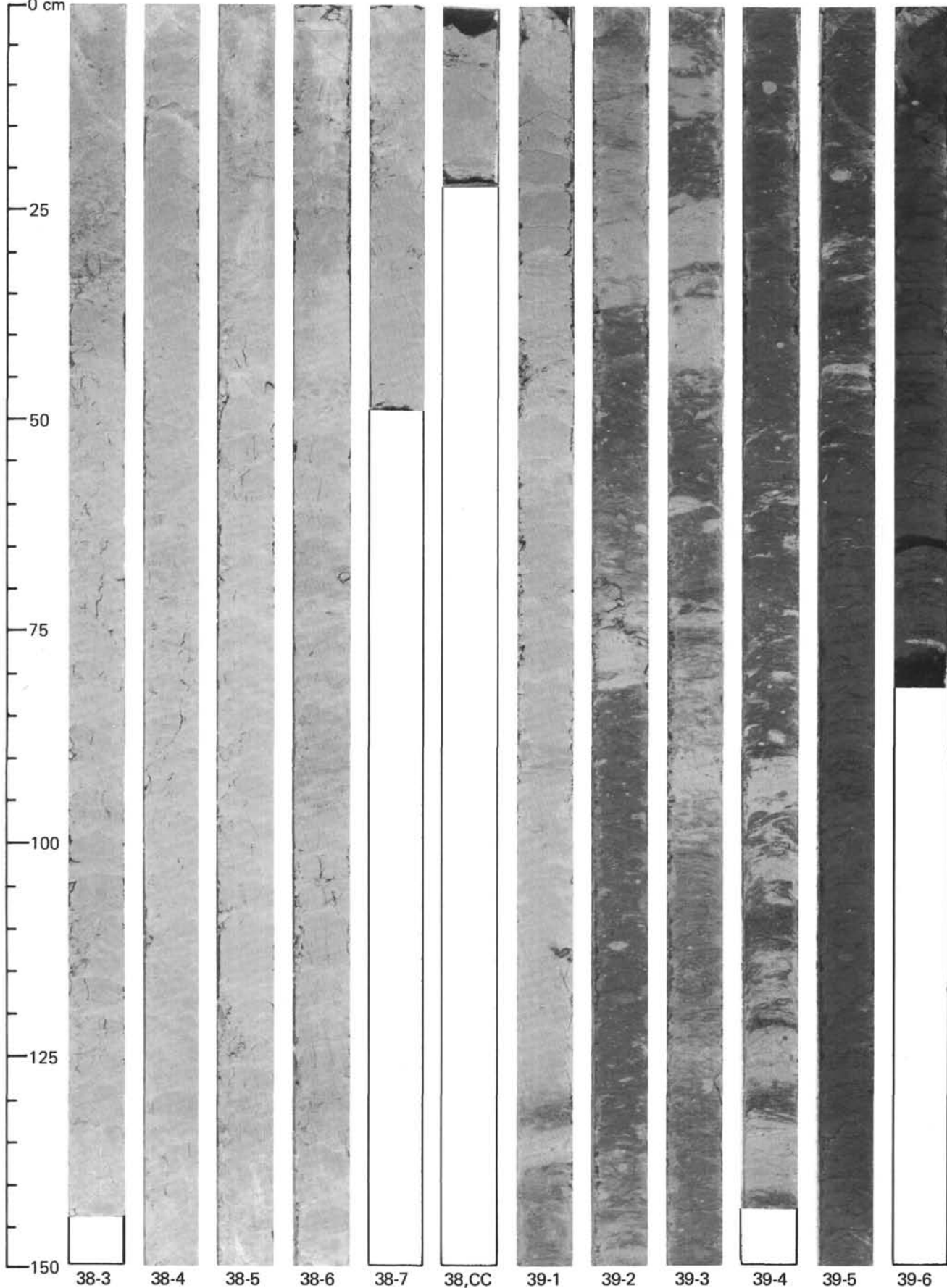
Site 436



Site 436



Site 436
0 cm



Site 436

0 cm

25

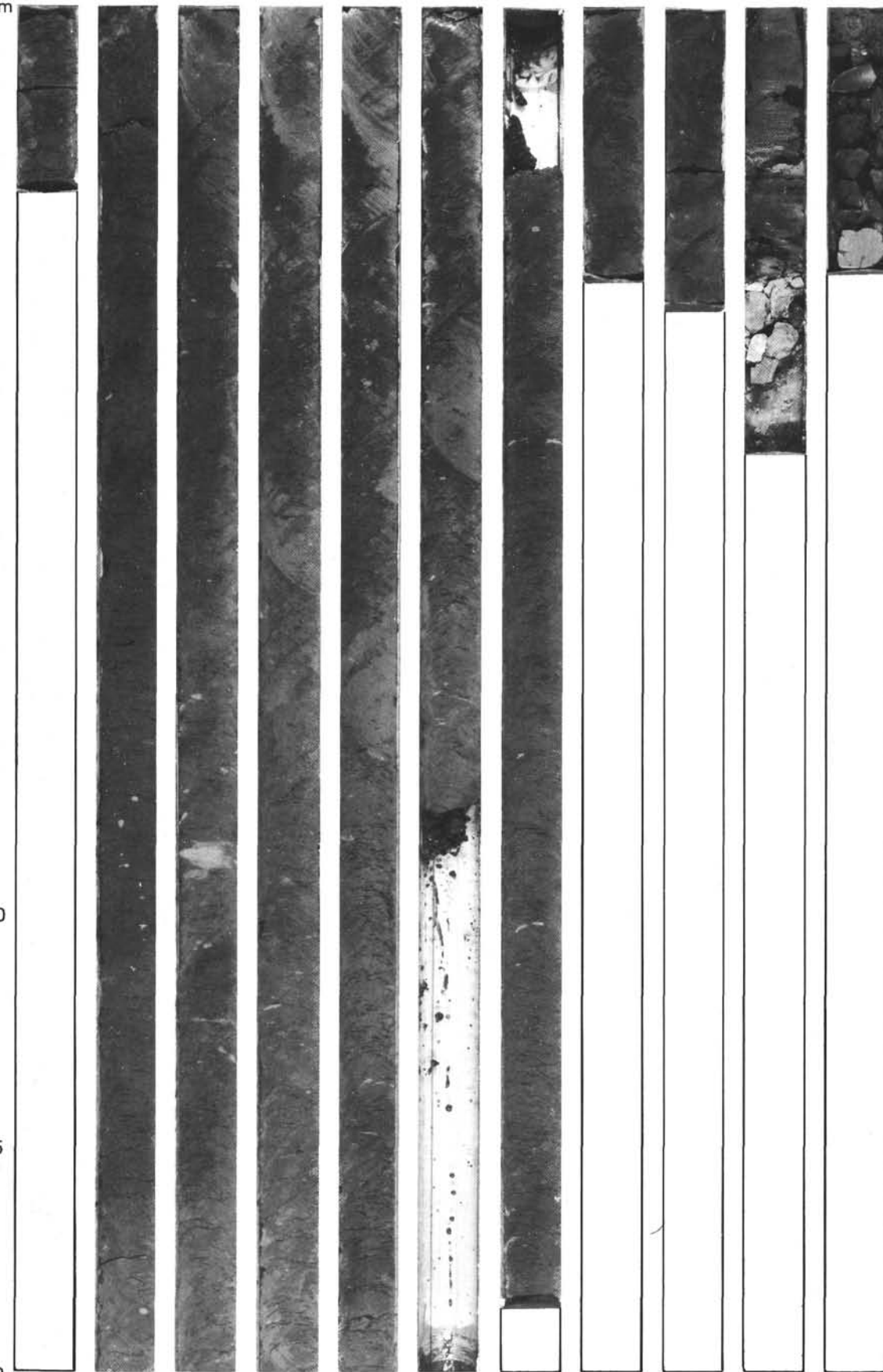
50

75

100

125

150



39,CC

40-1

40-2

40-3

40-4

40-5

40-6

40-7

40,CC

41-1

42-1